Alma Mater Studiorum – Università di Bologna

DOTTORATO DI RICERCA IN

Biologia Cellulare e Molecolare

Ciclo XXXIV

Settore Concorsuale: 05/E1 BIOCHIMICA GENERALE

Settore Scientifico Disciplinare: BIO/10 - BIOCHIMICA

INHERITED OPTIC NEUROPATHIES: WORKING ON MITOCHONDRIAL BIOENERGETICS AND DYNAMICS TO DISCOVER NEW THERAPEUTIC STRATEGIES

Presentata da: Serena Jasmine Aleo

Coordinatore Dottorato

Prof. Vincenzo Scarlato

Supervisore

Prof.ssa Anna Maria Ghelli

Co-supervisore

Dott.ssa Claudia Zanna

Esame finale anno 2022

INDEX

ABSTRACT

Inherited optic neuropathies are neurodegenerative disorders characterized by severe mitochondrial dysfunctions. Among these Leber's Hereditary Optic Neuropathy (LHON) and Dominant Optic Atrophy (DOA) are the most frequent and caused by mutations in respiratory complex I (CI) core subunits and OPA1 mutations, respectively. For both pathologies there is no established cure. For LHON the only approved drug is the ubiquinone-analogue idebenone. However, its effect is still controversial as only a limited subset of patients recovers. The antioxidant and bioenergetic effect of idebenone in CI-inhibited cells depend on its reduced form which can transport electrons to complex III, partially restoring the respiratory chain functionality bypassing the impaired CI. The enzyme identified as the key player in idebenone reduction is NAD(P)H-quinone dehydrogenase (NQO1), an inducible cytosolic enzyme involved in the antioxidant response through reduction of quinones. However, the demonstration of the role of NQO1 in promoting the idebenone therapeutical effect in cells with CI genetic defects is still lacking. DOA is caused by mutations in OPA1 gene encoding a mitochondrial dynamin-like GTPase involved in several mitochondrial functions such as mitochondrial fusion, energy metabolism, mitochondrial genome stability, cristae morphology, and apoptosis. Therapeutic strategies trying to mitigate mitochondrial dysfunctions associated with OPA1 mutations, to promote mitochondrial biogenesis, or directly stimulate the expression and activity of OPA1 have been proposed for DOA treatment. However, there is no approved drug and novel pharmacological strategies are needed to develop effective therapies. Here, we aim to better investigate the molecular mechanism of idebenone, as well as the role of NQO1 expression, in LHON treatment. Moreover, we aim to validate compounds as possible drugs for DOA treatment, using a "drug repurposing" approach. In the first part of our study, we show that in LHON CI-defective cellular models overexpressing NQO1, idebenone treatment was able to rescue rotenone-insensitive mitochondrial respiration. Furthermore, we find that in these cells mitochondrial ATP synthesis also occurs adding external NADH in presence of idebenone. We, therefore, demonstrate that NQO1 supports oxidative phosphorylation bypassing CI and directly transfers electrons to CIII via the NQO1-idebenone-CIII pathway. Additionally, we show that NQO1 overexpression significantly reduces ROS overproduction. Strikingly, only patient-derived fibroblasts expressing NQO1 are able to maintain respiration. Finally, treatment with NQO1 expression inducer dimethyl fumarate is able to rescue mitochondrial respiration in presence of idebenone. Hence, we show that NQO1 expression levels correlates with the efficacy of idebenone, providing the possibility to design strategies to enhance NQO1 activity to maximize idebenone therapeutic potential in LHON. In the second part,

we aim to validate FDA-approved molecules, here renamed “OPA1 rescuing molecules” (ORMs), able to rescue the mitochondrial dysfunctions induced by OPA1 mutations. Six ORMs were previously selected through a “drug repurposing” approach starting from 2,500 molecules. Here, we show the testing of these selected compounds in Opa1-ablated mouse embryonic fibroblasts (MEFs) expressing the human OPA1 isoform 1 bearing the R445H and D603H mutations. Some of these molecules ameliorate the energetic functions and/or the mitochondrial network morphology, depending on the type of OPA1 mutation. ORM14 is the most effective compound showing both energy and morphology rescuing in the final validation on patient-derived fibroblasts. Our results permit to translate into clinical trials the biochemical findings on the pivotal role of NQO1 expression and activity for LHON treatment, as well as the outcomes on the “drug repurposing” approach for DOA treatment.

1. INTRODUCTION

Optic neuropathies are neurodegenerative disorders affecting the prelaminar area of the optic nerve and can be either inherited or acquired, as well as non-syndromic or rare syndromic multisystem diseases. The progressive loss of painless bilateral visual acuity, central or caecocentral scotomas, and colour vision deficiency are caused by severe damage to retinal ganglion cells (RGCs), neural cells projecting their axons to the brain forming the optic nerve and sending the information elaborated by the retina to the brain cortex (Pilz et al., 2017). These cells are particularly vulnerable to mitochondrial dysfunction as they are highly energy dependent (Chinnery & Hudson, 2013). The two most frequent non-syndromic inherited optic neuropathies are Leber's hereditary optic neuropathy (LHON) and dominant optic atrophy (DOA) and both are related to mitochondrial dysfunction.

1.1 Mitochondria: from bioenergetics and beyond

Mitochondria are organelles arranged in a dynamic and interconnected reticulum within eukaryotic cells. These essential organelles produce the majority of cellular energy, in form of adenosine triphosphate (ATP), via oxidative phosphorylation system (OXPHOS) and harbour many metabolic pathways critical for cell survival and function. First and foremost, mitochondria host tricarboxylic acid cycle (TCA) which, besides being central in oxidative catabolism, is also involved in anabolism as its intermediates support diverse biosynthetic routes, such as fatty acid, amino acids, purine, pyrimidines, and haems biosynthetic pathways. Mitochondrial functions go far beyond those of bioenergetics and metabolism as they are also crucial in calcium homoeostasis, autophagy, apoptosis, and cell signalling (Nunnari & Suomalainen, 2012). Structurally, mitochondria are composed by an outer mitochondrial membrane (OMM) and a more selective inner mitochondrial membrane (IMM) which separates a thin intermembrane space (IMS) from the matrix compartment. Moreover, the IMM houses functionally important membrane domains protruding into the matrix space called *cristae* (Freya & Mannellab, 2000). Mitochondria have their own DNA (mtDNA) derived from the genome of a proteobacterium engulfed by an ancestral eukaryotic cell according to the so-called endosymbiotic theory (Sagan, 1967). During the course of evolution, this bacterial genome was almost entirely transferred to the nuclear genome (nDNA) leaving mitochondria with a modest genome. In fact, human mtDNA is a polyploid, 16,596 base pair, circular double stranded DNA encoding only 13 proteins involved in OXPHOS, as well as 2 mitochondrial rRNAs and 22 mitochondrial tRNAs, necessary for the *in situ* translation of the 13 mtDNA-encoded protein

(Taanman, 1999). mtDNA molecules, moreover, are associated to different proteins forming DNA-protein structures anchored to IMM called nucleoids (Bogenhagen, 2012). Mitochondria morphology and distribution, as well as the complexity of the network that they form within cells, are highly dynamic and intimately linked to their function. Mitochondrial dynamics is orchestrated by two interconnected processes, namely fission and fusion, and depends on cell type, metabolic status and physio-pathological variations (Mannella, 2006; Wai & Langer, 2016). Clearance of damaged mitochondria via a process called mitophagy is also important to prevent the onset of human diseases, especially neurodegenerative disorders. Regulation and balancing of mitophagy with fusion, fission and mitochondrial biogenesis, a process as a whole referred as "mitochondrial quality control", are essential to preserve a functional mitochondria network and prevent pathological conditions (Yoo & Jung, 2018). As mitochondria are involved in numerous cellular functions, their impairment is associated to many pathologies, such as metabolic disorders, cancer (Iommarini et al., 2017), and neurodegenerative diseases (Zeviani & Carelli, 2007). Indeed, neurons are highly mitochondrial dependent since they are particularly sensitive to energetic deficits and their function relies on several mitochondrial processes as regulation of calcium flux, neurotransmitter, and lipid biosynthesis (Nunnari & Suomalainen, 2012). The role of dysfunctional mitochondria in neurodegeneration and neuropathies has been extensively investigated but needs to be further explored to develop safe and effective therapeutic opportunities.

1.2 The bioenergetic role of mitochondria: OXPHOS

Mitochondria are well-known for the synthesis of most of the cellular ATP via OXPHOS (Fig.1). The reduced forms of the coenzyme nicotinamide adenine dinucleotide (NADH) and flavin adenine dinucleotide ($FADH_2$) storing the free energy derived from the catabolism are oxidised by the mitochondrial respiratory chain (MRC). During the electron transfer, protons (H^+) are transferred from the mitochondrial matrix to the IMS generating a H^+ electrochemical gradient across the IMM which drives the ATP production according to the Mitchell's chemiosmotic theory (Rich, 2008). This electrochemical gradient, moreover, generates the mitochondrial membrane potential ($\Delta\psi$) essential for mitochondrial homeostasis (Zorova et al., 2018). MRC is composed of four enzymatic complexes: complex I (CI) or NADH-ubiquinone oxidoreductase; complex II (CII) or succinate-ubiquinone oxidoreductase; complex III (CIII) or cytochrome *bc1*; and complex IV (CIV) or cytochrome *c* oxidase (Lenaz & Genova, 2010). Various redox cofactors enable the transfer of electrons within complexes, whereas coenzyme Q (CoQ) and cytochrome *c* (cyt *c*) allow the transfer of electrons between complexes. The entry point of the electron in the MRC is represented by CI which oxidises

NADH to NAD^+ by the transfer of two electrons to the flavin mononucleotide (FMN). The electrons are then transferred through seven iron-sulfur (Fe-S) clusters to CoQ, thereby reducing it to semiquinone and finally to ubiquinol. The energy released is used to translocate four protons out of the matrix. CII is another electron entry point which oxidises succinate and reduce CoQ without coupling the electron transfer to the proton translocation. CIII oxidises the ubiquinol pool - generated by CI, CII, and other alternative dehydrogenases. CIII reduces cyt *c* and translocates four protons to the IMS via two turns of the Q-cycle (Crofts, 2004). Finally, reduced cyt *c* transports the electrons to CIV which in turn reduces O_2 to H_2O pumping two protons to the IMS. The H^+ electrochemical gradient is used by complex V (CV), F_1F_o - ATP synthase, for ATP synthesis from adenosine diphosphate (ADP) and inorganic phosphate (Walker, 1998).

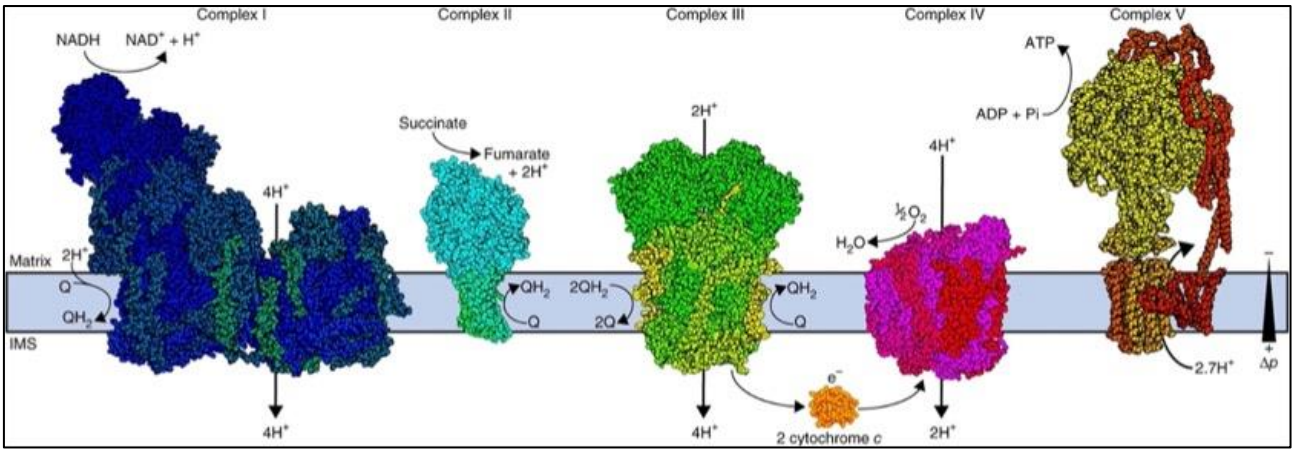

Figure 1 - Representation of the complexes of the electron transport chain (Letts & Sazanov, 2017)

1.3 Complex I: structure, function and its role in pathology

Mammalian CI is the largest MRC multiproteic complex made up of 45 subunits. 14 of these proteins are the core subunits involved in the enzymatic catalysis and evolutionary conserved (Hirst, 2013). The remaining 31 supernumerary subunits, although lacking any catalytic function, are essential for the stability and assembly of the enzyme (Stroud et al., 2016). CI subunits arrange in a L-shape structure forming a remarkable 1 MDa molecular "engine" with a peripheral arm, protruding into the mitochondrial matrix, and a membrane arm, embedded into the IMM (Fig.2) (Baradaran et al., 2013; Vinothkumar et al., 2014; Zhu et al., 2016).

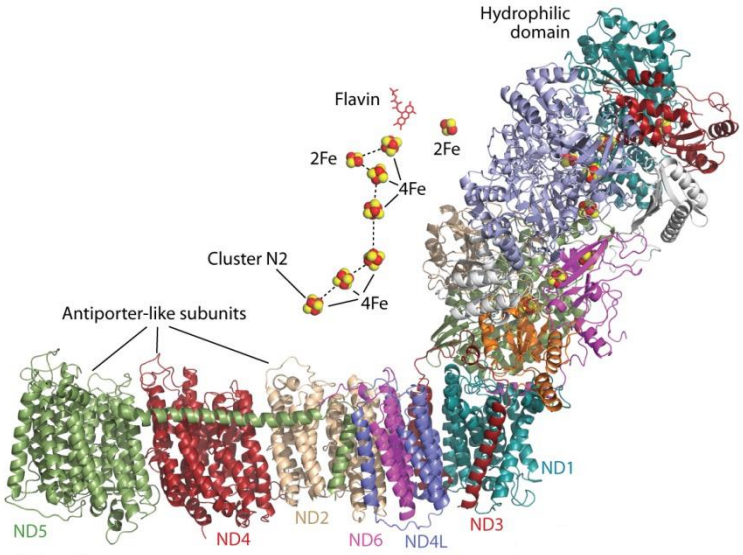

Figure 2 - Structure of Complex I from Thermus Thermophilus (Hirst, 2013)

The former is composed of 7 core and 7 supernumerary subunits, all nDNA-encoded. At the tip of this domain there is the NADH-binding site and the FMN cofactor. There, NADH is oxidised reducing the FMN which then donates two electrons, one by one, to the redox chain formed by 7 Fe-S clusters (N3, N1b N4, N5, N6a, N6a and N2). This chain transfers the electrons to CoQ reducing it to ubiquinol, as well as causing conformational changes which are transferred to the first proton channel of the membrane arm (Gutiérrez-Fernández et al., 2020). This domain comprises 7 mtDNA-encoded core subunits (ND1-6 and ND4L) and 24 nDNA-encoded supernumerary ones. The membrane arm core subunits harbours four half-closed channels for the proton pumping; indeed, the membrane domain is responsible for the translocation of four protons from the mitochondrial matrix to the IMS contributing to the generation of the proton motive force exploited for ATP synthesis by CV (Grba & Hirst, 2020; Kampjut & Sazanov, 2020). Specifically, ND2, ND4, and ND5 are antiporter-like subunits and represent three different proton translocation pathways, whereas the remaining mtDNA-encoded subunits form the fourth one named E-channel. A central role in the process of the coupling of Q reduction to proton pumping is played by electrostatic interaction between the conserved charged residues located in the central axis of the membrane domain (Grba & Hirst, 2020; Kampjut & Sazanov, 2020). Moreover, the involvement of only ND5 antiporter in the pumping of all four protons per catalytic cycle was recently proposed (Kampjut & Sazanov, 2020). Besides providing the driving force for ATP synthesis, CI is also a source of reactive oxygen species (ROS) as it produces superoxide anion ($O_2^{\cdot-}$), which is then dismutated to hydrogen peroxide (H_2O_2) by SOD_2. ROS production is a physiological event; however, CI disfunction can lead to its

pathological increase (Pryde & Hirst, 2011). On the basis of the described structural and functional characteristics, CI can be divided into three modules: the NADH dehydrogenase module (N-module), the ubiquinone-binding module (Q-module), and the proton translocating module (P-module) (Brandt, 2006). Furthermore, thorough studies on CI biogenesis which exploited quantitative proteomics confirmed its modular architecture and enabled to further divide the P-module into four submodules, namely ND1-, ND2-, ND4, and ND5-modules (Fig.3) (Guerrero-Castillo et al., 2017; Stroud et al., 2016). In fact, CI biogenesis occurs in a peculiar modular fashion and requires the intervention of various chaperons or proteins involved in prosthetic group incorporation, as well as in post-translational modifications, all referred as assembly factors (Formosa et al., 2018). CI modular organization was further corroborated by its disassembly analysed by the gradual depletion of a critical core subunit (D'Angelo et al., 2021). In addition, the near totality of CI interacts with CIII and CIV forming the respiratory supercomplexes (SCs) (Enríquez, 2016; Milenkovic et al., 2017). The function, as well as the biogenesis, of this supramolecular organization is still highly debated, with SCs deemed to maximise the efficiency of the electron transfer, to minimise ROS production, or to regulate the assembly or the respiratory complexes (Acín-Pérez et al., 2008; Milenkovic et al., 2017; Morán et al., 2012; Protasoni et al., 2020). Pathological mutations in the genes encoding CI subunits, as well as its assembly factors, cause a plethora of mitochondrial disorders characterised by CI deficiency, such as Leigh syndrome and Mitochondrial Encephalopathy, Lactic Acidosis and Stroke-like episodes (MELAS) (Fernandez-Vizarra & Zeviani, 2021). Complex I deficiencies are also causative of inherited neurodegeneration of the optic nerve such as Leber's hereditary optic neuropathy (LHON) and rarer forms of inherited optic neuropathies (Maresca & Carelli, 2021).

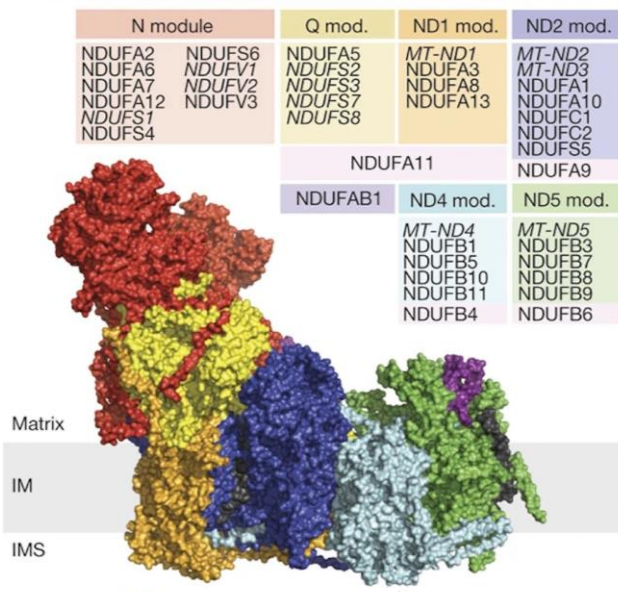

Figure 3 - Complex I modular architecture (Stroud et al., 2016).

1.4 LHON: Clinical and Biochemical Features

The first case LHON was described in 1871 by the German ophthalmologist Theodore Leber who, focusing on four families in which numerous cases of juvenile vision loss had been found with a higher incidence in males than females, hypothesized that the onset was due to mutations in the X chromosome (Erickson, 1972). Approximately 90% of LHON cases are caused by maternally inherited, homoplasmic, missense mutations in mtDNA-encoded CI core subunits, namely m.3460 G>A/*MT-ND1*, m.11778 G>A/*MT-ND4* and m.14484 T>C/*MT-ND6* (Chun & Rizzo, 2017; Vergani et al., 1995; Wallace & Lott, 2017). These mutations cause severe CI functional defect as the m.3460 G>A/*MT-ND1* mutation likely impairs the electron transfer to ubiquinone, whereas the remaining two affect the proton pumping (Fiedorczuk & Sazanov, 2018; Kampjut & Sazanov, 2020). In fact, the mutation on ND1 affect CI specific activity as this subunit, together with NDUFS2, NDUFS7 and ND3, is involved in the formation of the Q-binding site (Galemou Yoga et al., 2021). When ND1 is mutated, the binding of the semiquinone intermediate to this active site is highly compromised as indicated by the resistance to the inhibitory effect of rotenone (Carelli et al., 1997). On the contrary, mutation on ND4 and ND6 subunits do not decrease CI activity but may interfere with proton translocation and coupling of electron transfer to proton pumping (Brown et al., 2000; Carelli et al., 1997). All three LHON main mutations decrease CI-driven ATP synthesis rate confirming a CI functional deficiency (Baracca et al., 2005; Carelli et al., 2004). The defect on CI eventually leads to bioenergetic failure, ROS overproduction, as well as an increased propensity to apoptosis, which are all associated with RCGs' degeneration. However, the pathogenic mechanisms, albeit being

extensively investigated, has not been determined yet (Maresca & Carelli, 2021). Although all cells carry the mutations, their pathological effect is observed only in RGCs as they are more likely to be energy dependent and therefore vulnerable to respiratory chain defects and oxidative stress. RGCs susceptibility is related to their peculiar morphology and composition and change throughout their extension since myelin on the RGC axons is not uniformly distributed. In fact, in the posterior region of the lamina cribrosa the axon is myelinated and needs less energy for signal transmission, whereas in the anterior region the axon is unmyelinated, and action potential transmission depends only on ATP. Strikingly, the different composition of the axon leads to different mitochondrial distribution with more mitochondrial concentration in the unmyelinated region than in the myelinated one. Consequently, the anterior region is the most subject to damage in the presence of respiratory chain dysfunctions (Patrick Yu-Wai-Man, 2015).

LHON occurs with a prevalence of 1/30,000 and a frequency four times greater in male than female. Further, the age of onset in women is slightly higher, ranging from 19 to 55 years (mean 31.3 years) than in males, ranging 15 to 53 years (mean 24.3 years) (Man et al., 2003). The abovementioned mutations present with a ratio between male and female of 3:1 in the case of the *MT-ND1* mutation, 6:1 for the mutation in *MT-ND4*, and 8:1 for the mutation in *MT-ND6*, suggesting the influence of nDNA on disease onset. Specifically, X chromosome inactivation due to lyonization is deemed to be associated with the reduced disease onset in female, but to date there is no experimental evidence supporting this thesis (Hudson et al., 2007). Additionally, LHON onset is also associated with all the environmental factors that can induce oxidative stress such as smoking or alcohol abuse (Carelli et al., 2016). The onset of the disease occurs between the ages of 20 and 30 and is characterized by acute or subacute painless loss of vision in one eye, which in 2-4 months extends to the other eye. Only in 25% of cases the vision loss occurs simultaneously in both eyes and the persistence of unilateral loss of vision for a long period is rare (P. Yu-Wai-Man et al., 2014). Vision deterioration is severe but there may be a recovery of vision in the first year from disease onset depending on the mutation (Patrick Yu-Wai-Man, 2015).

1.4.1 LHON therapeutic strategies

LHON has been known for many years but there is still a lack of effective therapeutic treatment and so far, pharmaceutical therapy are essentially supportive. Gene therapy is still in clinical trial phase (Manickam et al., 2017). Pharmacological induction of mitochondrial biogenesis could be one of the possible strategies to limit LHON deleterious effects as mtDNA copy number, an index of

mitochondrial mass, is significantly higher in unaffected LHON patients (Bianco et al., 2017; C. Giordano et al., 2014). Interestingly, in vitro studies have found that tobacco toxins lead to a reduction in mtDNA copy number thus favouring the onset of the disease (L. Giordano et al., 2015). Among the drugs reported in literature, EPI-743, a new drug based on vitamin E, is exploited to treat vision loss triggered by oxidative stress (Chicani et al., 2013) and 70% of LHON patients treated with this drug have vision improvements without negative effects (Carelli et al., 2007). The block of ROS production and the prevention of respiratory chain uncoupling caused by treatment with Bendavia (MTP-131), a mitochondria-targeting peptide, suggest its use to target mitochondrial disfunction also in the case of optic atrophy (Manickam et al., 2017). In addition, a series of quinone short-chain antioxidant compounds are also undergoing clinical trials for the treatment of mitochondrial diseases (Patrick Yu-Wai-Man & Newman, 2017). This is in accordance with the hypothesis that the main factor influencing the pathology onset is chronic oxidative stress at the level of RGCs (Carelli et al., 2009). These compounds are supposed to improve the electron transport in the respiratory chain and to increase the endogenous antioxidant defences within cells as well. In particular, among these compounds several studies indicate idebenone as a potential drug capable of limiting the deleterious effects of mitochondrial optic neuropathies (Heitz et al., 2012). Encouraging results on its clinical efficacy came from a clinical trial and retrospective LHON patient's case series (Carelli et al., 2011a; Thomas Klopstock et al., 2011). As a consequence, idebenone was approved for LHON in 2015, under exceptional circumstances, by the European Medicine Agency (EMA; https://www.ema.europa.eu/en/medicines/human/EPAR/raxone), becoming the first and only approved therapy to date for a mitochondrial disease (Amore et al., 2021; Catarino et al., 2020). Moreover, administration of idebenone at early stages of the disease and for prolonged periods has been reported necessary to achieve a better vision recovery (Carelli et al., 2011a; Catarino et al., 2020).

1.4.2 Idebenone

Idebenone is a short-chain analogue of ubiquinone, having the same benzoquinone head as CoQ_{10} conjugated to a short lipophilic side chain formed by 10 carbon atoms with a terminal hydroxyl (Jaber & Polster, 2015). This modification allows it to be sufficiently hydrophilic to perform its functions (Heitz et al., 2012) (Fig.4).

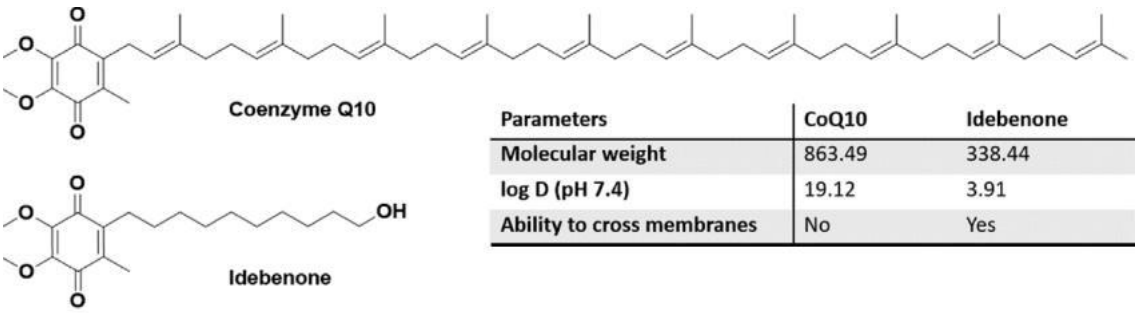

Parameters	CoQ10	Idebenone
Molecular weight	863.49	338.44
log D (pH 7.4)	19.12	3.91
Ability to cross membranes	No	Yes

Figure 4 - Comparison of the two quinones: CoQ10 and Idebenone (Varricchio et al., 2019).

Idebenone is exploited for the treatment of neurodegenerative mitochondrial pathologies as it can cross the blood-brain barrier and transports electrons from the cytosol to mitochondria carrying out its antioxidant role. In addition, several studies proposed idebenone as a drug able to restore the functionality of the respiratory chain through the transfer of electrons from cytoplasm directly to CIII when CI is impaired, as in the case of LHON (Giorgio et al., 2012; Haefeli et al., 2011). However, the positive effect of idebenone has not been clearly defined yet probably depending on its redox state. Indeed, when reduced, it has an antioxidant role and transports electrons maintaining the mitochondrial ATP synthesis, whereas in its oxidized form, idebenone probably binds the Q-binding site of CI, inhibiting its activity and causing the overproduction of superoxide and the consequent oxidative stress increase (Varricchio et al., 2020). CI-idebenone interaction, therefore, might aggravate a situation already compromised by CI mutations leading to undesired effects. Hence, the reduction of idebenone is essential for its therapeutic effect. There are numerous known enzymes capable of reducing idebenone but several studies have underlined the high affinity of idebenone to NAD(P)H:quinone oxidoreductases 1 (NQO1) identified as responsible for the pharmacological activity of idebenone (Haefeli et al., 2011).

1.4.3 NQO1: characteristic and function

NQO1 dehydrogenase is a cytosolic homodimeric flavoprotein catalysing the complete two-electron reduction of quinones to hydroquinones, thereby avoiding the generation of semiquinol intermediates. The enzyme requires NADH or NADPH as electron donor and FAD as the enzymatic prosthetic group. Specifically, FAD is reduced by NAD(P)H to $FADH_2$ and the oxidised cofactor $NAD(P)^+$ leaves the active site enabling the quinone to enter and be reduced by $FADH_2$ (Haefeli et al., 2011). NQO1 activity is inhibited by dicumarol which competes for the binding site of NAD(P)H preventing the transfer of electrons to FAD (Asher et al., 2006). Two-electron reduction bypasses the formation of semiquinones which may interact with molecular oxygen to generate aggressive ROS, *i.e.*

superoxide ($O_2^{\cdot-}$), causing oxidative stress and cellular damage (Dinkova-Kostova & Talalay, 2010; Ross & Siegel, 2004). In addition, reduced forms of quinones may show antioxidant activities making the reduction of quinones by NQO1 an important detoxification system within cells. Nevertheless, the antioxidant role of hydroquinones is highly related to theirs physicochemical features and bioactivation of some quinones by NQO1 can even lead to formation of pro-oxidant hydroquinones increasing the oxidative stress (Fig.5) (Ross & Siegel, 2017). NQO1-mediated reduction of some quinones also increases mitochondrial bioenergetic efficiency as some hydroquinones can enter mitochondria, transfer electron to CIII contributing to the generation of the proton gradient necessary for ATP synthesis. Therefore, this mechanism can be exploited to restore energy levels in CI deficiencies. Considering what has been highlighted so far, the right choice of quinone as NQO1 substrate is fundamental to have a beneficial effect for the treatment in mitochondrial disorders and avoid toxicity. Hence, thorough studies have analysed different short chain quinones and correlated their NQO1-mediated biological effect to their physicochemical properties (Erb et al., 2012; Haefeli et al., 2011). ATP rescue ability of short chain quinones in CI deficient conditions is highly related to lipophilicity (logD) rather than being linked to their structural features or Q moiety redox potential (Erb et al., 2012; Haefeli et al., 2011). Indeed, the compound has to be sufficiently hydrophilic to be reduced by NOQ1 in the cytoplasm and concomitantly lipophilic to localize into the IMM and transfer its electrons to CIII. CoQ_{10} is extremely hydrophobic (LogD = 19.12) and therefore it is found only into membranes and cannot be reduced by NQO1 in the cytoplasm. On the other hand, QS-10 can be reduced efficiently by NQO1, but being more hydrophilic than other quinones (LogD = 1.18) does not show the bioenergetic rescue in CI deficient models (Haefeli et al., 2011). Idebenone and CoQ_1 show optimal LogD values, 3.91 and 2.14 respectively, and therefore are efficiently reduced by NQO1 and perform ATP rescue ability. Lipophilicity influences the antioxidant property of hydroquinone compounds as well. In fact, in order to prevent lipid peroxidation quinones have to be sufficiently lipophilic to localize in the cellular membranes. In addition, modification on the alkylic side chain must be considered since it can influence the biological activity and pro-oxidant ability. CoQ_1 showed substantial oxidative damage when compared to idebenone in diverse cell models causing high toxicity. Among the tested quinone compounds, idebenone has all the characteristic to allow the energetic rescue in CI deficient models and prevent oxidative damage. These studies assessed the efficacy of short chain quinones in cells treated with rotenone to inhibit CI, but their effects on cells bearing CI pathogenic mutations have not been dissected yet. Additionally, NQO1 involvement in the putative NQO1-idebenone-CIII axis, as well as its ability to rescue the energy deficit in LHON cell lines, have not been fully demonstrated.

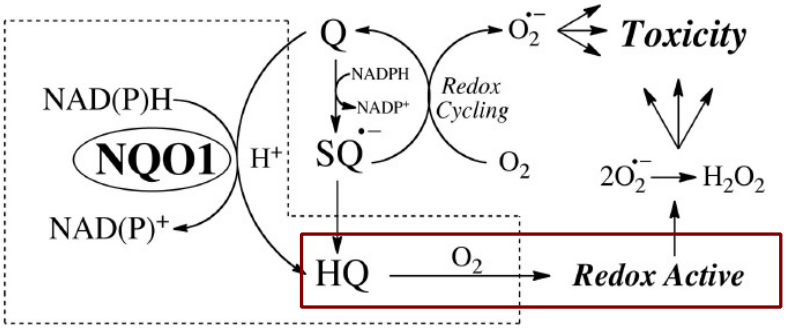

Figure 5 - Antioxidant activity of NQO1 (Ross & Siegel, 2017) *adapted.*

1.4.4 Regulation of the expression of NQO1

NQO1 expression is regulated by nuclear factor E2-related protein (Nrf2) which interacts with the antioxidant response element (ARE) region, a specific nucleotide sequence located in promoters of genes encoding cytoprotective enzymes. Under basal conditions, Nrf2 associates with its cytosolic inhibitor Keap1 and Cul3 protein forming the Cullin3-based E3-ligase ubiquitination complex which mediates Nrf2 ubiquitination and the consequent proteasomal degradation (Giudice & Montella, 2006; Tong et al., 2006). Under stress conditions, such as oxidative stress, ARE inducers' electrophilic motifs interact with Keap1 -SH groups determining the dissociation of the Keap1-Cul3 complex from the Nrf2 factor which can now migrate to the nucleus where it activates the transcription of the target genes (Dinkova-Kostova & Talalay, 2010; Zhang, 2006). The increase of NQO1 expression *via* Nrf2 pathway can also be mediated by natural or synthetic compounds such as sulforaphane, resveratrol or dimethyl fumarate (Hamed et al., 2016). In particular, sulforaphane is an isothiocyanate belonging to aliphatic hydrocarbons with a sulphur atom and it is possible to find it in cruciferous plants such as broccoli and cabbage (Dinkova-Kostova et al., 2004). It has a protective effect against various types of tumours, cardiovascular diseases and osteoporosis and, importantly, it is a well-tolerated substance with no reported adverse reactions (Fimognari et al., 2008; Vanduchova et al., 2019). Resveratrol is a non-flavonoid phenolic compound particularly abundant in grape skin and its anticancer, anti-inflammatory and antioxidant properties have made it of great interest in the therapeutic field (Stojanović et al., 2001). Finally, dimethyl fumarate (DMF) is a synthetic molecule, corresponding to the methyl ester of fumaric acid which is used both in the industrial and medical fields. Unlike the previous compounds, DMF can cause side effects such as redness of the skin, hot flashes, gastrointestinal disturbances such as diarrhea, nausea and abdominal pain. In this case, the dosage is fundamental as it is potentially harmful to humans at high dosages, whereas it can constitute

an effective pharmacological therapy at low dosages (Ropper, 2012). DMF is currently exploited in the therapeutic treatment of psoriasis and multiple sclerosis (Kappos et al., 2014).

1.5 Dominant optic neuropathy: clinical and molecular features

Dominant Optic Atrophy (DOA) is a mitochondrial neurodegenerative disease first described in 1959 (KJER, 1959). It is the most frequent form of hereditary optic neuropathy with a prevalence ranging from 1:12 000 to 1:50 000 (Patrick Yu-Wai-Man & Chinnery, 2013) with incomplete penetrance (Amati-Bonneau et al., 2009). DOA patients show a progressive and painless loss of vision between 10 and 20 years due to the optic nerve bilateral degeneration (Barboni et al., 2010). The disease selectively affects RGCs with the damage usually moderate but irreversible and variable between and within the same families (Votruba et al., 1998). In 60 - 80% of patients with DOA, the onset is caused by a mutation in the optic atrophy 1 (*OPA1*) nuclear gene, consisting of 30 exons on chromosome 3q28-q29 (Delettre et al., 2001). This gene encodes a high molecular weight GTPase of the dynamin family characterized by a mitochondrial targeting sequence (MTS), followed by transmembrane domains, coiled coil domains, and three highly conserved domains, namely GTPase, central or dynamin-like, and GTPase effector domain (GED) (Fig.6).

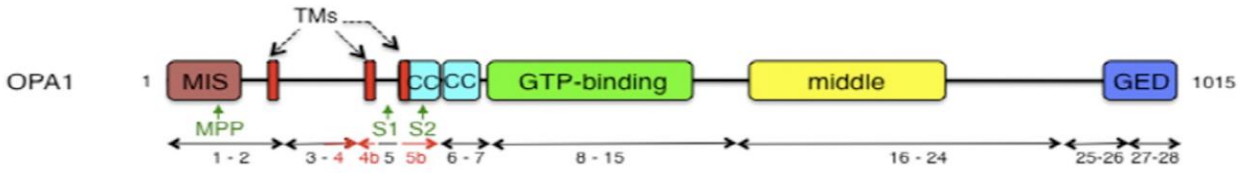

Figure 6 - Schematic representation of the OPA1 protein (Bertholet et al., 2016)

In humans, OPA1 has 8 different isoforms deriving from the alternative splicing exon 4, 4b and 5b (Fig.7) (Del Dotto, Fogazza, Carelli, et al., 2018). The MTS placed at the N-terminus is inserted into IMM and enters the matrix, where it is cut off by the specific mitochondrial processing peptidase. However, the transfer to the matrix is blocked by the presence of a hydrophobic region anchoring the protein to the membrane facing the intermembrane space. Through this mitochondrial protein import process “long” isoforms of the protein (L-OPA1) are generated. OPA1 can then undergo a second stage of proteolytic maturation at two cleavage sites, namely S1 and S2, located respectively in exon 5 and 5b. This proteolytic cleavage determines the detachment of the "short" isoforms of the protein (S-OPA1), lacking the trans-membrane domain and therefore soluble in the intermembrane space (Fig. 7) (Del Dotto et al., 2017; Del Dotto, Fogazza, Lenaers, et al., 2018).

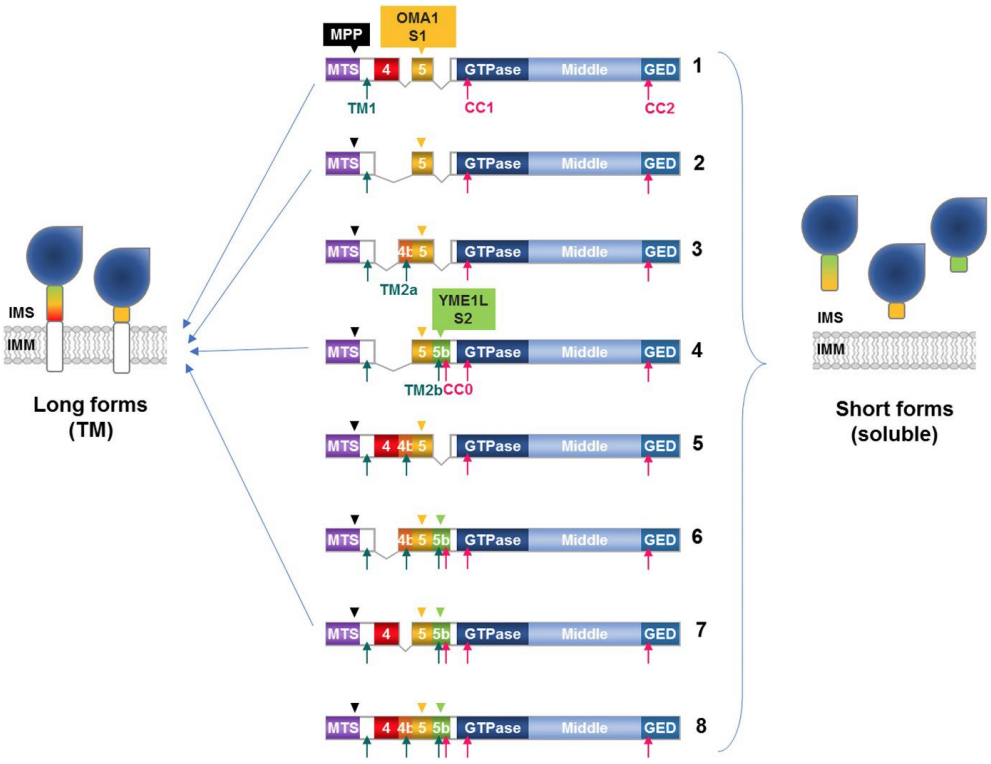

Figure 7 - Image showing the domains characterizing OPA1 protein including exons 4, 4b and 5b which by alternative splicing generate the eight isoforms of OPA1. The cutting sites S1 and S2 define the processing of long forms into short forms (Del Dotto, Fogazza, Carelli, et al., 2018)

The majority of missense and frameshift mutations are found either in the GTPase domain or in the GED domain causing the production of a truncated protein with a consequent loss of approximately half of the protein. This condition is called haploinsufficiency and is the main cause of the onset of DOA (Patrick Yu-Wai-Man, 2015). In addition, patients with multisystem syndromes associated with dominant-negative (DN) mutations in GTPase domain causing a severe form of DOA, namely DOA "plus", have been described. These severe forms occur mainly at a young age and involves sensorineural deafness, ataxia, myopathy, chronic external ophthalmoplegia and peripheral neuropathy in addition to optic atrophy (Amati-Bonneau et al., 2009).

1.6 Functions of OPA1

Numerous studies have clearly shown that OPA1 is a multifunctional protein being involved in several important mitochondrial functions such as mitochondrial network fusion, energy metabolism, mitochondrial genome stability, as well as cristae morphology and apoptosis (Del Dotto, Fogazza, Lenaers, et al., 2018).

1.6.1 Mitochondrial dynamics

OPA1 catalyses the fusion of the inner mitochondrial membrane in the contest of mitochondrial reticulum fusion and fission (van der Bliek et al., 2013). The former allows functional complementation between mitochondria *via* the exchange of proteins and mtDNA (L. Yang et al., 2015), thus playing a protective role in stress conditions, favouring the hyperfusion of the network and the concomitant increase in energy efficiency [Gomes et al., 2011]. Conversely, fission preserves a proper mitochondrial architecture and mtDNA distribution by fragmenting the network (Ishihara et al., 2015), as well as promoting the mitophagy-dependent clearance of damaged mitochondria (Sauvanet et al., 2012). The network morphology under physiological conditions is due to a dynamic balance of the two processes and depends on cell type and metabolic state. Mitochondrial reticulum dynamics are also mediated by other proteins of the GTPases family, namely mitofusins (Mfn1, Mfn2), involved in the fusion of the outer mitochondrial membrane, and the Dynamin Related Protein 1 (DRP1), which mediates mitochondrial fission (Ge et al., 2020). OPA1 involvement in fusion has been dissected in several studies showing that the absence of OPA1 determines the fragmentation of the mitochondrial network underlining its fusogenic activity (Olichon et al., 2003; Song et al., 2007). Furthermore, proper balance between the long and short forms is crucial to guarantee the dynamism of the mitochondrial reticulum providing a high degree of flexibility that allows a better adaptation to cellular needs (Del Dotto et al., 2017). The fundamental importance of the integrity of the GTPase domain was also highlighted because changes in the amino acids, directly or indirectly involved in the binding of GTP, determine the blocking of the fusion and the complete fragmentation of the mitochondrial network (Tadato et al., 2010).

1.6.2 Mitochondrial metabolism

OPA1 is also involved in mitochondrial metabolism. David Chen and colleagues characterized the biochemical alterations of cells lacking OPA1, highlighting a severe reduction in cellular respiration (Chen et al., 2005). It was initially speculated that this respiratory deficit was due to the ultrastructure disorganization of IMM in cells lacking OPA1 (Griparic et al., 2004; Wu et al., 2019). Strikingly, OPA1 depletion causes a decrease in the levels of some subunits of the respiratory complexes (Bertholet et al., 2016). In accordance, immunoprecipitation experiments indicated that OPA1 interacts with CI, CII and CIII, probably stabilizing them (Cogliati et al., 2013; Zanna et al., 2008). Moreover, in patient-derived fibroblasts bearing the R445H missense mutation in OPA1, a significant decrease in ATP synthesis compared to control has been described (Amati-Bonneau et al., 2005).

Zanna *et al*. described an energy defect in cells with various nonsense mutations in OPA1. Specifically, these fibroblasts showed reduced OPA1 expression accompanied by decreased CI-driven ATP synthesis rate. Furthermore, when the mutated fibroblasts were grown in a medium in which glucose had been replaced by galactose, forcing them to use oxidative metabolism, ATP content decreased compared to controls (Zanna et al., 2008). A final conclusive indication of the role of OPA1 in preserving OXPHOS efficiency derives from experiments performed in mouse models with severe defects in the respiratory chain caused by mutations in a nuclear-encoded CI subunit. The crossing of these mice with those overexpressing OPA1 induced a significant increase in CI activity and a marked improvement in muscle performance (Civiletto et al., 2015). Altogether these lines of evidence support the important role of OPA1 in cellular energy metabolism, in addition to reticulum morphology maintenance.

1.6.3 Maintenance of mtDNA

Multiple mtDNA deletions in muscles of patients with OPA1 mutations were reported, indicating the essential role of OPA1 in mtDNA maintenance (Amati-Bonneau et al., 2008; Hudson et al., 2008). In addition, mtDNA depletions were also observed in leukocytes of patients suffering from DOA (Kim et al., 2005). mtDNA deletions result in mitochondrial genetic material loss and are caused by mutations in genes encoding proteins involved in mtDNA duplication, as gamma polymerase, or stabilization, as twinkle helicase. The involvement of OPA1 in the binding of the nucleoid to the IMM was speculated. This hypothesis was then supported by analysis in HeLa cell lines where the specific silencing of OPA1 isoforms containing exon 4b caused a marked reduction in mtDNA content and a change in nucleoid distribution as well. In these cells, a peptide consisting only of OPA1 N-terminus containing either exon 4 or 4b was expressed and a ChiP experiment revealed that only the peptide containing the exon 4b co-immunoprecipitated with the mtDNA. This outcome supports the idea of the interaction between nucleoids and OPA1, most likely through the hydrophobic sequence of exon 4b which forms a folding facing the matrix compartment (Elachouri et al., 2011).

1.6.4 Structure of cristae

The IMM is both structurally and functionally subdivided into the inner boundary membrane (IBM), closer to the OMM, and cristae, representing membrane domains protruding into the matrix. These sub-compartments, which have different composition, are linked by tight and tubular invaginations

named cristae junctions (CJs). In addition, between CJs and IBM there are IMM regions in contact with the OMM, called contact sites (Freya & Mannellab, 2000). Crista morphology can be influenced by different factors such as $\Delta\psi$, lipid and protein composition (Ghochani et al., 2010), and OPA1 presence as well. Importantly, cristae are pivotal for mitochondrial bioenergetic efficiency as they increase significantly the IMM surface to harbor OXPHOS complexes (Gilkerson et al., 2003). Furthermore, multiproteic complex called mitochondrial contact site and cristae organizing system (MICOS) which acts as a bridge between the two mitochondrial membranes is involved in crista structure formation and maintenance. In yeast, MICOS includes 6 subunits: Mic10, Mic12, Mic19, Mic26, Mic27 and Mic60 (Pfanner et al., 2014), while in mammals its composition become more intricate with 9 subunits identified so far (Guarani et al., 2015). This complex interacts also with the Sorting Assembly Machinery (SAM), involved in the insertion of proteins with a β-barrel structure into the OMM (Pfanner et al., 2014). MICOS localizes in the CJs and its lack compromises cristae organization and affecting the mitochondrial respiratory chain (JR et al., 2015). OPA1 interacts with MICOS and Mic60 loss causes a decrease in OPA1 expression and other proteins involved in the processes of fission and fusion affecting the mitochondrial morphology (Ding et al., 2015). OPA1 is important in apoptosis regulation as evidenced by the resistance to apoptosis observed in mouse models when it was overexpressed (Cipolat et al., 2006; Costa et al., 2010; Merkwirth et al., 2008; Varanita et al., 2015). Conversely, OPA1 loss causes crista enlargement with the consequent release of cyt *c* in the cytoplasm and apoptosis activation (Cipolat et al., 2006; Frezza et al., 2006).

1.7 DOA: therapeutic strategies

1.7.1 Gene therapy

As for the LHON, even for DOA no cure is available. However, since DOA is a monogenetic pathology, it appears to be an excellent candidate for gene therapy. In fact, the expression of wild type OPA1 at the optic nerve level could allow recovery, especially in patients bearing mutations associated with haploinsufficiency, while in cases of mutations for which a dominant negative effect has been proposed the situation is more intricate (Del Dotto, Fogazza, Lenaers, et al., 2018). Considering the easy accessibility of the eye and the fact that it can be effectively monitored by non-invasive techniques, several clinical trials have been conducted using adeno-associated viral vectors (AAV) for the treatment of genetic pathologies affecting retinal cells. The intravitreal injection of AAV vectors is an effective and relatively safe procedure, despite the fact that there is a risk of an inflammatory response following the surgical operation (Petit et al., 2016). However, in this case, it

is necessary not only to express the correct amount of OPA1 but also the most appropriate isoform to ensure a balance between long and short forms and rescue the clinical phenotype given by a particular mutation. Furthermore, in the case of missense mutations associated with syndromic forms of DOA, increasing the levels of OPA1 expression may not be sufficient for an improvement in the clinical phenotype, although a possible beneficial effect cannot be excluded (Del Dotto, Fogazza, Lenaers, et al., 2018). For this type of pathology, a strategy that uses CRISPR-Cas9 technology, capable of precisely removing the pathogenic alleles and replacing them, would probably be more effective. This approach could be applied either by replacing the altered cells with ocular tissue derived from induced pluripotent stem cells (iPSCs) in which the mutation has been corrected, or by editing the gene directly in cells of the retina through the release of AAV2 containing CRISPR-Cas9 (Hung et al., 2016). Alternatively, gene therapy strategies have been developed to reduce retinal ganglion cell degeneration and treat a wide range of diseases including DOA as well as the more severe phenotypes associated with OPA1 missense mutations. These are approaches that aim to inhibit apoptosis, for example by increasing the expression of X-linked inhibitor of apoptosis (XIAP) or to induce neuronal survival through the overexpression on the one hand of growth factors with neuroprotective function, on the other hand of enzymes and transcription factors that result in an antioxidant effect (Petit et al., 2016).

1.7.2 Pharmacological Treatment

Increasing in-depth knowledge on the functions and pathological alterations of OPA1 and the mechanisms controlling biogenesis and mitochondrial signaling, has led to propose different pharmacological strategies for DOA treatment (Viscomi et al., 2015). A first hypothesis is to directly stimulate the expression and activity of OPA1 or to act on the other proteins involved in the regulation of mitochondrial dynamics. To date, however, components of the fusion and fission machinery have not been considered targets of pharmacological therapies yet. Another strategy is to try to mitigate the mitochondrial dysfunctions associated with OPA1 mutations. In this sense, a first approach is to use electron donors and acceptors to overcome the impairment of the respiratory chain, especially in the case of defects at CI level (P. Yu-Wai-Man et al., 2014). Indeed, a reduction of CI-driven ATP synthesis rate was observed in fibroblasts obtained from DOA patients, and therefore there is the possibility that ubiquinone analogues, such as idebenone and EPI-743, can improve the energy efficiency of mutated cells (P. Yu-Wai-Man et al., 2014; Zanna et al., 2008). This therapeutic

approach was carried out in a pilot study on seven DOA patients, who were administered idebenone, with promising results. After a treatment of at least 6 months, five of these patients showed some improvement and increase in vision, however the efficacy is limited to cases in which the therapy started in the early stages of the disease, when the visual acuity was not yet severely impaired (Barboni et al., 2013). It is well known that alterations at the level of respiratory chain complexes generally induce an increase in ROS production which can damage cell structures (Viscomi et al., 2015). Indeed, in DOA patients-derived fibroblasts levels of some antioxidant enzymes are perturbed reasoning the use of antioxidants such as lipoic acid, vitamin C and E to reduce the accumulation of these molecules (Millet et al., 2016; Viscomi et al., 2015). Considering that mutations in OPA1 are associated with mtDNA instability and alterations in the mitochondrial quality control, which eventually lead to the accumulation of dysfunctional and damaged organelles, another possible therapeutic strategy consists in promoting an increase in the number of mitochondria or the expression of respiratory complexes (Del Dotto, Fogazza, Lenaers, et al., 2018; Kane et al., 2017). Hence, pharmacologically activating mitochondrial biogenesis, possibly in combination with proper regulation of mitophagy, could be a promising strategy.

1.8 Models for the study of mutations in OPA1

1.8.1 Yeast Models

Saccharomyces cerevisiae was extensively used as a model for the study of DOA (Jones & Fangman, 1992). *Mgm1* is the orthologous gene of OPA1 in yeast cells presenting the same OPA1 functional domains, but low conservation of the aminoacidic sequence. Therefore, only a limited number of human mutations can be introduced and studied in yeast OPA1. Mgm1 ablation impairs OXPHOS, cristae biogenesis and cytochrome *c* levels (Amutha et al., 2004). Chimeric proteins containing Mgm1 N-terminal regions at various length fused to OPA1 catalytic domain have been generated (Nolli et al., 2015). All chimeras exhibited a growth defect under oxidative conditions as the null mutant, except for CHIM3 chimera which was able to restore the growth in Mgm1-null mutants. Specifically, the MTS, the transmembrane domain and the cleavage region derive from Mgm1, whereas the GTPase, central and GED domains derive from OPA1. Three OPA1 missense mutations have been introduced in this chimera: the I382M, a phenotypic modifier (Bonifert et al., 2014); R445H,

associated with DOA plus (Amati-Bonneau et al., 2003); and K468E, associated with DOA (Pesch et al., 2001). All haploid strains carrying the mutations, except for I382M, presented the complete mtDNA loss with inability of growing under oxidative conditions, absence of tubular mitochondria, and presence of fragmented or giant mitochondria. On the contrary, I382M mutation complemented Mgm1 ablation but to a lesser extent than the wild type, as demonstrated by higher frequency of *petite* yeasts and low levels of mtDNA. Petite yeasts are unable to grow on nonfermentable carbon sources, such as glycerol or ethanol, due to mitochondrial dysfunction. When grown in fermentable carbon sources (such as glucose), they form small anaerobic colonies. Indeed, I382M mutation is often asymptomatic but becomes pathogenic in association with other mutations (Bonifert et al., 2014; Carelli, Maresca, et al., 2015). The major advantage of using yeast is the chance to perform short-term and low-cost screening to identify molecules for the wild-type phenotype rescue.

1.8.2 Cell models

The most used cell model is represented by cells derived directly from patients, typically fibroblasts and lymphoblasts. In fact, numerous studies have been performed in patient-derived fibroblasts carrying OPA1 mutations (Agier et al., 2012; Amati-Bonneau et al., 2005; Chevrollier et al., 2008; Zanna et al., 2008). However, since the mutations are heterozygous the phenotype is often poorly evident. In addition, it is particularly difficult to obtain skin biopsies from patients and their culturing is a long and time-consuming process. Finally, the maintenance of patient-derived fibroblasts is limited as they undergo senescence. To overcome these drawbacks, our laboratory decided to exploit OPA1-null murine embryonic fibroblasts (MEF $OPA1^{-/-}$) (Davies et al., 2007). The wild-type human OPA1 isoform 1 (ISO1) or with different missense mutations associated with DOA or "plus" DOA (R445H, D603H) was introduced in these cells. Contrary to fibroblasts these models express only the mutated protein. Three mutations in the GTPase domain (c.1146A> G, p.I382M in exon 12; c.1316G> T, p.G439V in exon 14; c.1334G> A, p.R445H in exon 14) and a mutation in the dynamin domain (c.1807G> A, p.D603H in exon 18) have been identified in patients and consequently used in these cell models.

All these cell lines were biochemically characterized in our laboratory to verify their ability to adequately represent the pathology (Del Dotto, Fogazza, Musiani, et al., 2018). OPA1 expression was similar in MEFs when compared to control ($OPA1^{+/+}$), whereas in patient-derived fibroblasts OPA1 expression decreased for all mutations except for G439V mutation in which OPA1 levels increased. In the presence of glucose, cultured cells produce ATP through glycolysis and only in minimal part

from the oxidation of pyruvate. When glucose is replaced by galactose (DMEM-galactose), the glycolytic pathway becomes less efficient. In fact, galactose has to be converted into galactose-1-phosphate, then into glucose-1-phosphate before entering the glycolytic pathway as glucose-6-phosphate. Cells incubated in galactose are therefore forced to rely on OXPHOS to produce sufficient ATP to survive (Robinson, 1996). This change generally does not affect cell viability, unless there are mitochondrial defects, and it is used for revealing OXPHOS impairment. In DMEM-glucose, R445H, G439V and OPA1$^{-/-}$ MEF cell lines grew slower than isogenic controls, whereas in DMEM-galactose the same mutant cell lines showed a growth blockage. Conversely, D603H cells grew similarly to the isogenic control when cultured in DMEM-glucose and showed only a decrease in cellular growth in DMEM-galactose. The decrease in ATP content was evident only in G439V and R445H MEFs when compared to the isogenic control. G439V and R445H lines showed a significant decrease in mtDNA content, whereas ISO1, I382M and D603H MEFs behaved like the WT. Regarding patient-derived fibroblasts, filamentous mitochondrial network was observed in OPA1 WT cells and in those bearing the I382M mutation. On the other hand, R445H, G439V and D603H mutated lines showed an increase in the percentage of cells with intermediate and fragmented reticulum. In DMEM-galactose the morphology of OPA1 WT patient-derived fibroblasts did not change, whereas in the mutated ones the percentage of cells with fragmented mitochondria increased. ATP content was drastically reduced in patient-derived fibroblasts incubation in DMEM-galactose. Finally, mtDNA copy number in patient-derived fibroblasts with I382M and D603H mutations was similar to the isogenic control, whereas a variation was observed in fibroblasts with R445H and G439V mutations with significant decrease and increase, respectively (Del Dotto, Fogazza, Musiani, et al., 2018).

2. AIMS

Vision loss is a common feature of mitochondrial disorders, frequently characterized by complex phenotypes with different degrees of severity, possibly encompassing multisystem clinical manifestations. Selective degeneration of retinal ganglion cells (RGCs) is a hallmark of Leber's Hereditary Optic Neuropathy (LHON) and Dominant Optic Atrophy (DOA) (Chun & Rizzo, 2017), two well-known mitochondriopathies and commonly but not exclusively driven by mitochondrial subunits of respiratory complex I and OPA1 mutations respectively (Brown & Wallace, 1994; Lenaers et al., 2012). With no cure currently available and gene therapy under investigation (Amore et al., 2021), it has clearly become imperative to define new therapeutic strategies to hinder the onset and clinical symptoms manifestations.

Three main missense mutations are responsible for the majority of LHON cases, namely m.3460 G>A/MT-ND1, m.11778 G>A/MT-ND4, and m.14484 T>C/MT-ND6. In LHON patients, RGCs, whose axons form the optic nerve, degenerate due to OXPHOS impairment and chronic oxidative stress eventually leading to apoptosis. LHON lacks effective therapy and the only approved supportive treatment is the antioxidant idebenone, a ubiquinone short chain analogue. The positive effect of this compound is highly connected to its redox status. Indeed, in its oxidized form, idebenone inhibits CI causing superoxide overproduction, whereas, when reduced, it acts as an antioxidant and transports electrons to respiratory chain complex III maintaining the mitochondrial ATP synthesis. Idebenone reduction is catalysed by the cytosolic dehydrogenase NAD(P)H:quinone oxidoreductase 1 (NQO1) (Haefeli et al., 2011). However, the direct involvement of NQO1-idebenone synergism in the treatment of mitochondrial optic neuropathies is not clear yet. To address this issue, we sought to evaluate the efficacy of idebenone treatment on LHON *in vitro* models. Particularly, we characterized control and LHON mutated cells overexpressing or not NQO1 to assess the effect of idebenone on mitochondrial physiology by measuring oxygen consumption, ATP synthesis, cell viability, and ROS production. Furthermore, we analysed differently idebenone responsive patient-derived fibroblasts to prove a correlation between NQO1 expression and idebenone treatment efficacy. Finally, we tested the capacity of dimethyl fumarate, a likely NQO1 expression inducer to promote the cytoprotective effect associated with reduced idebenone in CI deficient LHON cell lines.

DOA is a neurodegenerative disease associated with *OPA1* mutations encoding a dynamin related GTPase processed in eight isoforms, either long or short, each one involved in mitochondrial dynamics, cristae and mtDNA maintenance, as well as bioenergetics. Protein-truncating mutations are causative of DOA, whereas missense variants in the GTPase domain are responsible for the syndromic multisystem disorder known as DOA plus. Although currently there is no therapy for

patients, off-label treatment with idebenone appears to stimulate the stabilization/recovery of visual acuity (Romagnoli et al., 2020). However, due to the complex effects of *OPA1* mutations on mitochondrial physiology, the discover of new potential drugs that can act at different levels of the biochemical defects associated with DOA is required. This prompted us to investigate the beneficial impact of known molecules we repurposed as "OPA1-Rescuing Molecules" (ORMs) to rescue DOA cellular defects. We firstly took advantage of OPA1-defective yeast strain to screen libraries of approved or highly heterogenous compounds, identifying six promising compounds. We, then, proceeded to test their efficacy in murine embryonic fibroblasts (MEFs) and patient-derived fibroblasts. Specifically, MEFs were knocked out for the murine *Opa1* isoform 1 and the correspondent human wild type gene (ISO1) or mutated genes (D603H, R445H) were overexpressed. To determine the efficacy of the selected compounds we focused on mitochondrial bioenergetics, network morphology, and cellular autophagy.

3. MATERIALS AND METHODS

3.1 Cell cultures: cybrids, murine embryonic fibroblasts (MEFs) and human fibroblasts

For the first part of this study, two cybrid lines were used: a control line (H42A) and a line harboring the m.3460G>A LHON mutation (RJ206), both generated as previously described (M. P. King & Attardi, 1996). Human fibroblasts were collected from three healthy donors and six affected patients, after informed consent, bearing the m.3460 G>A/*MT-ND1* or m.11778 G>A/*MT-ND4* mutations. For the second part, three murine embryonic fibroblasts (MEFs) were used (ISO1, D603H, R445H), generated as previously described (Del Dotto, Fogazza, Musiani, et al., 2018). Each cell line was knocked out for the murine *Opa1* isoform 1 gene and the correspondent human orthologue gene (wild type or mutated) was overexpressed, obtaining a cell line overexpressing the human ISO1 OPA1 isoform or the ISO1 D603H isoform or the ISO1 R445H. In addition, human fibroblasts were collected, following informed consent, from five healthy donors and two DOA patients each carrying one of the two mutations considered.Cybrids, MEFs and human fibroblasts were grown in Dulbecco's Modified Eagle Medium containing 25 mM glucose (DMEM, Gibco, Life Technologies) supplemented with 10% foetal bovine serum (FBS, South America, Gibco, Life Technologies), 2 mM L-glutamine, 100 units/mL penicillin and 100 µg/mL streptomycin, in an incubator with a humidified atmosphere of 5% CO_2 at 37 °C. This growth medium was called DMEM-glucose.

3.2 Overespression of NQO1

Control cybrids (H42A, also indicated as WT) and LHON cybrids (RJ206 carrying the m.3460 G>A/*MT-ND1* mutation) were used to generate four stable cell lines overexpressing or not NQO1 human isoform 1. Lentivirus particles containing a pLenti-C-Myc-DDK-P2A-Puro plasmid empty (OriGene, PS100092) or with human NQO1 isoform 1 (OriGene, RC200620L3) were prepared using the Lentiviral Packaging Kit (OriGene, TR30037) following manufacturer's instructions and used to infect the cybrid cell lines. Infected cells were selected using 0.25 µg/mL puromycin for the control line and 0.75 µg/mL for LHON cybrids. Subsequently, a clonal selection was performed and the overexpression of NQO1 in the individual clones was evaluated by Western blot. For each cell line, three clones with higher NQO1 overexpression were pooled together. Three clones were also pooled for the mock cell lines.

3.3 Measurement of the rate of oxygen consumption in intact cells

Oxygen consumption rate (OCR) was measured using the Seahorse XFe24 Extracellular Flux Analyzer. Cells were seeded in DMEM-glucose ($3x10^4$ cells/well for fibroblasts, $2.5x10^4$ and $3x10^4$ cells/well for H42A and RJ206 cybrids respectively) into XFe24 cell culture plate and allowed to attach for 24 h. The following day 750 µL of Seahorse medium (DMEM not buffered supplemented with 1 mM L-glutamine, 5 mM Na^+ pyruvate, 10 mM glucose) were added to each well of the plate, then the medium was aspirated. One additional wash with 1 mL of Seahorse medium was performed and 525 µL of Seahorse medium with 10 µM Idebenone or the corresponding volume of vehicle (DMSO) were added. Cells were incubated for one hour at 37 °C in a CO_2-free incubator. During the incubation, the cartridge was loaded with the inhibitors (oligomycin, rotenone or antimycin) or the uncoupler (carbonyl cyanide-p-trifluoromethoxyphenylhydrazone, FCCP) to inhibit or activate oxidative phosphorylation. After incubation, OCR measurements were performed starting from basal conditions (without any addition), then oligomycin (1 µM), FCCP (0.5 µM for cybrids, 1 µM for fibroblasts), rotenone (1 µM) and antimycin A (1 µM) were sequentially added to each well. At the end of the experiment, sulforodamine B assay (SRB) was performed (see below). Data were normalized to SRB absorbance and expressed as pmoles of O_2 per minute per protein content.

3.4 SRB assay

SRB assay was used to evaluate the protein content since this is related to the number of cells in a well (Porcelli et al., 2008). SRB assay was used for cell viability assays and for protein content measurements as follow. LHON Cybrids ($3x10^4$ cells/well) and DOA MEFs ($10x10^3$ cells/well) were seeded in a 24 multiwells in DMEM-glucose. After 24 hours, cells were washed with PBS before the specific treatment. In particular, cybrids were incubated with 10 µM Idebenone or the same volume of DMSO in DMEM supplemented with 10 mM glucose, 5 mM Na^+ pyruvate and 1 mM L-glutamine. MEFs were incubated in glucose-free DMEM supplemented with 5 mM galactose, 2 mM L-glutamine, 5 mM Na^+ pyruvate and 5% FBS (DMEM-galactose) or in DMEM-galactose with ORMs at the concentration (Table 1). After 48 hours of incubation, cells were fixed with 50 % trichloroacetic acid (TCA) for 1 hour and then washed with BDW 5 times. When the plates were dried, cells were stained with 0,4% SRB in 1% acetic acid for 30 minutes, subsequently they were washed with acetic acid 4 times. SRB was solubilized in 10 mM Tris-HCl buffer pH 10.4, and the absorbance was measured. SRB absorbance in the absence of idebenone corresponds to 100% of viable cells.

SRB absorbance was measured at 540 nm using a plate reader (VICTOR^3 Multilabel Plate Counter). For each experiment two wells without cells were fixed and stained with SRB and used as blank. Data were normalized to SRB absorbance measured in DMEM-glucose (T_0) and expressed as percentage.

ORMs	Chemical name	Concentration (μM)
ORM0	Benzbromarone	2
ORM2	Chlorexine	1
ORM11	Retapamulin	1
ORM12	Salicylanilide	10
ORM14	Tolfenamic acid	10
ORMA	Ovalicin	1

Table 1 – Concentrations of functional ORMs

3.5 Mitochondrial ATP synthesis

Mitochondrial ATP synthesis rate was assessed in digitonin-permeabilized cells, growth at sub-confluent density in DMEM-glucose, by a luciferase-dependent luminometric assay, as previously described with few modifications(Giorgio et al., 2012). Briefly, cells were trypsinized and resuspended 10x10^6/mL in 150 mM KCl, 25 mM Tris–HCl, 2 mM EDTA (ethylenediaminetetraacetic acid), 10 mM potassium phosphate and 0.1 mM $MgCl_2$, pH 7.4, then incubated with 50 μg/mL digitonin for 1' at RT until 80-90% of cells were positive to erythrosine b staining. ATP synthesis driven by CI, CII and NQO1 was measured as Δchemiluminescence over time with a Sirius L Tube luminometer (Titertek-Berthold, Pforzheim, Germany), using aliquots of 3x10^5 permeabilized cells incubated in the same buffer, to which 0.1% BSA and luciferin/luciferase (Sigma Aldrich) were added. Substrate concentrations were as follows: 1 mM malate, 1 mM Na^+ pyruvate, 5 mM malonate (Complex I); 5 mM succinate, 5 μM rotenone (Complex II). NQO1-driven ATP synthesis was assessed in the presence of 0.2 mM NAD(P)H, 5 μM rotenone, 5 mM malonate. Each ATP synthesis reaction was started with 0.1 mM ADP after proper stabilization. Where indicated 10 μM idebenone was added to the assay, pre-incubated 5' at RT before starting the reaction. In each assay the reaction was stopped with 5 μM oligomycin and 11 μM ATP was added as a standard for internal signal calibration. Data were normalized by protein content detected with Bradford method (Bradford, 1976), and by citrate synthase activity as indicator of mitochondrial content (Trounce et al., 1996).

3.6 Preparation of total lysates

Confluent cells were trypsinized and centrifuged at 1500 rpm for 10 minutes. Pellets from the different LHON cell models were resuspended in Phosphate Buffer Saline Solution (PBS: NaCl 9.0 g/L, KH_2PO_4 0.144 g/L, Na_2HPO_4 x $2H_2O$ 0.534 g/L at pH 7.4) containing 1% Triton-X 100, 0.5 mM EDTA, 0.6 mM PMSF, whereas pellets from the different DOA cell models were resuspended in 50-100 µL RIPA buffer (1% Triton X-100, 0.5 Mm EDTA, 0,6 mM PMSF in PBS). A cocktail of protease (Roche #04693116001; 100 µl/ml) and phosphatase (Sigma-Aldrich P5726; 10 µl/ml) inhibitors were added to each buffer immediately before cellular lysate preparation. Samples were incubated 15 minutes on ice, then frozen/thawed twice. Only the samples resuspended in the first buffer were sonicated at high frequency for 10 min in an ice-bath sonicator. Finally, all samples were centrifuged for 15 minutes at 4 °C at 13 000 rpm. Supernatant was stored at -80 °C.

3.7 Protein quantification

Protein quantification was carried out with the Bradford method (Bradford, 1976). The Bradford reagent is an acidic solution based on Coomassie Brilliant Blue G-250, which binds basic and aromatic residues of proteins and turns from red (cationic form, acidic, doubly protonated) to blue (anionic, basic, deprotonated form). Its absorption peak is at 595 nm. A standard calibration curve is necessary to quantify the protein content in a sample: absorbance values of samples will be interpolated in the curve and their concentration derived. We used BSA (Bovine Serum Albumin) as standard: the initial solution is 10mg/ml concentrated and through serial dilution in water we prepared the standard curve with decreasing concentration of BSA: 5 mg/mL, 2.5 mg/mL, 1.25 mg/mL e 0.625 mg/mL. Both points of the curve and samples were prepared in duplicate:

- **blank**: 3 µl of buffer (the same in which samples were resuspended) + 3 µl of water
- **points of the curve**: 3 µl of buffer (the same in which samples were resuspended) + 3 µl of BSA at the different concentrations.
- **samples**: 3 µl of sample + 3 µl of water

Then 1ml of Bradford reagent was added to each sample and 250 µl of the resultant solution were loaded into a 96 wells plate and absorbance was measured with a plate reader (Victor^3, 1420 Multilabel Counter-PerkinElmer, Turku, Finland). Using the calibration curve the protein concentration of samples was calculated.

3.8 SDS-PAGE e WB

35-50 µg of cell lysates were separated by SDS–PAGE using different acrylamide percentage (8%, 10%, 12%, 16%), depending on the molecular weight of protein analyzed, and transferred onto nitrocellulose membranes (Bio-Rad). After, membranes were incubated in 5% powdered milk solved in TBS 1X-Tween 0.05% (25 mM Tris-HCl pH 7.4, 137 mM NaCl, 0,05% Tween) for 1 hour at room temperature and incubated with primary antibodies, diluted in 5% milk-1X TBS-0.05% (Table 2). Then membranes were incubated with the proper horseradish peroxidase-conjugated secondary antibody (Jackson Immuno Research; Mouse 115-035-146, Rabbit 111-035- 144) dissolved 1:5000 in 5% milk-1X TBS-0.05%. The chemiluminescence signals were revealed by using an ECL Western blotting kit (Biorad, #1705061) and measured with Gel Logic 1500 Imaging System-Kodak (Ronchester, NY, USA).

Antibody	Diluition	Manufacturer	Catalog number
OPA1	1:1000	BD Biosciences	612607
TIM23	1:1000	BD Biosciences	611222
DRP1	1:1000	Abnova	H00010059-M01
MFN2	1:1000	Abnova	H00009927-M01
HSP60	1:1000	Santa Cruz	SC-13966
DRP1-pS616	1:1000	Cell Signalling	3455
ATG5	1:1000	Cell Signalling	12994
ATG7	1:1000	Cell Signalling	8558
TOM20	1:1000	Cell Signalling	42406
NDUFA9	1:1000	Abcam	Ab14713
SDHA	1:1000	Abcam	Ab14715
UQCRC2	1:1000	Abcam	Ab14745
COXIV	1:1000	Abcam	Ab14744
ATP5A	1:1000	Abcam	Ab1801
CS	1:1000	Abcam	Ab129095
NQO1	1:1000	Thermo fisher Scientific	39-370-0
PRX3	1:2000	Abfrontier	LF-PA0030
MNSOD	1:1000	Sigma-Aldrich	06-984
CATALASE	1:2000	Sigma-Aldrich	C0979
GAPDH	1:10 000	Millipore	MAB374
ACTIN	1:5000	Sigma-Aldrich	12994
TUBULIN	1:10 000	Sigma-Aldrich	T6557
LC3	1:2000	Sigma-Aldrich	L7543

Table 2 - Primary antibodies (Diluition, Manufacturer and Catalog nunmber)

3.9 Measurement of ROS levels

Cell-ROX Deep Red reagent (Thermo fisher Scientific #C10422), a probe that can detect the oxidative stress in cells by reacting with produced H_2O_2 to become brightly fluorescent, and IncuCyte S3 Live-Cell Analysis System, were used to measure H_2O_2 levels.Cells were seeded in DMEM-glucose $12x10^3$ and $15x10^3$ cells/well for $H42A^{Mock/NQO1}$ and $RJ206^{Morck/NQO1}$ respectively and 24 hours later they were incubated in DMEM supplemented with Cell-ROX probe (5 μM), 10mM glucose, 5 mM pyruvate and 1 mM L-glutamine in the presence or absence of 10 μM idebenone. The probe is a Deep Red reagent for measuring cellular oxidative stress in live cell imaging, with absorption/emission maxima at ~ 644/665 nm. ROS production was measured as a function of red fluorescence over time and expressed as RCU x $\mu m^2/mm^2$. Phase-contrast and red fluorescent images were collected to detect the probe retention. Specifically, images were segmented to identify individual objects, counted, and reported on a *per-area* (mm^2) basis for each time point. The integrated red object counting algorithm was used to isolate the fluorescent signal from background. Raw data were analyzed by Microsoft excel software: the fluorescence of each time point is divided to the fluorescence of T_0 and expressed as percentage (%).

3.10 Total cellular ATP levels measurement

Total amount of cellular ATP in all DOA cell models was measured using luciferin/luciferase assay (Sigma). $25x10^4$ cells/well were seeded in a 6 multiwell in DMEM-glucose. After 24 hours, cells were washed two times with PBS and incubated in DMEM-galactose in the absence or presence of the ORMs at the concentrations indicated in Table 1. After the incubation time (24h), cells were removed with a scraper, centrifuged and resuspended in 500 μL of PBS. They were divided into two aliquots: 200 μL were used for the protein assay, 300 μL were deproteinized with 120 μL of 12% perchloric acid, vortexed, kept in ice for 1 'and finally neutralized with K_2CO_3 3 M in Tris-HCl 2 M and centrifuged for 1' at 13000 at 4°C. ATP content was measured adding 5 μL of sample to each tube containing 200 μL of assay buffer containing luciferin/luciferase and using the luminometer previously described. Finally, 0.125 μM of ATP was added to each tube as an internal standard.
Data are expressed as percentage of the ATP content measured in each cell line in DMEM-glucose before switching to DMEM-galactose (T_0).

3.11 Mitochondrial reticulum analysis

Cells were seeded in a 6 well plate with cover glass in DMEM-glucose ($40x10^3$ for MEFs and $15x10^4$ for fibroblasts). The following day cells were incubated for 24 hours in the absence or presence of the ORMs at concentrations reported in Table 1 in DMEM-glucose or DMEM-galactose. At the expiry of the established times, each petri dish was incubated with 10 nM MitoTracker Red (Mitotracker CMX Ros, M7512, ThermoFisher Scientific) for 15 ' at 37 °C. At the end of the incubation, the medium was aspirated and 2 mL of phenol red-free medium containing 10 mM Na-HEPES were added. A Nikon Eclipse Ti-U epifluorescence microscope was used, equipped with a Photometrics Cascade digital camera (Roper Scientific), and an excitation wavelength of 579 nm and an emission wavelength of 599 nm was used. Images were acquired with a 63X / 1.4 NA immersion objective and analyzed using Metamorph software. The quantification of the percentage of cells with filamentous, intermediate or fragmented reticulum was determined by a blind test, carried out by at least three different people, which were previously trained to recognize the three conditions analyzing some representative images.

3.12 Statistical analysis

All numerical data are expressed as mean ± SD or SEM, as indicated. Student's unpaired two-tailed test was used for statistical analysis, unless otherwise indicated. Differences were considered statistically significant for $p < 0.05$.

4. RESULTS

4.1 Study on LHON

4.1.1 Idebenone treatment increases mitochondrial energetic efficiency in cybrids overexpressing NQO1

The aim of this study was to investigate the role of NQO1 expression and activity on the effect of idebenone treatment in cells with CI deficiency as in LHON, to better understand the relationships between NQO1 and idebenone effectiveness.

Firstly, we took advantage of two cybrids cell lines, a control (H42A) and a cell line bearing the m.3460 G>A/*MT-ND1* mutation (RJ206), which showed very low levels of NQO1 protein, to generate four cell lines, two carrying the empty expression vector ($H42A^{Mock}$ / $RJ206^{Mock}$) and two carrying the cDNA encoding the NQO1 human isoform 1 ($H42A^{NQO1}$ / $RJ206^{NQO1}$) as described in Materials and Methods. As shown in Figure 8A, cells infected with the empty vector barely expressed NQO1 protein, whereas both lines infected with the viral vector containing the NQO1 cDNA showed an increase in the expression of the protein, stronger in $H42A^{NQO1}$ than in $RJ206^{NQO1}$.We then evaluated cellular respiration profile both in the presence and absence of idebenone. The $H42A^{Mock}$ line in the presence of DMSO (vehicle) showed a cellular basal respiration around 700 pmolO_2/min.prot which increased after the addition of the mitochondrial uncoupler FCCP and was inhibited in presence of rotenone (CI inhibitor) and antimycin (CIII inhibitor) (Figure 8B, open circles). This is a typical OCR profile of cultured cells in which the mitochondrial respiration is mostly dependent from CI. In the same cells, in presence of idebenone, the basal respiration was around 400 pmolO_2/min.prot, inhibited by oligomycin but not enhanced by FCCP, indicating a partial inhibition of the respiratory chain (Fig.8B, red squares). The addition of rotenone partially reduced the residual oxygen consumption, that in turn was completely inhibited by antimycin. $RJ206^{Mock}$ cell line showed a respiration profile similar to $H42A^{Mock}$ cells (Figure 8C, open circles), even if the basal oxygen consumption rate (OCR) in presence of DMSO was lower (around 400 pmolO_2/min.prot), congruent with previous literature showing that 3460/ND1 mutation induced a reduction in respiration of about 50% (Brown et al., 2000). Furthermore, incubation with idebenone completely inhibited OCR dependent from CI, maintaining a slight respiration that was inhibited by antimycin (Figure 8C, red squares). These results indicated that when NQO1 is expressed at very low levels, probably idebenone is only partially reduced exhibiting an inhibitory effect on respiratory chain with its oxidized form and sustained a low residual respiration through CIII with its reduced form. NQO1 overexpression in presence of

DMSO did not alter OCR in both cell lines compared to mock cells (Figure 8D, E, open circles), indicating that the enhanced expression of NQO1 did not influence mitochondrial respiration *per se*. However, in presence of idebenone, basal respiration significantly increased in both cell lines, reaching similar values (Figure 8D, E, red squares) and OCR was also sustained in presence of rotenone in a CI-independent but complex III-dependent way (antimycin sensitive). As an internal control in cells overexpressing NQO1, we used dicumarol, a specific inhibitor of NQO1, to evaluate if the measured OCR was due to the activity of NQO1 specifically. In these cells, in presence of idebenone and dicumarol, respiration was completely inhibited (Figure 8D, E, green triangles). Altogether, these results demonstrate that idebenone is able to restore respiratory chain defects linked to CI deficiency when NQO1 is overexpressed.

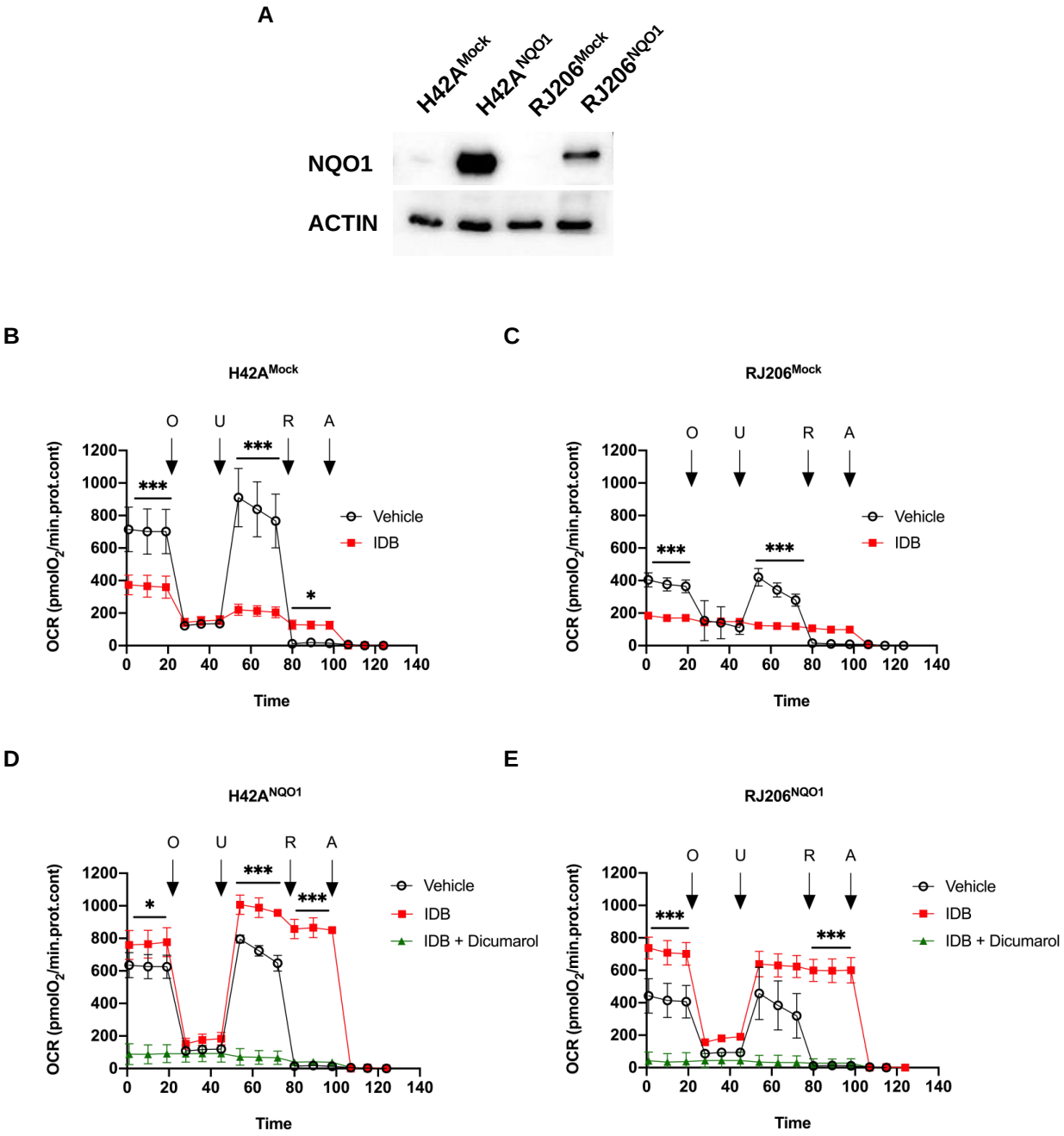

*Figure 8 – (A) Expression of NQO1 in in H42A$^{Mock/NQO1}$ and RJ206$^{Mock/NQO1}$. Actin (45KDa) was used as reference protein. (B-C) OCR in in H42A$^{Mock/NQO1}$ and RJ206$^{Mock/NQO1}$in presence or absence of idebenone. (D-E) OCR in control and 3460 mutated cybrids overexpressing NQO1 in presence or absence of idebenone or dicumarol. Data are reported as mean ± SD of three independent experiments using an unpaired t-test (Holm-Sidàk test). *p<0.05; ***p<0.001*

The demonstration that NQO1 and idebenone are involved in electron transport along the respiratory chain, bypassing complex I, was not sufficient to conclude that reduced idebenone could restore the mitochondrial energetic efficiency in cells with complex I deficiency. To address this point, we measured the mitochondrial ATP synthesis rate driven by complex I and/or NQO1 substrates NADH/NADPH in mock and NQO1 cybrids.

Figure 9A shows that, in digitonin-permeabilized cells, CI-driven ATP synthesis rate was significantly reduced in LHON cells (RJ206) compared to control cells (H42A) in both mock and NQO1 overexpressing cells considering the effect of 3460 mutation on CI activity. However, NQO1 overexpression did not significantly alter CI-driven ATP synthesis. The addition of idebenone strongly inhibited CI-driven ATP synthesis in all cell lines, suggesting that idebenone is present in its oxidized form and cannot be reduced by NADH-linked substrates inside the mitochondria. However, the addition of exogenous NAD(P)H together with idebenone induced ATP synthesis rates similar to CI-driven ATP in cells overexpressing NQO1, while in mock cells the effect is negligible. Also, in this case we used dicumarol to confirm that it was really NQO1 to bring back the value of ATP synthesis to the basal condition (not shown). After the incubation with this inhibitor the ATP synthesis was completely inhibited. In these experimental conditions, NAD(P)H can be oxidized only by cytosolic NAD(P)H dehydrogenases like NQO1, therefore, these results demonstrate that NQO1 can oxidize NAD(P)H outside of mitochondria and in turn can reduce idebenone sustaining mitochondrial ATP synthesis. Finally, we evaluated the long-time effect of idebenone in cells overexpressing NQO1 compared to mock cells, performing a viability assay after 48 hours of treatment with idebenone. In Figure 9B, cell viability was expressed as percentage of viable cells treated with 10μM idebenone relative to non-treated cells. Both H42A and RJ206 mock cell lines showed a decrease in cell viability, 40% and 60% respectively, when treated with idebenone, suggesting a toxic effect of this drug in its oxidized form. However, the overexpression of NQO1 induced a significant increase of cell survival in both cell lines, completely and partially restoring the viability of $H42A^{NQO1}$ and $RJ206^{NQO1}$, respectively. Taken together, these results indicate that NQO1 can oxidize cytosolic NAD(P)H reducing idebenone that loses its toxic effect and sustains the respiratory chain ameliorating the mitochondrial energetic efficiency particularly in cells with defective CI.

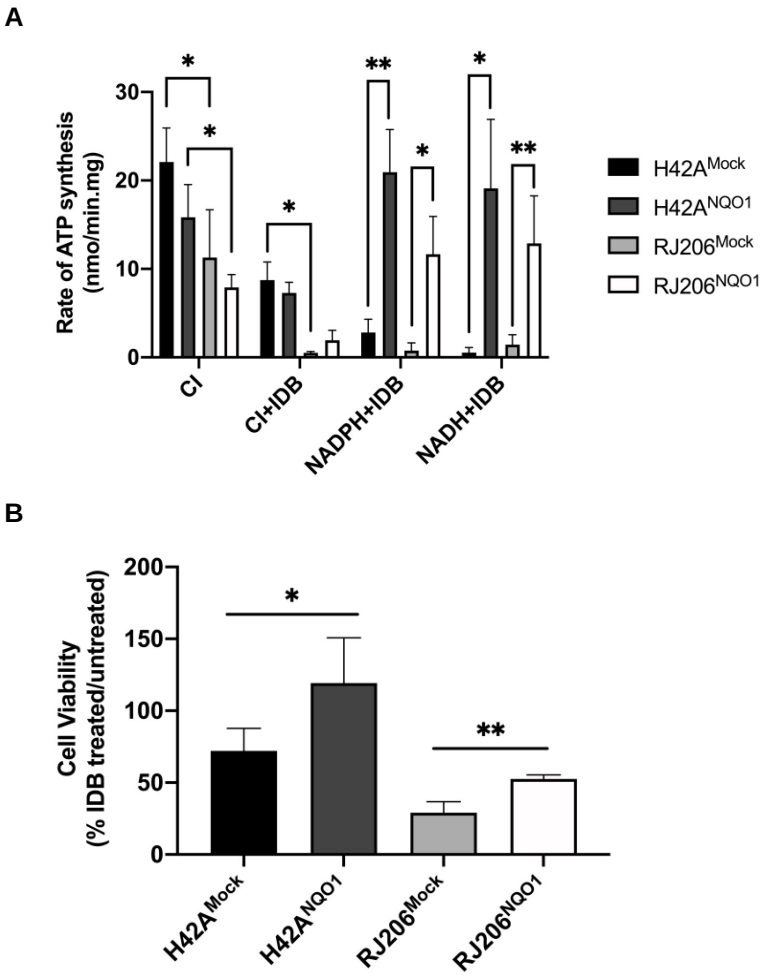

*Figure 9 - (A) ATP synthesis of CI measured in digitonin-permeabilized cells in presence or absence of exogenous NAD(P)H and/or idebenone (IDB) at the final concentration of 10μM and incubated for 5 minutes before the measurement as detailed in Materials and Methods. Data are means ± SD of at least three independent experiments. (B) Cell viability in 10mM glucose, 5mM pyruvate and 1mM L-glutamine DMEM in presence or absence of 10μM idebenone. Values are expressed as percentage of the ratio between idebenone treated and non-treated cells. Statistical analysis was performed using unpaired t test. *p < 0.05 and **p < 0.01.*

4.1.2 Idebenone treatment ameliorates oxidative stress in cybrids overexpressing NQO1

It is well known that common LHON mutations cause partial CI defects, reducing ATP production and increasing mitochondrial ROS (Wallace & Lott, 2017). Firstly, we evaluated the expression levels of antioxidant proteins of different cellular compartments in cell lines overexpressing or not NQO1 (Figure 10A-B). In particular, we analysed the expression of catalase, acting at the level of peroxisomes, as well as manganese superoxide dismutase (MnSOD) and peroxiredoxin 3 (PRX3), localized inside to mitochondria. As shown in Figure 3A-B, the levels of all proteins were significantly increased in RJ206^{Mock} compared to H42A^{Mock} cells, suggesting a response to cellular oxidative stress in LHON cybrids as previously demonstrated by several authors (Brown et al., 2000; Floreani et al., 2005; Ghelli et al., 2008). Furthermore, the overexpression of NQO1 reduced these

differences, and in particular in RJ206^{NQO1} a reduction of PRX3 expression was observed compared to the respective mock cells. ROS production was also directly measured in the same cells, confirming that RJ206^{Mock} cells generated significantly more ROS than H42A^{Mock} and that overexpression of NQO1 considerably reduced ROS production in RJ206 cells (Figure 10C). However, the differences in terms of ROS production between both cell lines overexpressing NQO1 was still significative. These results suggest that NQO1 overexpression only could mitigate the oxidative stress induced by 3460 mutation. In addition, the therapeutic action of idebenone has also been associated to its antioxidant effect in its reduced form (Erb et al., 2012), therefore ROS production was also measured in cells treated with 10 µM idebenone (Figure 10D), showing that H_2O_2 production was significantly reduced in RJ206^{NQO1} compared to RJ206^{Mock} cells, clearly revealing an antioxidant effect of idebenone in presence of NQO1. Noteworthy, ROS levels measured in idebenone treated RJ206^{NQO1} line are similar to the levels of the H42A^{Mock} line (Figure 10D), suggesting that the protective role of NQO1 in mitigating ROS production is enhanced by idebenone treatment.

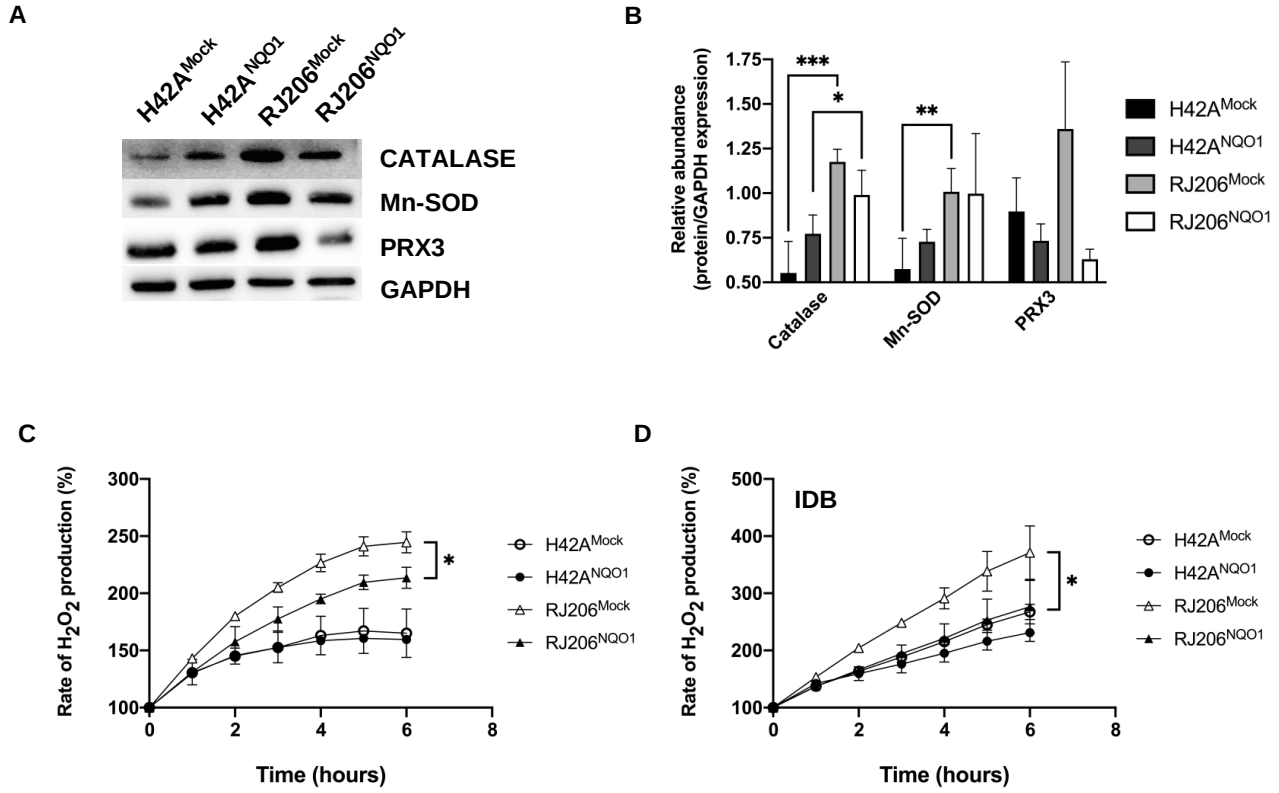

*Figure 10 – (A) Western Blot analysis of Catalase (60 kDa), PRX3 (24 kDa) and MnSOD (24 kDa) proteins in H42A$^{Mock/NQO1}$ and RJ206$^{Mock/NQO1}$. GAPDH (37 kDa) was used as reference protein (C-D) Rate of H_2O_2 production in cells grown in 10mM glucose, 5mM pyruvate and 1mM L-glutamine DMEM in presence or absence of 10µM idebenone. The H_2O_2 production rate are expressed as percentage considering 100% the fluorescence at time zero. Data are reported as mean ± SD of two independent experiments (*p<0.05; **p<0.01) using a paired two tailed t-test.*

4.1.3 Idebenone effectiveness depends on NQO1 levels in fibroblasts from controls and LHON patients

As cybrids are constructed by transferring only the mtDNA from donor cells and carry the same nuclear background, the next step was to study the effect of idebenone related to NQO1 expression directly in fibroblasts derived from healthy controls and LHON patients, which present the full genetic complement of original nuclear and mitochondrial genomes. Therefore, we firstly analyzed NQO1 expression levels using three fibroblast cell lines from healthy donors, three from LHON patients with the m.3460G>A/*MT-ND1* and three with the m.11778G>A/*MT-ND4* mutation. Figure 11A-B show the Western Blotting analysis of NQO1 expression in the different cell lines revealing that in three samples (WT2; 3460/1 and 11778/3) the protein was undetectable and two cell lines (WT1 and 11778/1) showed significant lower levels of NQO1, considering as reference WT3, which is the control cell line that express higher levels of NQO1 (Figure 11A-B).

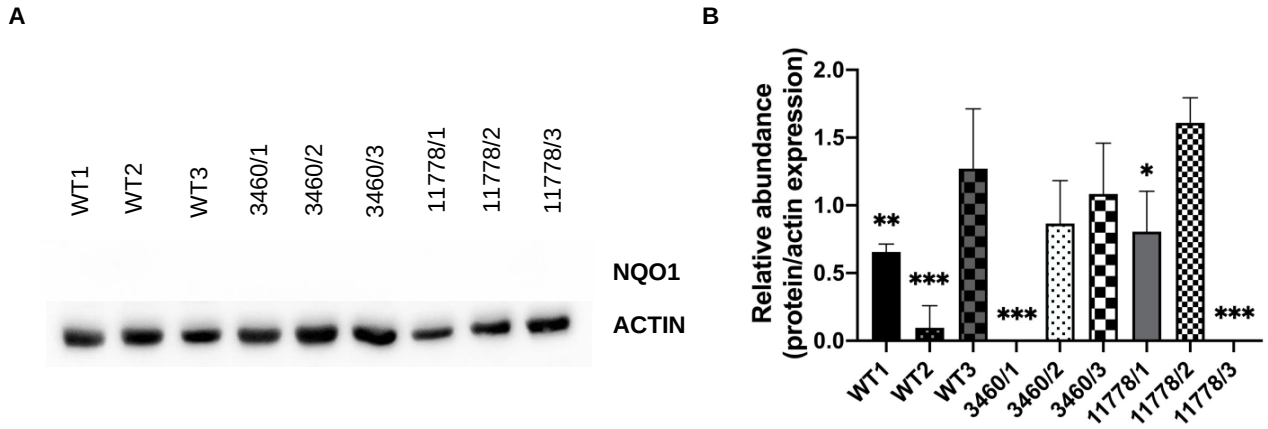

*Figure 11 – (A) Representative blot and (B) quantification of NQO1 expression in cellular lysates from control (WT1, WT2, WT3) and LHON (3460/1, 3460/2, 3460/3, 11778/1, 11778/2, 11778/3) fibroblasts. Actin (45KDa) was used as loading control. The relative abundance of protein expression is normalized considering as reference the wild type fibroblast showing the higher expression of NQO1 (WT3). Data are reported as means±SD (*p<0.05; ***p<0.001) using ANOVA test.*

Then, we assessed whether the physiological levels of NQO1 expression could maintain mitochondrial respiration in presence of the LHON genetic disfunction or pharmacological inhibition of CI. Firstly, we measured OCR in controls fibroblasts in presence or absence of idebenone (Figure 12 A-C), showing that idebenone treatment did not alter basal respiration and uncoupled respiration (FCCP) in fibroblasts expressing NQO1 (WT/1 and WT/3). However, in presence of idebenone, cellular respiration was also maintained when rotenone was added, indicating the presence of a mitochondrial oxygen consumption independent from CI. Conversely, in WT/2 which did not express NQO1, uncoupled respiration was inhibited in presence of idebenone and only partially maintained

after addition of rotenone. This result suggests a correlation between NQO1 expression and idebenone effectiveness in feeding respiratory chain through NQO1 expression and activity.

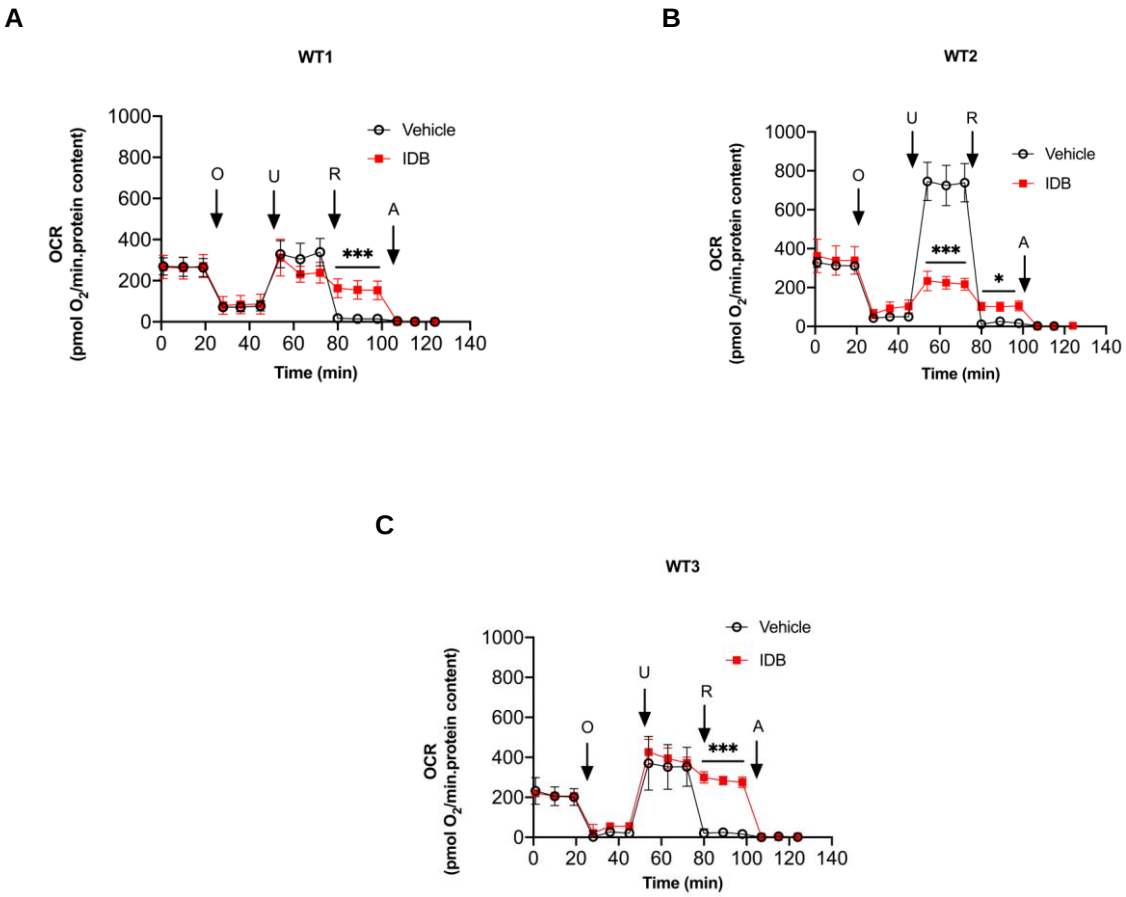

*Figure 12 – (A-C) OCR measurements in control fibroblasts in presence or absence of idebenone. Data are reported as mean ± SD of three independent experiments (*p<0.05; ***p<0.001) using an unpaired t-test (Holm-Sidàk test).*

Furthermore, in fibroblast carrying the 3460/ND1 mutation (Figure 13A-C), idebenone treatment significantly inhibited uncoupled respiration in cells that did not express NQO1 (3460/1; Figure 13A), while enhanced mitochondrial respiration in both basal and uncoupled conditions as well as sustained respiration in the presence of rotenone in cells expressing NQO1 (3460/2 and 3460/3; Figure 13B-C).

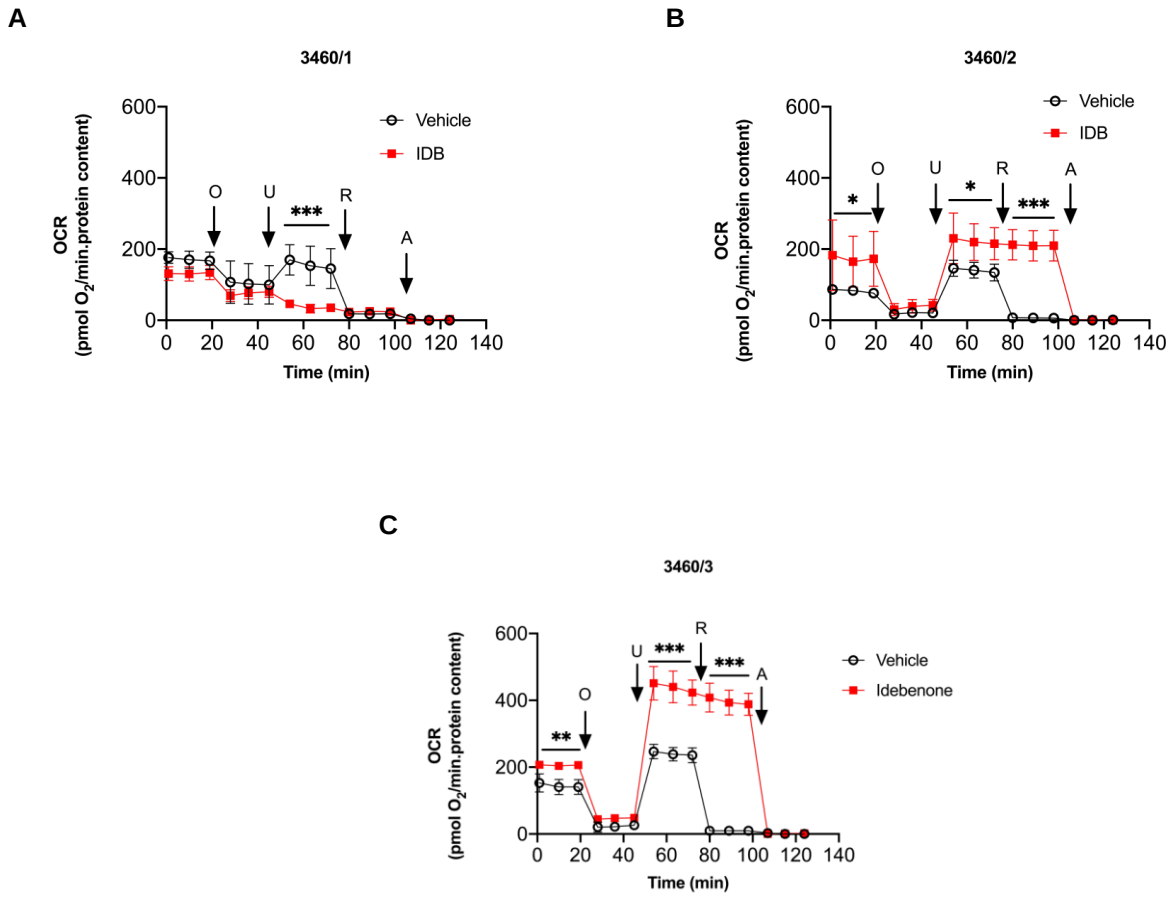

*Figure 13 – (A-C) OCR measurements in 3460 LHON fibroblasts in presence or absence of idebenone. Data are reported as mean ± SD of three independent experiments (*p<0.05; ***p<0.001) using an unpaired t-test (Holm-Sidàk test).*

A similar behaviour was mainly observed also in fibroblasts carrying the 11778/ND4 mutation, suggesting a general effectiveness of idebenone in LHON fibroblasts on mitochondrial respiratory chain depending on NQO1 expression (Fig. 14A-C).

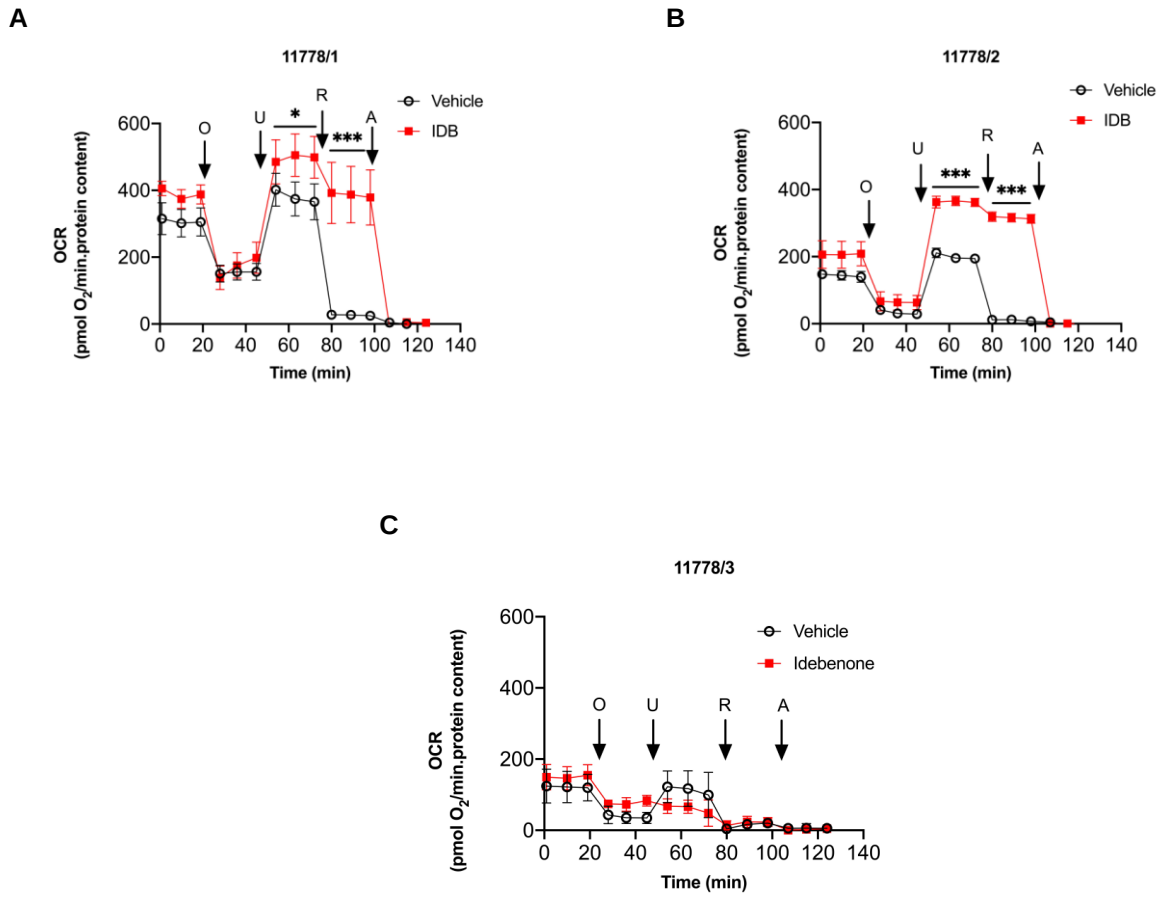

*Figure 14 – (A-C) OCR measurements in 11778 LHON fibroblasts in presence or absence of idebenone. Data are reported as mean ± SD of three independent experiments (*p<0.05; ***p<0.001) using an unpaired t-test (Holm-Sidàk test).*

To match these *in vitro* results with the *in vivo* real-world experience, in collaboration with the laboratory of neurogenetics of IRCCS Institute of Neurological Science of Bologna, Bellaria Hospital headed by Professor Valerio Carelli, we obtained the clinical information of the six LHON patients from which fibroblasts were derived and we classified these patients as idebenone treatment Responders (R) or Non-Responders (NR). Table 3 summarizes the LHON mutations, NQO1 expression, OCR in presence of idebenone and rotenone (OCR-ROTE-IDB) and the clinical response to idebenone treatment. These results suggest a general concordance among non-responders (NR), fibroblasts which had a reduced NQO1 expression and did not sustain respiration in presence of idebenone and rotenone, with the exception of a case corresponding to fibroblasts 3460/3 which was not treated with idebenone but with EPI-743 and the case corresponding to fibroblasts 11778/1 which was a patient with a peculiar LHON story triggered by toxic chemicals (Carelli et al., 2007). Moreover, the two patients classified as responders showed high NQO1 expression levels and OCR sustained by idebenone after addition of rotenone. Taken together these results indicate that NQO1-Idebenone-CIII pathway, can recover the energy deficit in LHON cells bypassing CI defect, fitting in the large majority of cases the clinical *in vivo* response to idebenone therapy.

Cell line	LHON mutation	NQO1 expression	OCR-ROTE-IDB	Clinical response to idebenone treatment
WT 1	-	0.62	169	
WT 2	-	0.08	58	
WT 3	-	0.90	286	
3460/1	3460	0.17	29	NR
3460/2	3460	0.93	194	R
3460/3	3460	0.70	396	NR*
11778/1	11778	0.67	463	NR
11778/2	11778	1.41	312	R
11778/3	11778	0.00	30	NR

*Table 3 - Summary table of cell line types, LHON mutation, protein expression, OCR ROTE IDB (pmolO2/min.prot.cont) and clinical response to Idebenone treatment in patients *indicate a non-responder patient treated with EPI-743 and not idebenone.*

4.1.4 Induction of NQO1 as an option to optimize idebenone efficacy

NQO1 is a highly inducible enzyme regulated by the Keap1/Nrf2/ARE pathway and its induction, by different modulators, has been proposed as a pharmacological approach for different diseases in which this pathway is involved. There are many molecules acting on this pathway, one of these, dimethyl-fumarate (DMF), has received by the US Food and Drug Administration clinical approval for multiple sclerosis and psoriasis treatment (Cuadrado et al., 2019). Therefore, we treated some selected control and LHON fibroblasts, from the previously studied, with DMF to induce the expression of NQO1 and to assess the effect of idebenone on OCR. Figures 15A-B illustrates NQO1 protein amounts in fibroblasts treated or not with 5μM DMF for 48h, showing that DMF increased NQO1 protein expression at different levels.

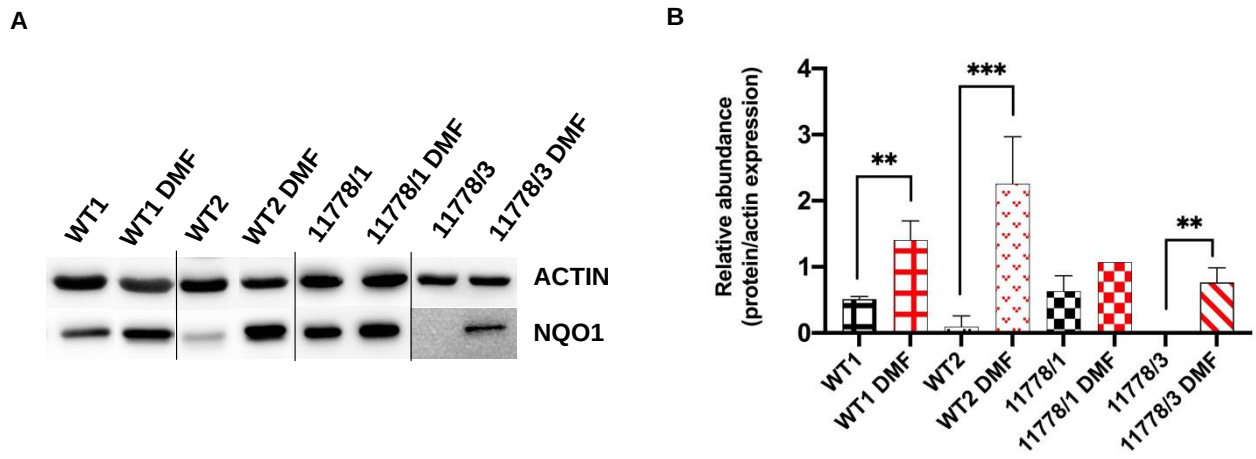

*Figure 15 – (A) Representative blot and (B) quantification of NQO1 expression in cellular lysates from control (WT1, WT2) and LHON (11778/1, 11778/3) fibroblasts treated or untreated with 5μM DMF for 48h. Actin was used as loading control. Statistical analysis was performed using unpaired t test. **p < 0.01 and ***p < 0.001.*

Furthermore, the OCR measurements indicated that DMF treatment did not significantly alter mitochondrial respiration except for 3460/1 line in uncoupled conditions (Figure 16D), while the presence of idebenone maintain respiration after rotenone addition depending on NQO1 protein expression levels. Indeed, WT1 and WT2 cell lines showed a significant increase of protein expression after DMF treatment, and a more robust respiration compared to cells treated with idebenone only (Fig.12A). Moreover, 11778/1 fibroblasts slightly increased NQO1 expression and maintained an OCR similar to that measured in Figure 14A, whereas in 11778/3 cell line, DMF increased NQO1 expression significantly but not sufficiently to enable idebenone to maintain respiration after rotenone addition.

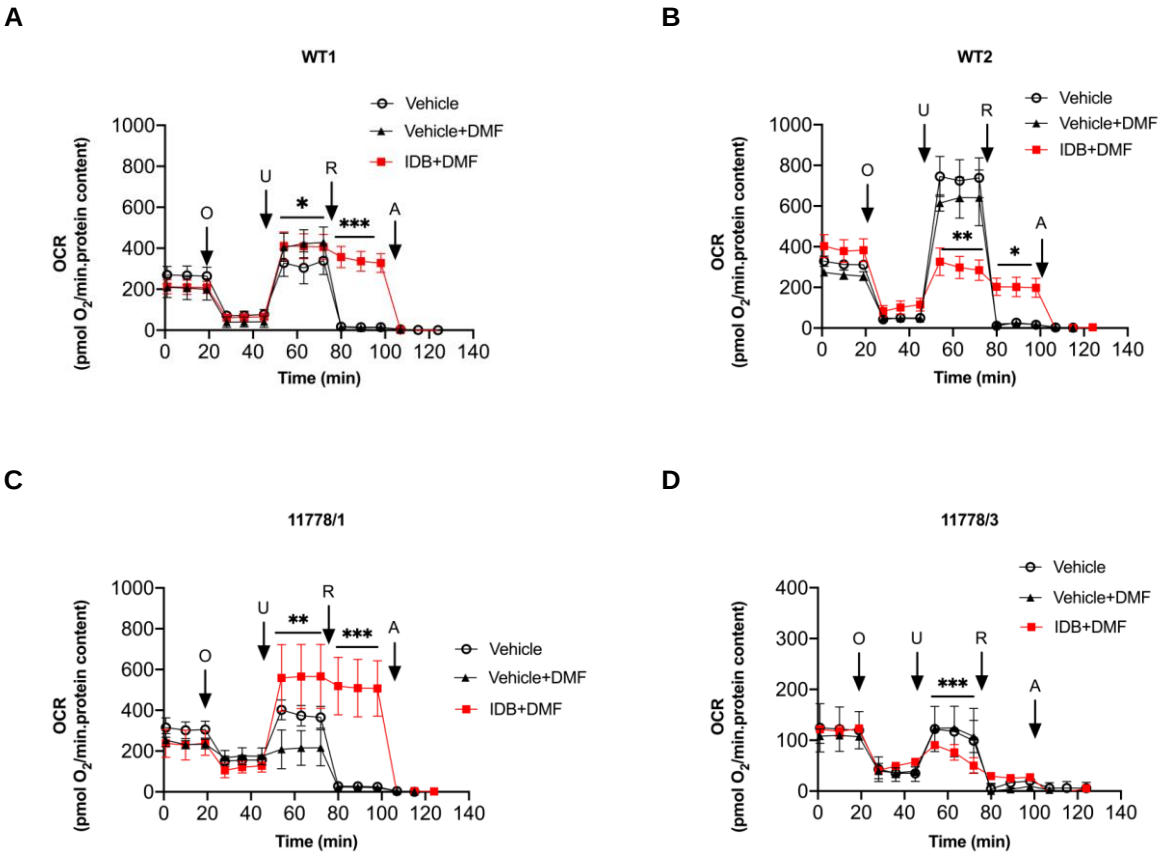

*Figure 16 - (A-C) OCR measurements in controls and LHON fibroblasts treated or not with DMF for 48 hours in presence or absence of idebenone. Data are reported as mean ± SD of three independent experiments. *p<0.05; ***p<0.001 using an unpaired t-test (Holm-Sidàk test).*

These results indicate that, in general, the expression of NQO1 induced by DMF is able to enhance idebenone effectiveness, however this topic deserve further investigations to understand the threshold of NQO1 levels useful for idebenone therapeutic effect.

4.2 Study on DOA

OPA1 mutations cause either DOA or DOA plus, pathologies for which there is no cure. Firstly, we used yeast models to analyse FDA-approved molecules able to rescue the mitochondrial dysfunctions induced by mutations. In particular, a strain of *Saccharomyces cerevisiae* bearing the I322M mutation in OPA1 ortholog *mgm1* was used. This strain is characterised by a limited growth at 37°C in nonfermentable carbon sources, glycerol or ethanol, associated with poor mtDNA maintenance, resulting in high *petite* frequency. The screening was based on the capability of the drug to rescue the growth defect of such strain. From the screening of 2500 molecules, 42 molecules, called OPA1 Rescuing Molecules (ORMs), rescuing the growth defect were selected. These 42 hits were further tested on a yeast strain harbouring MGM/OPA1 chimeric gene, named CHIM3. In this strain different

OPA1 mutations causing growth defect were introduced and only 16 hits were able to rescue the growth defect in these mutant strains. Among these, only 6 reduced *petite* frequency indicating an increase in mtDNA stability. Here, we show the assessment of these six selected molecules on MEF models previously described and DOA patient-derived fibroblasts. Before starting our analysis, we evaluated the maximum non-toxic concentration after 24 hours of incubation in DMEM-galactose for each ORM to perform experiments in which mitochondrial dysfunction and OXPHOS impairment were highlighted. (Table 1 of Materials and Methods) (Aleo et al., 2020).

4.2.1 Validation of ORMs efficacy in MEFs with OPA1 mutations

4.2.1.1 Effect of the ORMs on MEFs viability

Mutations in OPA1 can determine an impairment in oxidative phosphorylation. To highlight this impairment, control cells expressing human isoform 1 (ISO1) and mutated cells expressing ISO1 carrying D603H or R445H mutations were grown in DMEM-galactose medium in presence or absence of ORMs and cell viability was measured by SRB assay. In this experimental condition D603H grew slower than ISO1, whereas R445H did not proliferate. ISO1 growth was not influenced by any ORMs. ORM12 determined a significant increase in R445H cell viability, whereas ORMs 0, 2, 12 and 14 increased the number of D603H viable cells, without reaching statistical relevance (Fig.17 A-B).

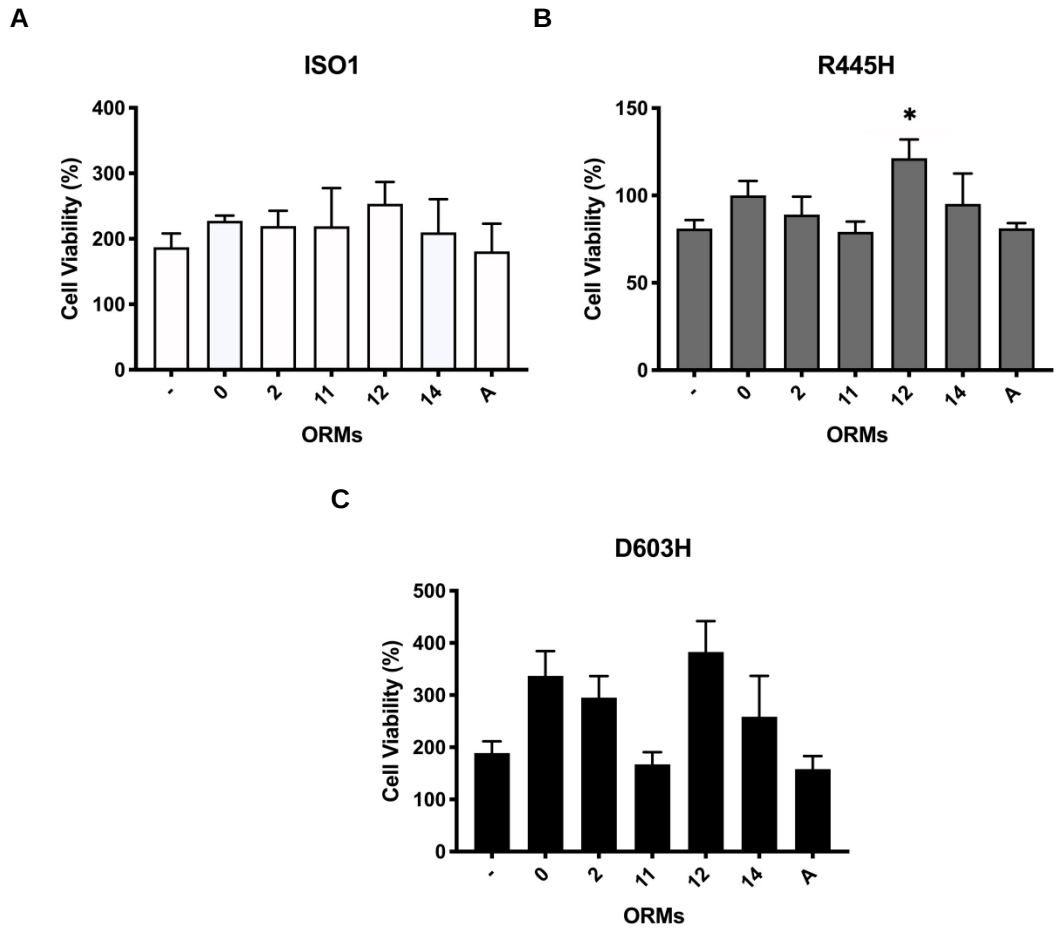

Figure 17 - Viability of OPA1 mutated MEFs with ORMs. (A–C) Number of viable cells of ISO1, R445H and D603H, after incubation for 24 h in DMEM-galactose in the absence or presence of ORMs. Data are expressed as percent of the SRB absorbance measured in DMEM-glucose at time = 0, considered as 100% value. Data are means±SEM of 19 experiments in DMEM-galactose and 3–7 experiments in DMEM-galactose with ORMs treatment (ORMs 0, 2, 11, 12: n = 3; ORM14, A: n =7). ∗Denotes P < 0.05.

Altogether, these data indicate that ORM12 is the more effective on increasing cell viability in both mutant cell lines and ORM0, 2 and 14 show a tendency to ameliorate it (Aleo et al., 2020).

4.2.1.2 Effect of the ORMs on MEFs ATP content

To obtain an indication of the energetic metabolism, we assessed cellular ATP levels in DMEM-galactose in presence or absence of ORMs. Indeed, as previously reported in Del Dotto et al., 2018, after 24 hours of incubation with galactose, ISO1 show a significant increase of ATP content due to the switch from a more glycolytic to a more oxidative metabolism. Conversely, D603H did not exhibit the same increase and R445H ATP content significantly decreased. Figure 18 shows that in DMEM-galactose the total ATP content of ISO1 (A) and D603H (C) cell lines was the same in presence or absence of ORMs, suggesting that they did not improve or impair the energetic charge of cells. On

the contrary, R445H showed a clear decline in ATP content when cells were incubated in DMEM-galactose, whereas ORM0 and 2 significantly increase the total ATP levels (Fig.18B).

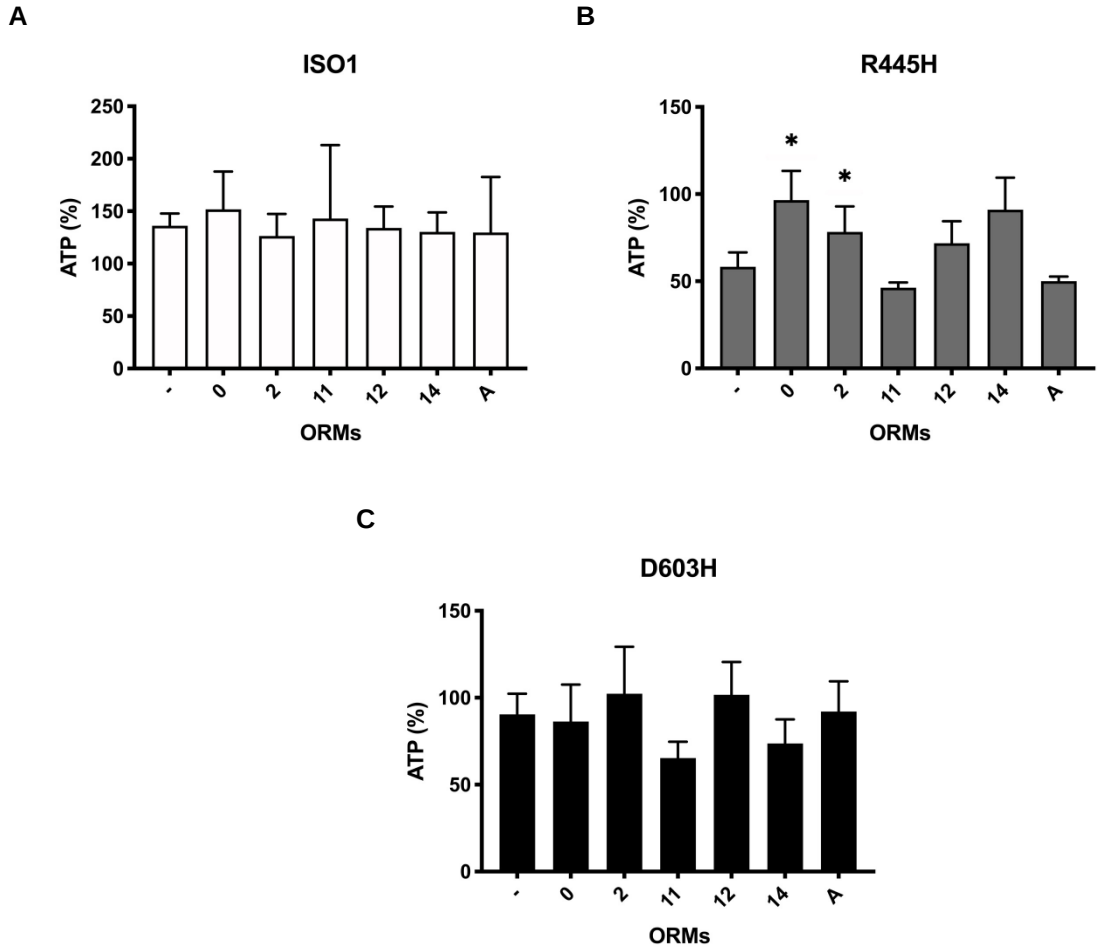

Figure 18 – ATP content of OPA1 mutated MEFs with ORMs. (A-C) Cellular ATP levels of ISO1, R445H and D603H after incubation for 24 h in DMEM-galactose ± ORMs. Data are expressed as percentage of ATP content measured in DMEM-glucose at time = 0. Values are means ± SEM of 14 experiments in DMEM- galactose and 3–4 experiments in DMEM-galactose + ORMs (ORMs 0, 2, 11, 12, 14 n = 4, ORMA n = 3). ⁎Denotes P < 0.05.

4.2.1.3 Effect of the ORMs on mitochondrial network morphology

OPA1 plays a key role in the fusion process of the inner mitochondrial membrane. We analysed the mitochondrial network morphology of cells loaded with Mitotracker Red by fluorescence microscope. Cells were classified into 3 different categories: cells with filamentous and interconnected mitochondria (filamentous), cells with an intermediate network (intermediate) and cells with totally fragmented mitochondria (fragmented). In DMEM-glucose, ISO1 cells showed mainly filamentous mitochondria, D603H showed mitochondria intermediate or fragmented, whereas R445H showed mitochondria completely fragmented (Del Dotto, Fogazza, Musiani, et al., 2018). As show in Fig. 19A-B, in ISO1 cells incubated in DMEM-glucose in presence or absence

of ORMs, ORM0 caused a significant increase of cells with filamentous mitochondria associated with a significant decrease of cell with fragmented mitochondria. In addition, the treatment with ORM2 and 14 induced a significant decrease of cells with fragmented mitochondria only. Instead, in D603H, ORM2 caused a significant increase in the percentage of cells with filamentous and intermediate mitochondria associated with a significant decrease of cells with fragmented mitochondria, which was more evident in the presence of ORMA. In the same cell line, ORM0 induced a significative reduction of cells with fragmented mitochondria due to a redistribution of cells in the intermediate group. On the contrary, ORM11 caused a significant decrease of cells with intermediate mitochondria associated with a significant increase of cells with fragmented mitochondria (Fig. 19A-C).

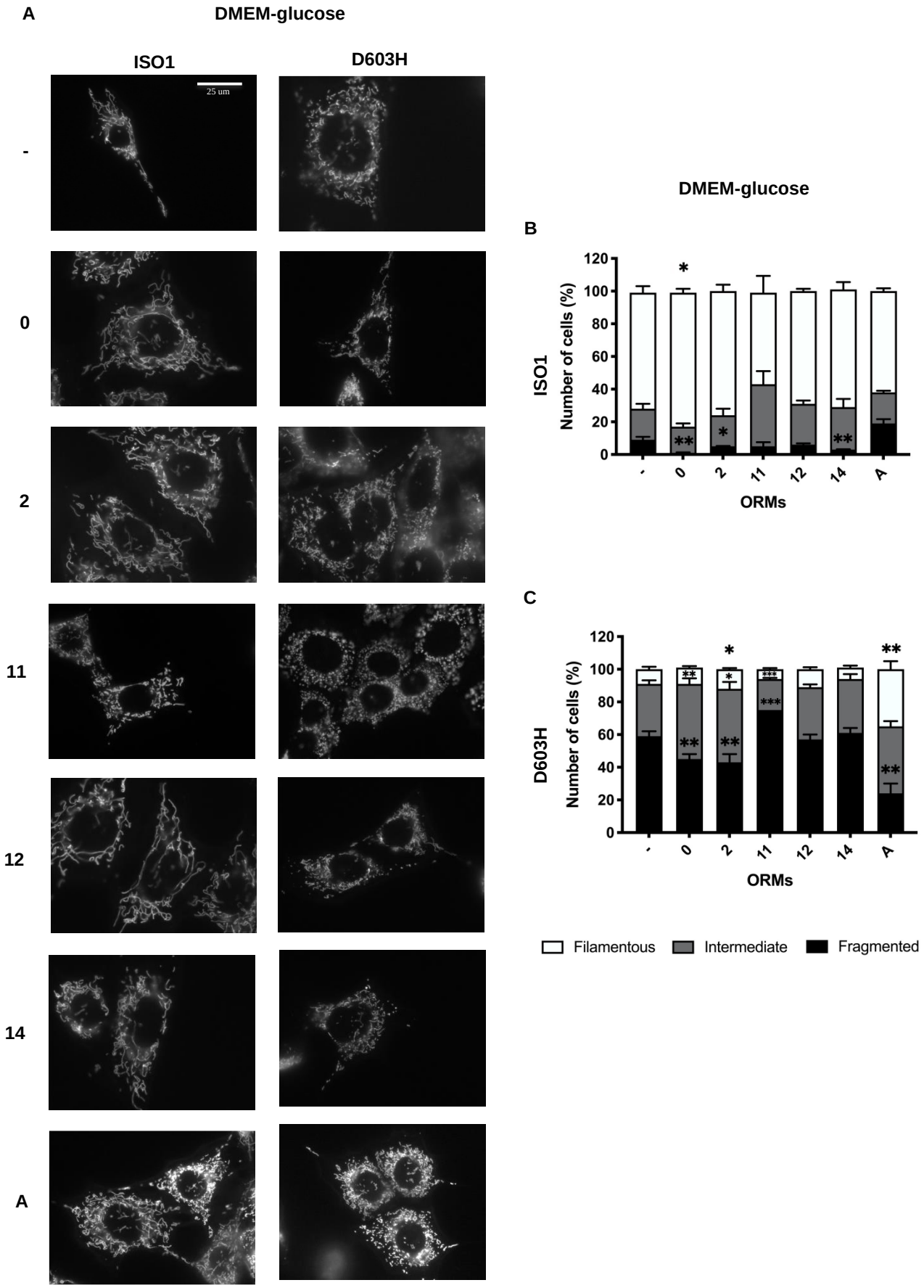

Figure 19 - Mitochondrial network morphology of OPA1 mutated MEFs incubated with ORMs. (A) Representative images of mitochondrial network of ISO1 and D603H after labeling with Mitotracker Red. MEFs lines were incubated for 24 h in DMEM-glucose in absence or presence of the ORMs. Cells were scored in three categories on the basis of mitochondrial network morphologies: cells

with filamentous and inter- connected network (filamentous), cells with short filamentous mitochondria (intermediate) and cells with fragmented mitochondria (fragmented). 100–120 cells were analyzed for ISO1 (B) and D603H (C) in each condition and for each experiment. Data are means±SEM of 3–4 independent experiments. ∗P < 0.05, ∗∗P < 0.01, ∗∗∗P < 0.001.

In DMEM-galactose the mitochondrial shape distribution in ISO1 was similar to DMEM-glucose condition; on the contrary, in D603H the mitochondrial morphology was almost completely fragmented. In ISO1, ORM2 significantly decreased the percentage of cells with fragmented mitochondria whereas ORMA significantly increased the percentage of cells with filamentous mitochondria associated with a decrease in the percentage of cells with intermediate mitochondria. In addition, ORM14 induced a significant decrease of cells with fragmented and intermediate mitochondria associated to a significant increase of cells with filamentous mitochondria. Conversely, ORMs 11 and 12 showed a negative effect on mitochondrial network significantly reducing cells with filamentous mitochondria (Fig. 20A-B). The incubation of D603H with ORMs 0, 2, 14 and A, significantly recovered the filamentous phenotype with a corresponding reduction of cells with fragmented mitochondria, suggesting a similar effect on control and mutated cell lines. The intermediate component also increased at the expense of the fragmented one. In fact, in presence of ORMs 0, 2 and 14 a significant decrease in fragmented cells was evident. On the contrary, ORM12 showed a negative effect (Fig. 20A-C).

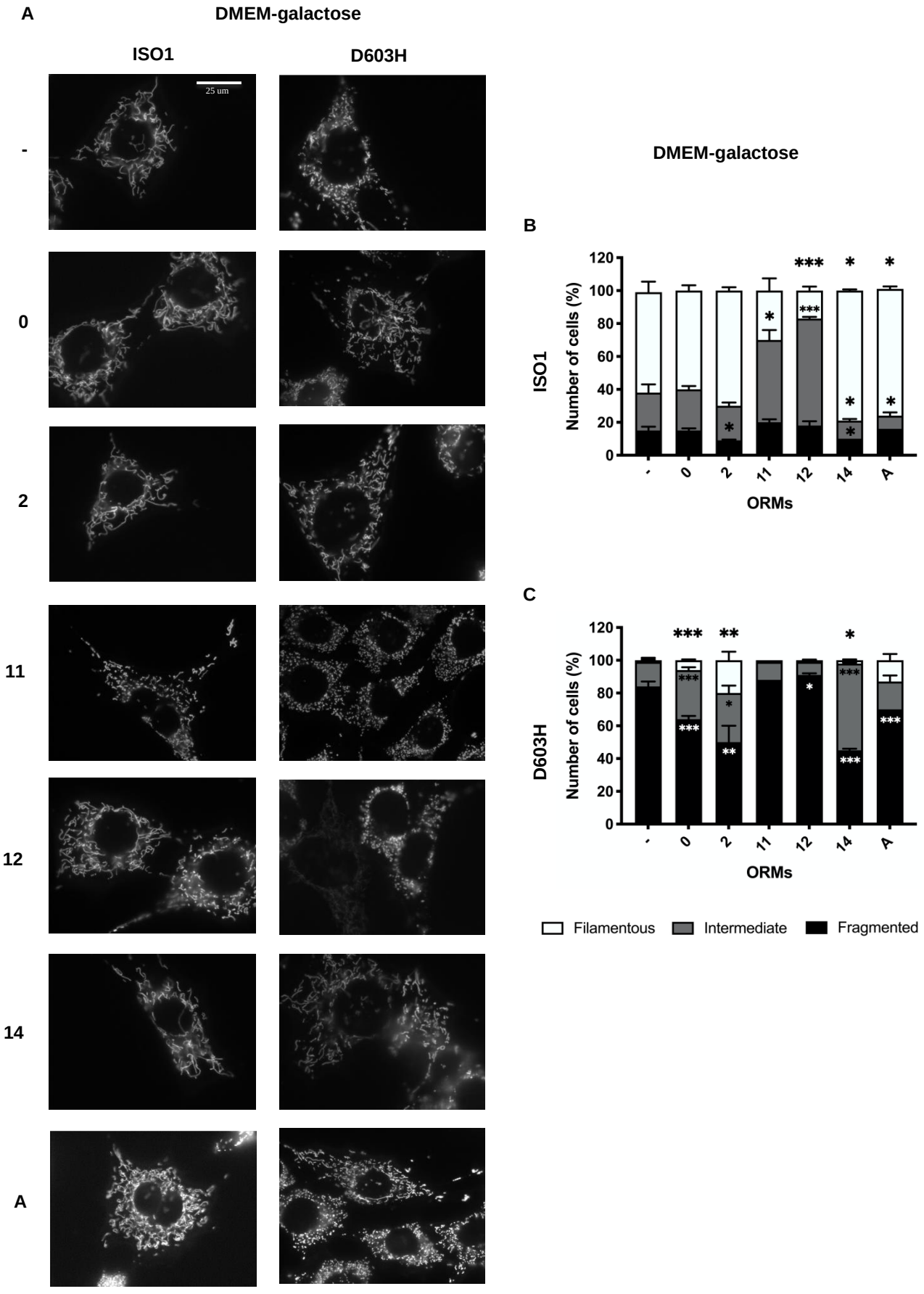

Figure 20 - Mitochondrial network morphology of OPA1 mutated MEFs incubated with ORMs. (A) Representative images of mitochondrial network of ISO1 and D603H after labeling with Mitotracker Red. MEFs lines were incubated for 24 h in DMEM-galactose in absence or presence of the ORMs. Cells were scored in three categories on the basis of mitochondrial network

morphologies: cells with filamentous and inter- connected network (filamentous), cells with short filamentous mitochondria (intermediate) and cells with fragmented mitochondria (fragmented). 100–120 cells were analyzed for ISO1 (B) and D603H (C) in each condition and for each experiment. Data are means±SEM of 3–4 independent experiments. ∗P < 0.05, ∗∗P < 0.01, ∗∗∗P < 0.001.

Furthermore, we tested the same set of ORMs on R445H both in DMEM-glucose and galactose media, showing no effect for any compound on mitochondrial network of these cells (Fig.21 A-C). This result suggests that the mitochondrial fragmentation induced by this mutation is too deleterious for a pharmacological rescuing.

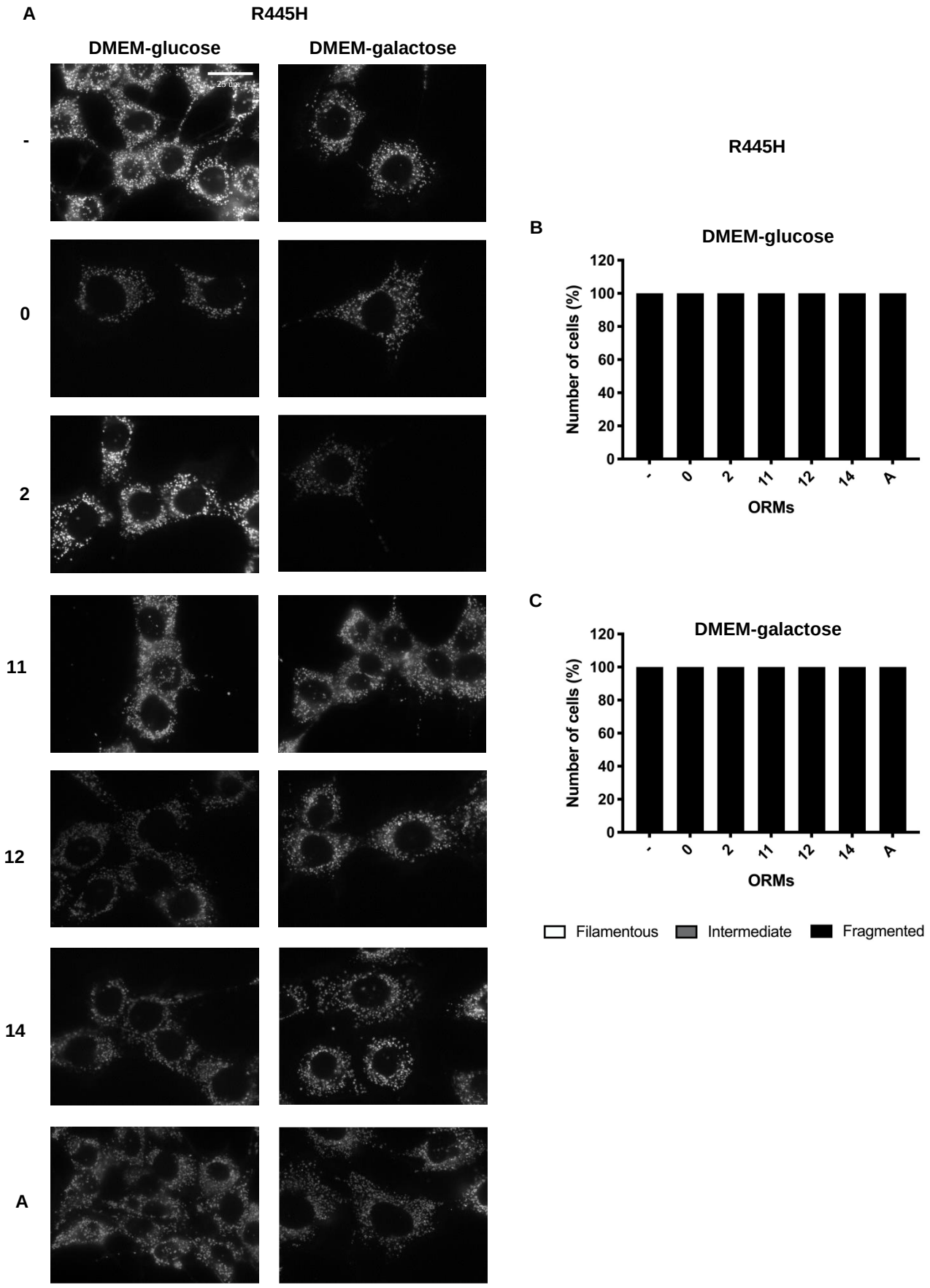

Figure 21 - Mitochondrial network morphology of R445H MEFs incubated with ORMs. (A) Representative images of mitochondrial network of R445H after labeling with Mitotracker Red. MEFs lines were incubated for 24 h in DMEM-glucose or DMEM-galactose in absence or presence of the ORMs. Cells were scored in three categories on the basis of mitochondrial network morphologies: cells

with filamentous and inter- connected network (filamentous), cells with short filamentous mitochondria (intermediate) and cells with fragmented mitochondria (fragmented). 100–120 cells were analyzed for R445H (B-C) in each condition and for each experiment. Data are means±SEM of 3–4 independent experiments.

Summarizing, the results derived from the analysis of cellular mitochondrial network indicated that , ORM0, 2, 14, and A showed a significant reduction of cells with fragmented mitochondria both in ISO1 and D603H. Furthermore, considering that ORM11 often showed negative effects on cell viability, ATP cellular levels and mitochondrial network, we decided to rule out it in the following analysis.

4.2.2 Identification of putative ORMs-target pathways

4.2.2.1 Mitochondrial shaping proteins

Having observed that some ORMs induced a shift towards a more filamentous mitochondrial morphology, we aimed to assess the expression of mitochondrial proteins involved in the process of mitochondrial fission and fusion by western blot in presence or absence of ORMs in DMEM-galactose. It was previously reported that in DMEM-glucose MEFs carrying D603H and R445H mutations showed similar levels of OPA1, OPA1 long/short ratio, MFN2, and DPR1, indicating that their protein expression was not influenced by mutated OPA1 (Del Dotto, Fogazza, Musiani, et al., 2018). In addition, cell treatment with ORMs in DMEM-galactose for 24h did not modify the content of OPA1 and its long/short form ratio indicating no effect on the balance between these two forms (Fig.22 A-C).

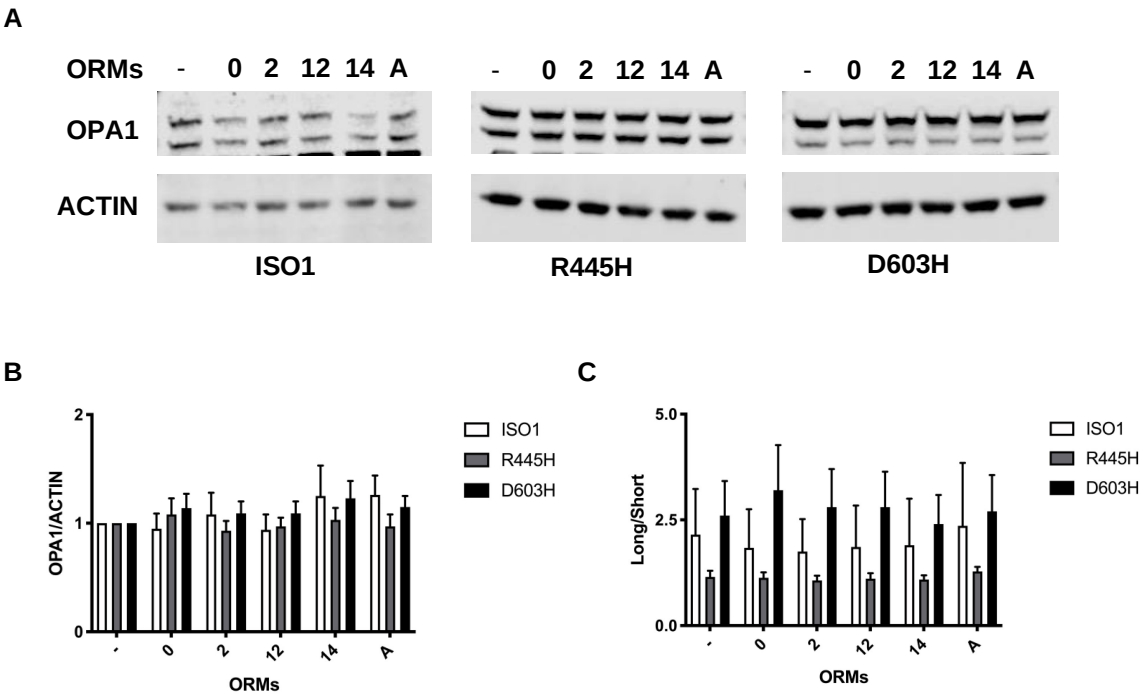

Figure 22 - Levels of OPA1 in OPA1 mutated MEFs. (A) Representative blots of OPA1 after incubation in DMEM-galactose whit or without ORMs for 24 hours. ACTIN was used as a loading control (B) Densitometric analysis of OPA1 protein levels. (C) Densitometric analysis of OPA1 long-/short- forms ratio Data are normalized on the untreated cells in DMEM- galactose. Data are means ± SEM of 3 experiments.

Further, we analysed the expression levels of other mitochondrial shaping proteins like MFN2, DRP1 and its active form phosphorylated at position S616 (DRP1-p-S616), observing no variations in cells treated with ORMs in DMEM-galactose (Fig.23 A-E).

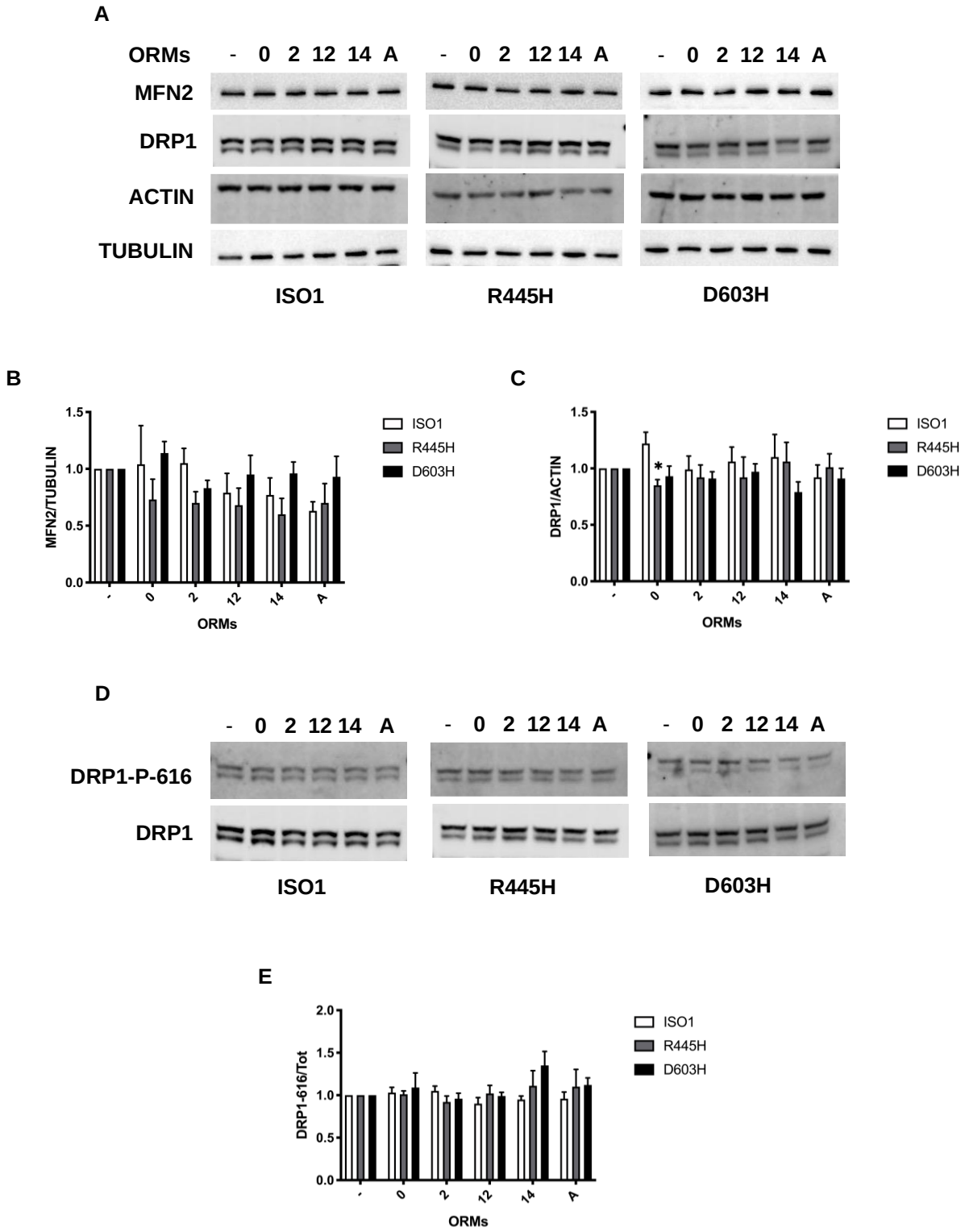

*Figure 23 - Expression levels of proteins involved in mitochondrial fusion and fission in OPA1 mutated MEFs. (A, D) Representative blots of MFN2, DRP1, DRP1-P-616 after incubation in DMEM-galactose whit or without ORMs for 24 hours. ACTIN or TUBULIN were used as a loading control (B-C) Densitometric analysis of MFN2, DRP1 protein levels. (E) Densitometric analysis of DRP1-P-616/DRP1 ratio. Data are normalized on the untreated cells in DMEM- galactose. Data are means ± SEM of 3 experiments. * Indicates $P < 0,05$.*

This suggests that ORMs do not directly influence the key proteins of the mitochondrial shaping dynamics but rather their interactors or, they possibly use different pathways to achieve this result.

4.2.2.2 Mitochondrial mass and OXPHOS complexes

To understand the mechanism underlying the increase of cell viability and ATP content induced by the treatment with some ORMs in the two mutant cell lines, we evaluated the mitochondrial mass and the expression of the OXPHOS complexes in DMEM-galactose with or without ORMs. Firstly, we analysed the levels of representative proteins of different mitochondrial compartments by western blot. The protein levels of TOM20 subunit of the translocase of the outer membrane were similar in ISO1 and R445H, while a significant decrease was evident in D603H after incubation with ORM12 (Fig.24 A-B). However, no differences were observed in protein expression of TIM23 subunit of the inner mitochondrial membrane translocase as well as the heat shock protein 60 (HSP60) and the citrate synthase (CS), which are in the matrix (Fig.24 A, C-E).

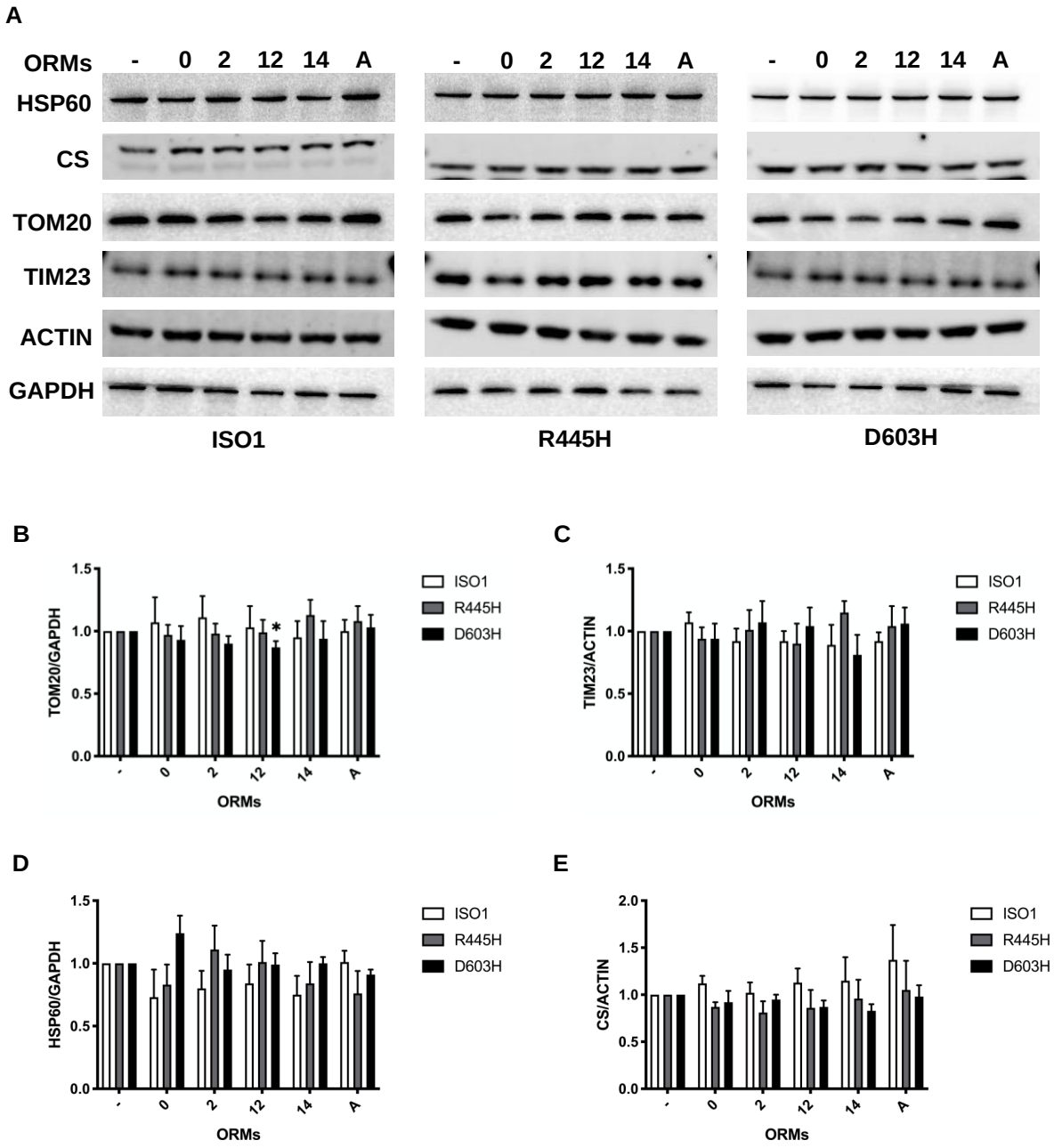

Figure 24 - Mitochondrial protein content of OPA1 mutated MEFs incubated with ORMs. MEFs were incubated for 24 h in DMEM-galactose in the absence or presence of ORMs. (A) Western blot of representative proteins of outer (TOM20) and inner (TIM23) mitochondrial membrane and of the matrix (citrate synthase and Hsp60). ACTIN or GAPDH were used as a loading control. (B–E) Densitometric analysis of the mitochondrial mass proteins; data are normalized to those of untreated cells in DMEM-galactose. Values are means ± SEM (n = 4–8). ∗P < 0.05, one simple t test.

Finally, we determined the expression of the representative subunits of the OXPHOS complexes: NDUFA9 for CI, SDHA for CII, UQCRC2 for CIII, COXIV for CIV and ATP5a for CV but also in this case no significant difference was underlined (Fig.25 A-F).

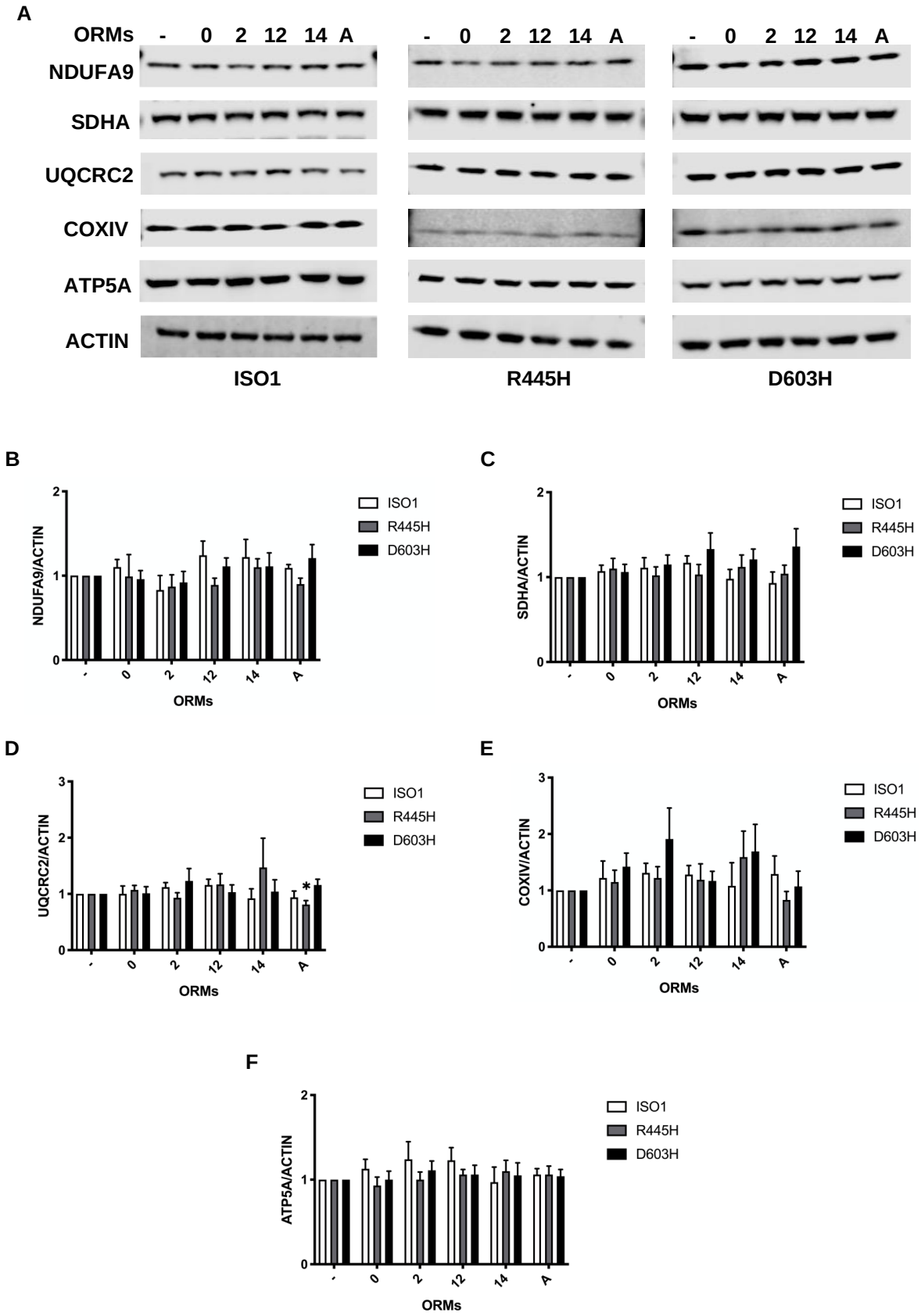

*Figure 25 - Expression levels of OXPHOS complexes in OPA1 mutated MEFs in DMEM-galactose in presence or absence of ORMs. (A) Representative blots of OXPHOS complexes after incubation whit or without ORMs for 24 hours. ACTIN was used as a loading control (B-F) Densitometric analysis of considered proteins. Data are normalized on the untreated cells in DMEM- galactose. Data are means ± SEM of 3 experiments. * Indicates P < 0,05.*

Taken together these data suggest that the increase of cell viability and cellular ATP content is not associated with an increase of mitochondrial biogenesis.

4.2.2.3 Protein involved in the autophagic process

OPA1 is also involved in the autophagy and mitophagy processes which are essential for maintaining the clearance of damaged organelles (L. Liu et al., 2012). Consequentially, we evaluated the autophagic marker microtubule-associated proteins 1A/1B light chain 3B (LC3) expression, considering its cytoplasmic form (LC3-I) and its membrane-bound form (LC3-II) (Lamb et al., 2013). In DMEM-glucose the two mutants showed a reduced LC3II/I ratio compared to ISO1. The incubation in DMEM-galactose, an activator of autophagy (Carelli, Musumeci, et al., 2015) increased proportionally this ratio in all cell lines, remaining lower in R445H and D603H (Fig.26A-B). Hence, this decrease in the LC3II-I ratio in mutant compared to ISO1 suggested a possible impairment of the autophagic process. To verify this, we analysed the autophagic pathway by treating MEFs with the autophagic inducer and mTOR inhibitor rapamycin (1 μM for 24 hours), as well as with chloroquine (80 μM for 2 hours), which blocks lysosome-mediated proteolysis producing an increase of autophagosome numbers (DJ et al., 2016). These two treatments caused accumulation of lipidated LC3 both in ISO1 and OPA1 mutated MEFs (Fig.26 C-D), indicating that the autophagic flux was not affected in our cells, but the only general process of autophagy is reduced in mutant cells.

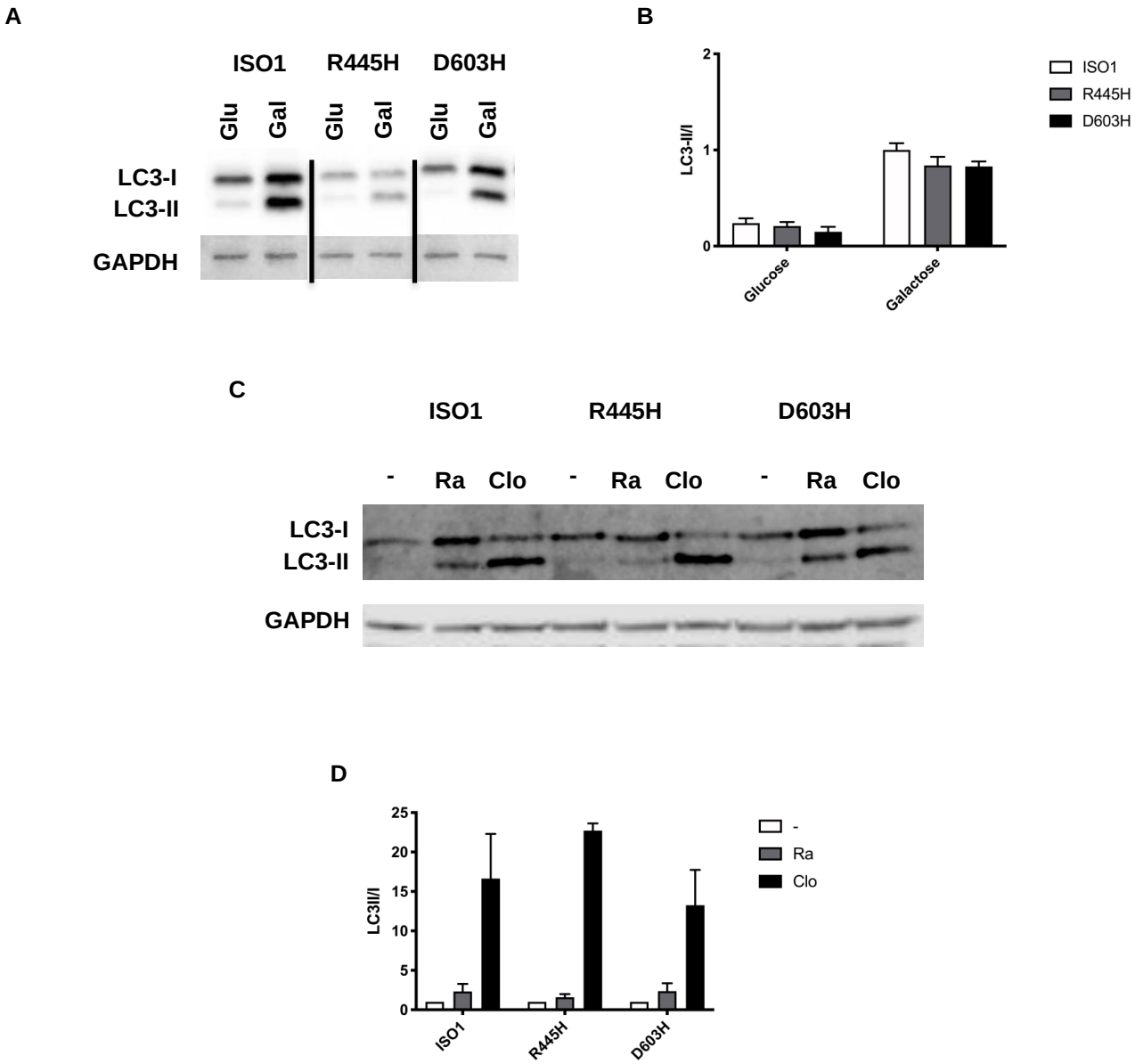

Figure 26 - Expression levels of LC3 in OPA1 mutated MEFs. (A) Representative blots of LC3 in DMEM-glucose and DMEM-galactose in control and mutated cell lines. (B) Densitometric analysis of LC3II/I ratio. (C) Representative blots of LC3 after the treatment with Clorexine and Rapamycin. (D) Densitometric analysis of LC3II/I ratio after Cloroquine (80 μM for 2 hours) and Rapamycin (1 μM for 24 hours) treatment. Data are means ± SEM of 3 experiments.

Incubations with ORMs induced an increase in LC3II/I ratio in R445H, being significant for ORM14, whereas they were ineffective on ISO1 and D603H indicating that this compound may induce autophagy in R445H only (Fig.27 A-B). The first stage of the autophagy process, the phagophore formation, requires activation of ATG12 by ATG7 and then conjugation of ATG12 and ATG5 proteins (Wesselborg & Stork, 2015; Yu et al., 2018).

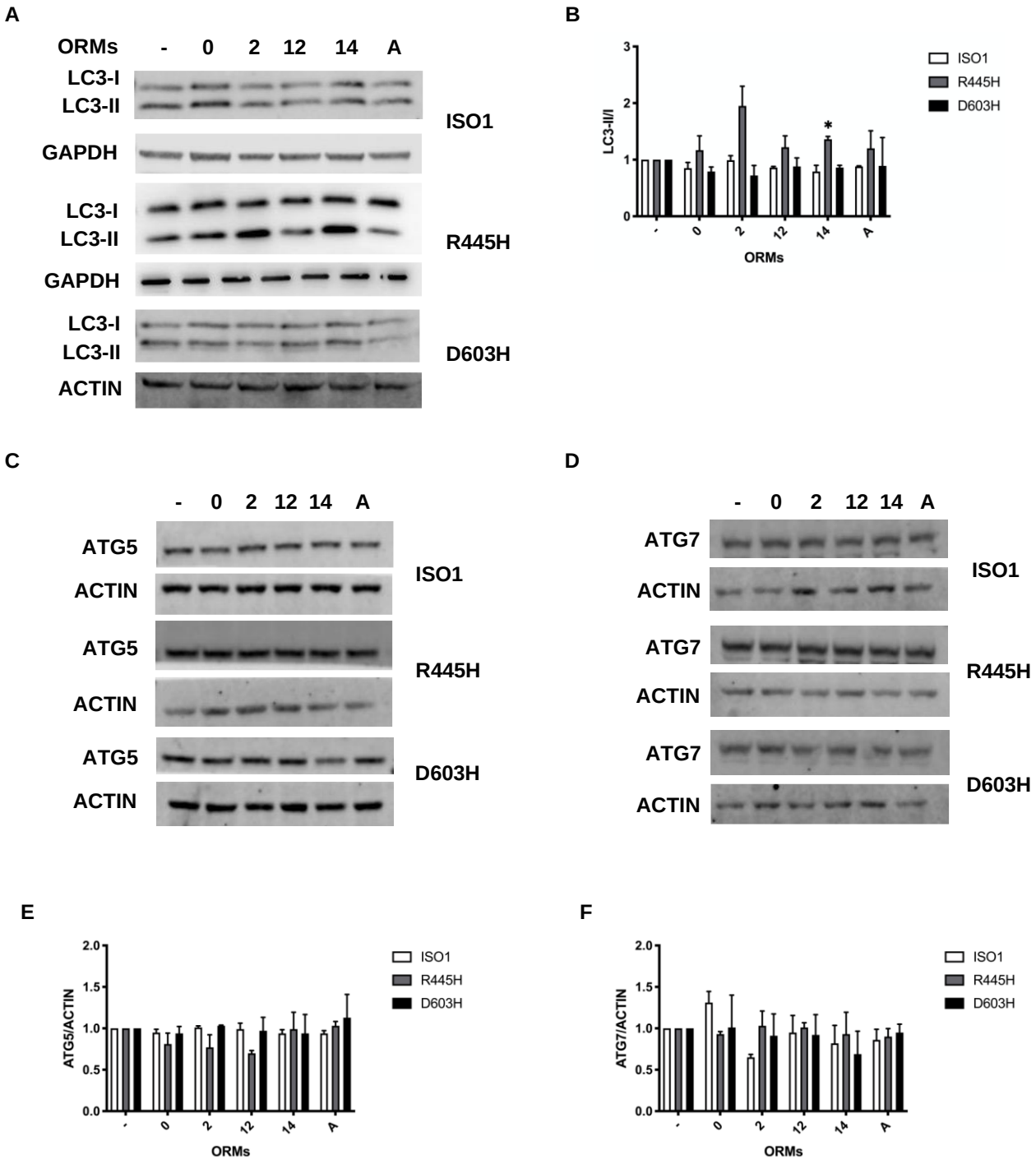

*Figure 27 - Expression levels LC3/ATG5/ATG7. (A, C, D) Representative blots of LC3/ATG5/ATG7 in ISO1 and OPA1 mutated MEFs in DMEM-galactose whit or whitout ORMs. (B, E, F) Densitometric analysis of LC3/ATG5/ATG7. Data are means ± SEM of 3 experiments. * Indicates P < 0,05.*

Therefore, we investigated the expression levels of ATG5 and ATG7 l in all three cell lines in DMEM-galactose medium in presence or absence of ORMs observing that their amounts were not significantly changed by any ORMs, except for ORM12 and ORM2 which reduced ATG5 in R445H (Fig.27C, E) and ATG7 in ISO1 (Fig.27D, F) respectively. Altogether these results indicate that, despite there was no evidence for an impairment in the autophagic process, the basal autophagic

activity seems to be slowed down in the two OPA1 mutants compared to ISO1 in both DMEM-glucose and DMEM-galactose and that in R445H cell line ORM2, 12 and 14 can improve the autophagic process.

4.2.3 Efficiency of ORMs in human fibroblasts

The last step of this study was focused on fibroblasts derived from healthy donors and DOA patients carrying the same R445H and D603H mutations. We were aware that this cellular model suffers several limitations, such as the presence of the wild-type gene in heterozygosis and the heterogeneity of OPA1-induced defect due to the individual nuclear and mitochondrial genomes variability. However, the aim was to validate the effects of these five selected molecules in a more complicated but more physiological model to consolidate the results and get a further step towards a possible therapy. It has previously reported that in fibroblasts, the presence of the wild-type allele mitigates the effect of the mutation and in fact the energy efficiency is not severely compromised, and the morphology of the mitochondrial network shows less impairment which is more evident following metabolic stress (Agier et al., 2012; Amati-Bonneau et al., 2005; Del Dotto, Fogazza, Musiani, et al., 2018; Zanna et al., 2008). Since morphology is a parameter strongly correlated with the severity of the patients' clinical profile, we used this indicator to test the effect of the selected ORMs. In DMEM-galactose, the mitochondria of wild-type and D603H fibroblasts were mainly filamentous and intermediate, those of R445H fibroblasts were intermediate or fragmented. In wild-type fibroblasts, incubation in DMEM-galactose with ORMs determined an increase (significant for all except ORMA) in the percentage of filamentous cells compared to untreated cells (Fig.28 A-B). In R445H fibroblasts, all the ORMs (except ORM2) cause a significant increase in the number of cells with filamentous mitochondria to the detriment of the fragmented ones (Fig.28 A-C). Finally, in D603H fibroblasts the treatment with ORMs increased the percentage of cells with filamentous reticulum being significant for ORM12, 14 and A (Fig.28 A-D).

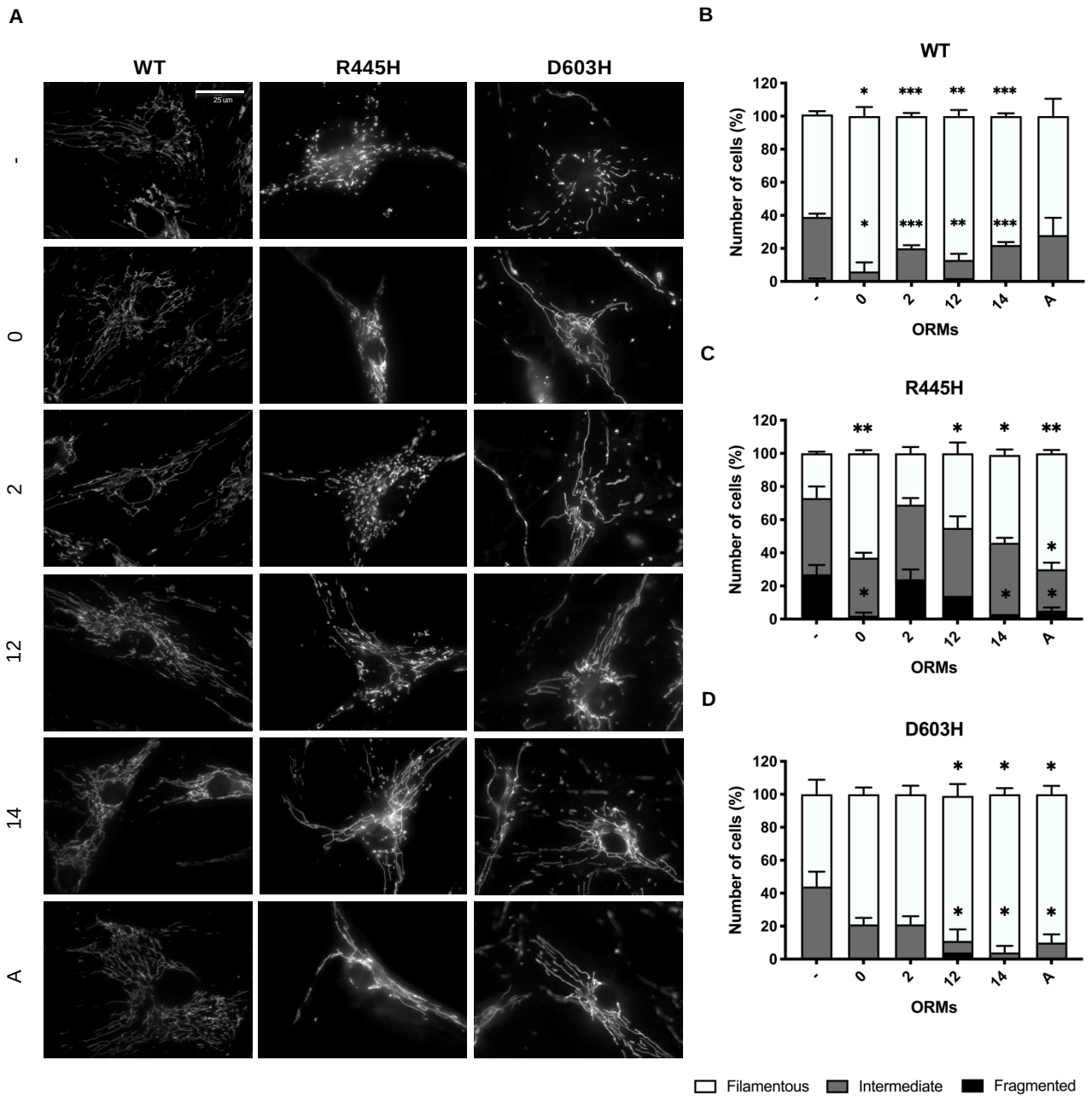

*Figure 28 - Mithocondrial network morphology of DOA patient's fibroblasts in presence or absence of ORMs. (A) Representative images of mitochondrial network whit Mitotracker Red. (B-C) Analysis of the number of cells present in each category considered. 60-80 cells were observed for the analysis. Data are means ± SEM of 3-4 independent experiments. * p < 0,05, ** p < 0,01, *** p < 0,001.*

This first study allowed us to exclude from subsequent analysis ORM2 for the R445H fibroblasts and ORM0 and 2 for the D603H fibroblasts as they did not produce statistically significant results. We then measured the levels of cellular ATP in order to evaluate the energy efficiency after incubation in DMEM-galactose in presence or absence of the ORMs. In DMEM-galactose, the ATP levels of wild-type fibroblasts markedly increased, whereas OPA1 mutated fibroblasts were unable to rise the ATP content (Del Dotto, Fogazza, Musiani, et al., 2018). In the control line, incubation with ORMs did not cause alterations in the percentage of cellular ATP present except for ORM0 in which there

was an increase of about 2 times compared to DMEM-galactose (Fig.29A). In R445H fibroblasts, only ORM14 appeared to increase cellular ATP levels while ORM0 appeared to have a negative effect (Fig.29B). In D603H fibroblasts the treatment with all the ORMs seemed to determine a tendency to increase ATP levels, although not statistically significant (Fig.29C).

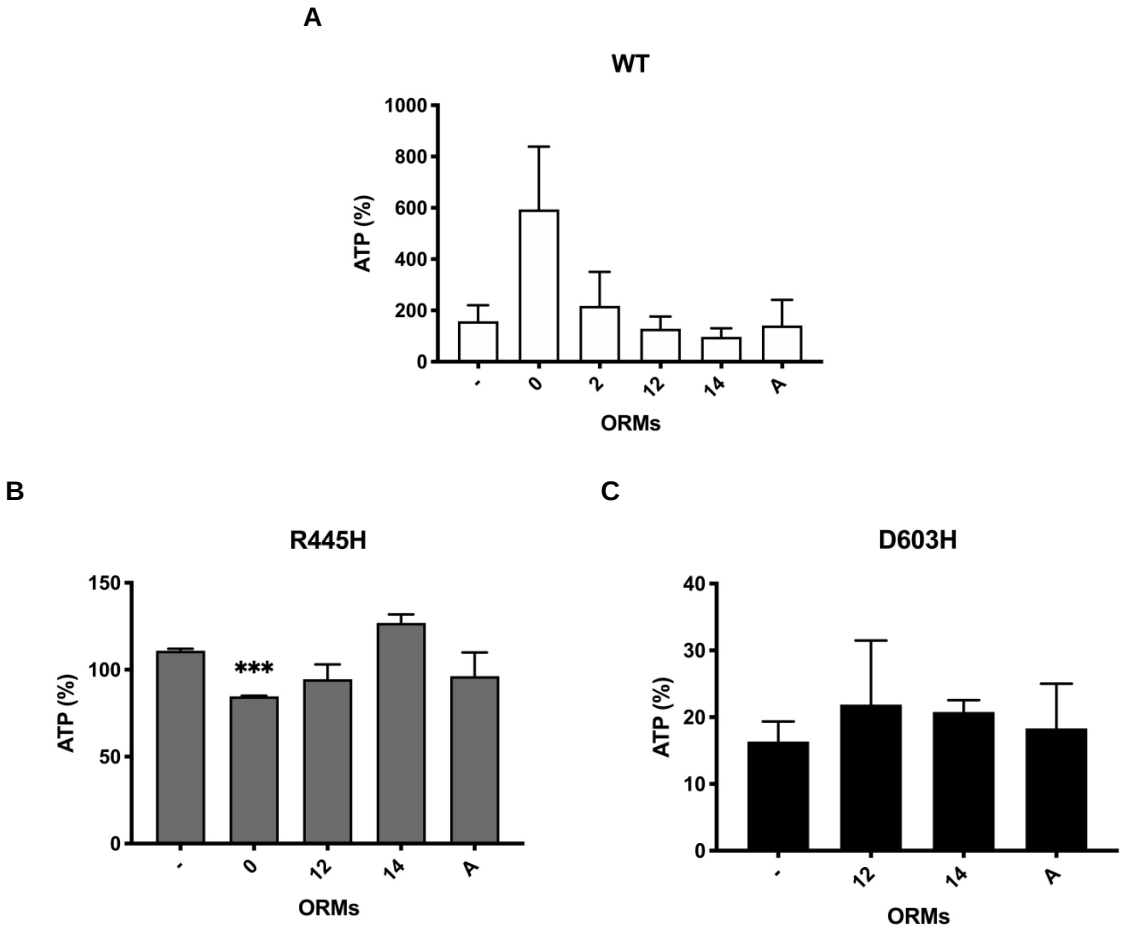

*Figure 29 - ATP content of DOA patient's fibroblast. (A-C) Cellular ATP content of WT, R445H and D603H fibroblasts after 24 hours of incubation in DMEM-galactose ± ORMs. Data are normalized on DMEM at time 0 and expressed as means ± sem of 3 experiments. *** p < 0,001.*

In conclusion, considering the above results, the most of ORMs had a positive effect on mitochondrial morphology in controls and mutants which, as previously mentioned, is the parameter in line with the severity of the patient's clinical phenotype. ORM14 also induces a slight increase in ATP levels in both DOA mutants, thus it seems reasonable to propose this molecule as the best candidate for therapeutic use in DOA patients.

5. DISCUSSIONS AND CONCLUSIONS

In this study, we aimed to better investigate the molecular mechanism of action of idebenone, the first and only approved therapy to date for LHON, and to validate compounds as possible drugs for DOA treatment using a "drug repurposing" approach. Mitochondrial dysfunction is a well-known hallmark of these optic neuropathies. We, therefore, gauged mitochondrial function, especially focusing on bioenergetic status and mitochondrial dynamics, in different cellular models recapitulating the genetic background of these two neurodegenerative diseases.

In the first part of our study, we sought to evaluate the efficacy and the mechanism of idebenone treatment in LHON. In the first clinical trial named Rescue of Hereditary Optic Disease Outpatient Study (RHODOS), although patients treated with idebenone showed an increased frequency of recovery of visual acuity, a portion of them did not respond to the treatment. Moreover, the recovery was significant in patients carrying the m.11778 G>A/*MT-ND4* mutation which is responsible for approximately 70% of LHON cases in Europe (Thomas Klopstock et al., 2011). A retrospective analysis on a cohort of 103 patients confirmed the results of the clinical trial (Carelli et al., 2011b) and a follow-up analysis revealed that idebenone beneficial effect persisted over time (T. Klopstock et al., 2013). Besides these encouraging clinical results, the molecular mechanism and the beneficial effect of idebenone are still poorly understood. Moreover, novel therapeutic strategies are needed for the cure of patients not responding to the current approved therapy. Idebenone effect is deemed to depends on its redox status. When oxidized, idebenone has a negative effect as it increases oxidative stress by inhibiting CI. On the contrary, reduced idebenone exhibits both an antioxidant activity and energetic function transporting electrons to CIII, thereby preserving the energetic status of CI deficient cells (Erb et al., 2012; Haefeli et al., 2011). Hence, the reduction of idebenone seems to be crucial for its therapeutic effect. Idebenone is mainly reduced by the cytosolic dehydrogenase NQO1 but its involvement in idebenone action in LHON has so far remained unexplored. We, therefore, investigated the involvement of NQO1-idebenone-CIII axis in a cybrid cell line harboring the m.3460G>A/*MT-ND1* LHON mutation. Here, we demonstrated for the first time the direct involvement of NQO1 in the bioactivation of idebenone for the rescue of the energetic status in LHON cell models. Two main lines of evidence support this thesis. First, rescue of rotenone-insensitive mitochondrial respiration in idebenone-treated LHON cybrid cells is observed only when NQO1 is overexpressed, whereas when NQO1 is poorly expressed, the treatment has a detrimental effect on mitochondrial respiration as evidenced by a plummeting in oxygen consumption rate. Second, ATP synthesis rate in LHON cells overexpressing NQO1 is rescued only when NADH and idebenone, NQO1 substrates, were added. Moreover, our data also highlight the importance of NQO1

in preventing oxidative stress in LHON. In fact, we observed a decrease in ROS production in untreated LHON cybrids overexpressing NQO1. Noticeably, idebenone-treated LHON cells show elevated ROS levels. Interestingly, when NQO1 was overexpressed, ROS production in LHON cybrids treated with idebenone significantly reduced. Idebenone is CI inhibitor impairing OXPHOS and increasing ROS production. Thus, idebenone treatment may worsens an already impaired situation, as suggest also by previous reports (Degli Esposti et al., 1996; Fato et al., 2008; Jaber & Polster, 2015; M. S. King et al., 2009). A note of caution on the use of Idebenone for LHON patients is therefore advisable. Our biochemical data are in accordance with a previous study in which the crucial role of NQO1 in idebenone bioactivation and toxicity was demonstrated in different cell lines and CI-impaired mouse retinal cells (Varricchio et al., 2020). Importantly, some patients do not respond to idebenone treatment. Klopstock and colleagues suggested that the therapeutic potential of idebenone depends on whether the treatment is initiated early in the disease, when RGCs loss is still minimal, and on the type of mutation. On the basis of our investigation, however, we propose that the different response to idebenone may also depends on NQO1 expression levels. Indeed, our data set revealed a correlation between NQO1 expression and idebenone effectiveness in rescuing mitochondrial respiration. We observed a differential expression of NQO1 in six patient-derived fibroblasts and measured a rescue of rotenone-insensitive respiration in cells expressing NQO1 treated with idebenone. Conversely, in fibroblasts with poor levels of NQO1 idebenone treatment induced a decrease of oxygen consumption rate. Remarkably, we found that NQO1 expression showed a good match with idebenone response in patients. In addition, idebenone efficacy did not depend on LHON mutations since responder and non-responder patients carried both m.3460 G>A/*MT-ND1* or m.11778 G>A/*MT-ND4* mutation. These results confirm that the effect of idebenone on respiratory chain activity depends on its reduction by NQO1. The expression of this dehydrogenase is therefore important in the outcome of the therapy with idebenone. Indeed, when NQO1 is poorly expressed idebenone cannot be properly reduced and may even exhibit a detrimental toxic effect. Considering this, before idebenone administration, NQO1 expression levels should be evaluated in patients since only good levels of NQO1 expression could lead to better outcomes. A clinical trial should be performed to correlate NQO1 expression, possibly in peripheral blood, with idebenone efficacy. The difference of expression levels of NQO1 in cells deserve further investigation. It is well known that NQO1 expression is regulated by the Nrf2 pathway in response to oxidative stress (Dinkova-Kostova & Talalay, 2010; Zhang, 2006), therefore this pathway should be investigated in cells of LHON patients. Furthermore, it has been reported that the presence of some polymorphisms in *NQO1* gene may affect its expression and activity (Siegel et al., 1999; Traver et al., 1997). In particular, previous studies, documented that NQO1*2 polymorphism (NM_000903.3:

c.559C>T known by old nomenclature as c.609C>T) induces a missense mutation P187S, resulting in a protein that is rapidly ubiquitinated and degraded with a consequence of a loss of protein in homozygotes and a reduced expression in heterozygotes. NQO1*3 polymorphism (NM_000903.3: c.415C>T known by old nomenclature as m.465C>T) affects the splicing of NQO1 mRNA, impairing the enzyme expression. Hence, it would be interesting in the future to test NQO1 polymorphisms in patients to evaluated whether there is a correlation with the effectiveness of idebenone therapy. Despite the interesting results obtained studying the relationship between NQO1 and idebenone efficacy, we cannot rule out that *in vivo* idebenone metabolites might have some therapeutic activity. It has been already reported that QS-10, the first idebenone metabolite, was able to be reduced by NQO1 but not to restore ATP levels in cells inhibited with rotenone (Haefeli et al., 2011). However, these data are in contrast with another study that showed that chemically reduced QS-10 is able to sustain cellular respiration in cells with defective CI and increases respiration and survival in *Zebra fish* treated with rotenone (Giorgio et al., 2018). At present, it is unclear how these discrepancies can be explained and further experiments are required. Finally, since NQO1 expression is regulated via Nrf2 pathway, a combination with Nrf2-inducing agent, such as sulforaphane, resveratrol, and dimethyl fumarate (DMF) may improve idebenone efficacy. Also different compounds derived from medical plants have been shown to increase the Nrf2-mediated NQO1 increase expression (Hamed et al., 2016). Our preliminary data support the idea of a possible synergic treatment with idebenone and Nrf2-inducing agents. In fact, treatment with DMF in patient-derived fibroblasts poorly expressing NQO1 led to an increase of NQO1 expression and a rescue of mitochondrial respiration. In conclusion, we suggest that the induction of NQO1 expression might increase the neuroprotective potential of idebenone and may have a beneficial effect *per se* as it has a direct antioxidant role (Dinkova-Kostova & Talalay, 2010; Ross & Siegel, 2004).

In the second part of the study, we aimed to validate FDA-approved compounds as possible drugs for DOA treatment using a “drug repurposing” approach. We have therefore gauged the efficacy of six compounds, renamed OPA1 rescuing molecules (ORMs), previously identified via yeast-based drug screening on more than 2,500 molecules, in DOA cell models, namely MEFs and patient-derived fibroblasts bearing the R445H and D603H. Among the six ORMs identified in yeast, five (ORM0, 2, 12, 14, and A) showed an improvement in mitochondrial function and/or morphology in OPA1 mutated MEFs. In particular, ORM12 ameliorated only cell viability, ORMA rescued mitochondrial reticulum morphology, whereas ORMs 0, 2 and 14 improved both mitochondrial morphology and ATP content, thereby resulting the most effective compounds in these cell models. In patient-derived fibroblasts, however, only ORM14 improved both mitochondrial network morphology and bioenergetics. We also investigated the molecular mechanism of ORMs identifying the activation of

autophagy as a possible common mechanism of these molecules. Furthermore, our investigation allowed us to rule out the direct action of ORMs on mitochondrial biogenesis and shaping proteins expression to explain the observed network morphology amelioration. Overall, since ORM14, tolfenamic acid, was the most effective on both cell models, we suggest it as the most promising compound to be used for drug repurposing in clinical trial for DOA or other neurodegeneration associated with OPA1 mutations.

Tolfenamic acid is a non-steroidal anti-inflammatory drug (Shao et al., 2015) which inhibits cyclooxygenase-2 (COX-2) and NF-κB (Pathi et al., 2014; Wilson et al., 2016). This molecule has been widely tested on different neurodegenerative disease models (Guan & Wang, 2019; Kaur et al., 2017). Importantly, tolfenamic acid downregulates transcriptional targets of Specific protein 1 (Sp1), *i.e.* Alzheimer's diseases related proteins including Cyclin Dependent Kinase 5 (CDK5) (Adwan et al., 2015; Chang et al., 2018; Subaiea et al., 2013, 2015). Strikingly, CDK5 is known to phosphorylate DRP1 inducing mitochondrial fission and apoptosis in neurons (Guo et al., 2018; Jahani-Asl et al., 2015). Thus, the positive effect of tolfenamic acid on mitochondrial network morphology in OPA1 mutant cell models may depend on a downregulation of mitochondrial fission due to decreased CDK5 protein levels and a consequent DRP1 inhibition. Interestingly, a recent work showed that tolfenamic acid exhibits antioxidant properties increasing the expression of NRF2, NQO1 and HO1, as well as pro-autophagic effect in a Huntington's disease model (P. Liu et al., 2019). We also observed an autophagic activation in R445H MEFs, suggesting that tolfenamic acid may increase the autophagic function in models of different neurodegenerative diseases. Also, ORMs 0, 12 and A have been tested for similar diseases and seem to activate autophagy as well. Indeed, these ORMs have been reported to reduce the oxidative stress via NRF2 activation, increase autophagy through mTOR/Akt pathway inhibition, and decrease inflammation by downregulation of NF-kB signalling. ROS production and mitochondrial filamentous reticulum have been reported to be inversely corelated (Willems et al., 2015). Indeed, both ORMs 0 and 14, which improve mitochondrial network morphology in our models, show an antioxidant activity involving NRF2, the master regulator of cellular redox homeostasis (Holmström et al., 2016). NRF2 is involved also in autophagy since it activates transcription of macroautophagy genes, such as p62 (Pajares et al., 2016). Autophagy is impaired in mutated MEFs as evidenced by our metabolomic analysis also showing a significant decrease in cellular amino acids content, more severe in the R445H than in D603H MEFs (Chao De La Barca et al., 2020). ORMs 0, 2 and 14 were able to increase the ATP content and to reactivate autophagy in R445H MEFs, as indicated by the induction of LC3-I cleavage in these cells. This outcome suggests that autophagy activation in cells having a severe energetic failure may act as a compensatory mechanism for ATP production (J. Yang et al., 2019). The lack of effect of ORMs on the LC3-I

cleavage on D603H MEFs, which do not present a severe energetic impairment, may support this hypothesis. Furthermore, autophagy is linked to inflammasomes, multi-protein platforms assembled in responses to different stimuli, including damage-associated molecular patterns (DAMPs). In fact, autophagy reduces the release of mitochondria-derived DAMPs suppressing inflammasome activation, which is associated with neurodegenerative disease onset and progression (Chitnis & Weiner, 2017; Grazioli & Pugin, 2018; Sun et al., 2017) Indeed, a study showed that the specific muscle Opa1 knock out in mice induced mtDNA-mediated inflammation and activation of NF-kB and TLR9 pathways (Rodríguez-Nuevo et al., 2018). Additionally, several studies demonstrated the link between OPA1 and NF-kB signaling (Albensi, 2019; Herkenne et al., 2020; Laforge et al., 2016). Remarkably, ORMs 0, 12 and 14 present anti-inflammatory activity, supporting the hypothesis of a role of inflammation and NF-kB pathway in DOA pathogenesis. Our results, moreover, suggest the possibility that both ROS and inflammation are activated in mutated cells and that ORM treatment induces both NRF2 and autophagy to counteract the dysregulation of these pathways.

In conclusion, by performing thorough molecular and biochemical analyses we have dissected the mechanism of action of idebenone, finding in its NQO1-mediated reduction the principal mechanism for bioactivation and toxic prevention. These results open new perspectives to optimize the effect of idebenone in LHON therapy performing genetic analysis on NQO1 polymorphisms in patients and/or enhancing NQO1 expression by Nrf2 pathway inducers to increase the idebenone effect. In addition, the possible correlation between the lack of effect of idebenone in some patients and a reduced expression of NQO1 leads to carefully evaluate NQO1 polymorphisms and expression in LHON patients before idebenone treatment, since its effect is strictly linked to NQO1 activity. However, it is well known that idebenone is well tolerated in human, probably because it is reduced not only by NQO1 but also by other dehydrogenases, therefore further studies are required to investigate the role of these enzymes, idebenone, and its metabolites in LHON.

The study conducted in cellular DOA models highlights the efficacy of these models to perform a screening to discover drugs for a disease that is orphan of a therapy. From this study, we propose tolfenamic acid as the most promising compound to be used for DOA treatment as it caused the major recovery from mitochondrial dysfunctions probably via the induction of autophagy, decrease of ROS production, or inflammation reduction. The results presented in this thesis arise from two parallel and independent projects, however considering that DOA share some common feature with LHON and idebenone is used also for DOA treatment, but its efficacy is poorly investigated, future studies are planned to also evaluate the effect of idebenone and NQO1 in DOA cell models.

6. BIBLIOGRAPHY

Acín-Pérez, R., Fernández-Silva, P., Peleato, M. L., Pérez-Martos, A., & Enriquez, J. A. (2008). Respiratory Active Mitochondrial Supercomplexes. *Molecular Cell*, *32*(4), 529–539. https://doi.org/10.1016/j.molcel.2008.10.021

Adwan, L., Subaiea, G. M., Basha, R., & Zawia, N. H. (2015). Tolfenamic acid reduces tau and CDK5 levels: Implications for dementia and tauopathies. *Journal of Neurochemistry*, *133*(2), 266–272. https://doi.org/10.1111/jnc.12960

Agier, V., Oliviero, P., Lainé, J., L'Hermitte-Stead, C., Girard, S., Fillaut, S., Jardel, C., Bouillaud, F., Bulteau, A. L., & Lombès, A. (2012). Defective mitochondrial fusion, altered respiratory function, and distorted cristae structure in skin fibroblasts with heterozygous OPA1 mutations. *Biochimica et Biophysica Acta - Molecular Basis of Disease*, *1822*(10), 1570–1580. https://doi.org/10.1016/j.bbadis.2012.07.002

Albensi, B. C. (2019). What is nuclear factor kappa B (NF-κB) doing in and to the mitochondrion? In *Frontiers in Cell and Developmental Biology* (Vol. 7, Issue JULY). Front Cell Dev Biol. https://doi.org/10.3389/fcell.2019.00154

Aleo, S. J., Del Dotto, V., Fogazza, M., Maresca, A., Lodi, T., Goffrini, P., Ghelli, A., Rugolo, M., Carelli, V., Baruffini, E., & Zanna, C. (2020). Drug repositioning as a therapeutic strategy for neurodegenerations associated with OPA1 mutations. *Human Molecular Genetics*, *29*(22), 3631–3645. https://doi.org/10.1093/hmg/ddaa244

Amati-Bonneau, P., Guichet, A., Olichon, A., Chevrollier, A., Viala, F., Miot, S., Ayuso, C., Odent, S., Arrouet, C., Verny, C., Calmels, M. N., Simard, G., Belenguer, P., Wang, J., Puel, J. L., Hamel, C., Malthièry, Y., Bonneau, D., Lenaers, G., & Reynier, P. (2005). OPA1 R445H mutation in optic atrophy associated with sensorineural deafness. *Annals of Neurology*, *58*(6), 958–963. https://doi.org/10.1002/ana.20681

Amati-Bonneau, P., Milea, D., Bonneau, D., Chevrollier, A., Ferré, M., Guillet, V., Gueguen, N., Loiseau, D., Crescenzo, M. A. P. de, Verny, C., Procaccio, V., Lenaers, G., & Reynier, P. (2009). OPA1-associated disorders: Phenotypes and pathophysiology. In *International Journal of Biochemistry and Cell Biology* (Vol. 41, Issue 10, pp. 1855–1865). Int J Biochem Cell Biol. https://doi.org/10.1016/j.biocel.2009.04.012

Amati-Bonneau, P., Odent, S., Derrien, C., Pasquier, L., Malthiéry, Y., Reynier, P., & Bonneau, D. (2003). The association of autosomal dominant optic atrophy and moderate deafness may be due to the R445H mutation in the OPA1 gene. *American Journal of Ophthalmology*, *136*(6), 1170–1171. https://doi.org/10.1016/S0002-9394(03)00665-2

Amati-Bonneau, P., Valentino, M. L., Reynier, P., Gallardo, M. E., Bornstein, B., Boissière, A., Campos, Y., Rivera, H., De La Aleja, J. G., Carroccia, R., Iommarini, L., Labauge, P., Figarella-Branger, D., Marcorelles, P., Furby, A., Beauvais, K., Letournel, F., Liguori, R., La Morgia, C., … Carelli, V. (2008). OPA1 mutations induce mitochondrial DNA instability and optic atrophy "plus" phenotypes. *Brain*, *131*(2), 338–351. https://doi.org/10.1093/brain/awm298

Amore, G., Romagnoli, M., Carbonelli, M., Barboni, P., Carelli, V., & La Morgia, C. (2021). Therapeutic Options in Hereditary Optic Neuropathies. In *Drugs* (Vol. 81, Issue 1, pp. 57–86). Drugs. https://doi.org/10.1007/s40265-020-01428-3

Amutha, B., Gordon, D. M., Gu, Y., & Pain, D. (2004). A novel role of Mgm1p, a dynamin-related GTPase, in ATP synthase assembly and cristae formation/maintenance. *Biochemical Journal*, *381*(1), 19–23. https://doi.org/10.1042/BJ20040566

Asher, G., Dym, O., Tsvetkov, P., Adler, J., & Shaul, Y. (2006). The crystal structure of NAD(P)H quinone oxidoreductase 1 in complex with its potent inhibitor dicoumarol. *Biochemistry*, *45*(20), 6372–6378. https://doi.org/10.1021/bi0600087

Baracca, A., Solaini, G., Sgarbi, G., Lenaz, G., Baruzzi, A., Schapira, A. H. V., Martinuzzi, A., &

Carelli, V. (2005). Severe impairment of complex I-driven adenosine triphosphate synthesis in leber hereditary optic neuropathy cybrids. *Archives of Neurology*, *62*(5), 730–736. https://doi.org/10.1001/archneur.62.5.730

Baradaran, R., Berrisford, J. M., Minhas, G. S., & Sazanov, L. A. (2013). Crystal structure of the entire respiratory complex i. *Nature*, *494*(7438), 443–448. https://doi.org/10.1038/nature11871

Barboni, P., Carbonelli, M., Savini, G., Foscarini, B., Parisi, V., Valentino, M. L., Carta, A., Negri, A. De, Sadun, F., Zeviani, M., Sadun, A. A., Schimpf, S., Wissinger, B., & Carelli, V. (2010). OPA1 mutations associated with dominant optic atrophy influence optic nerve head size. *Ophthalmology*, *117*(8), 1547–1553. https://doi.org/10.1016/j.ophtha.2009.12.042

Barboni, P., Valentino, M. L., La Morgia, C., Carbonelli, M., Savini, G., De Negri, A., Simonelli, F., Sadun, F., Caporali, L., Maresca, A., Liguori, R., Baruzzi, A., Zeviani, M., & Carelli, V. (2013). Idebenone treatment in patients with OPA1-mutant dominant optic atrophy. In *Brain* (Vol. 136, Issue 2). Brain. https://doi.org/10.1093/brain/aws280

Bertholet, A. M., Delerue, T., Millet, A. M., Moulis, M. F., David, C., Daloyau, M., Arnauné-Pelloquin, L., Davezac, N., Mils, V., Miquel, M. C., Rojo, M., & Belenguer, P. (2016). Mitochondrial fusion/fission dynamics in neurodegeneration and neuronal plasticity. In *Neurobiology of Disease* (Vol. 90, pp. 3–19). Neurobiol Dis. https://doi.org/10.1016/j.nbd.2015.10.011

Bianco, A., Bisceglia, L., Russo, L., Palese, L. L., D'Agruma, L., Emperador, S., Montoya, J., Guerriero, S., & Petruzzella, V. (2017). High mitochondrial DNA copy number is a protective factor from vision loss in heteroplasmic leber's hereditary optic neuropathy (LHON). *Investigative Ophthalmology and Visual Science*, *58*(4), 2193–2197. https://doi.org/10.1167/iovs.16-20389

Bogenhagen, D. F. (2012). Mitochondrial DNA nucleoid structure. In *Biochimica et Biophysica Acta - Gene Regulatory Mechanisms* (Vol. 1819, Issues 9–10, pp. 914–920). Biochim Biophys Acta. https://doi.org/10.1016/j.bbagrm.2011.11.005

Bonifert, T., Karle, K. N., Tonagel, F., Batra, M., Wilhelm, C., Theurer, Y., Schoenfeld, C., Kluba, T., Kamenisch, Y., Carelli, V., Wolf, J., Gonzalez, M. A., Speziani, F., Schüle, R., Züchner, S., Schöls, L., Wissinger, B., & Synofzik, M. (2014). Pure and syndromic optic atrophy explained by deep intronic OPA1 mutations and an intralocus modifier. *Brain*, *137*(8), 2164–2177. https://doi.org/10.1093/brain/awu165

Bradford, M. (1976). A Rapid and Sensitive Method for the Quantitation of Microgram Quantities of Protein Utilizing the Principle of Protein-Dye Binding. *Analytical Biochemistry*, *72*(1–2), 248–254. https://doi.org/10.1006/abio.1976.9999

Brandt, U. (2006). Energy converting NADH:quinone oxidoreductase (complex I). In *Annual Review of Biochemistry* (Vol. 75, pp. 69–92). Annu Rev Biochem. https://doi.org/10.1146/annurev.biochem.75.103004.142539

Brown, M. D., Trounce, I. A., Jun, A. S., Allen, J. C., & Wallace, D. C. (2000). Functional analysis of lymphoblast and cybrid mitochondria containing the 3460, 11778, or 14484 leber's hereditary optic neuropathy mitochondrial DNA mutation. *Journal of Biological Chemistry*, *275*(51), 39831–39836. https://doi.org/10.1074/jbc.M006476200

Brown, M. D., & Wallace, D. C. (1994). Molecular basis of mitochondrial DNA disease. *Journal of Bioenergetics and Biomembranes*, *26*(3), 273–289. https://doi.org/10.1007/BF00763099

Carelli, V., D'Adamo, P., Valentino, M. L., La Morgia, C., Ross-Cisneros, F. N., Caporali, L., Maresca, A., Polosa, P. L., Barboni, P., De Negri, A., Sadun, F., Karanjia, R., Salomao, S. R., Berezovsky, A., Chicani, F., Moraes, M., Filho, M. M., Belfort, R., & Sadun, A. A. (2016). Parsing the differences in affected with LHON: Genetic versus environmental triggers of disease conversion. In *Brain* (Vol. 139, Issue 3, p. e17). Brain. https://doi.org/10.1093/brain/awv339

Carelli, V., Franceschini, F., Venturi, S., Barboni, P., Savini, G., Barbieri, G., Pirro, E., La Morgia, C., Valentino, M. L., Zanardi, F., Violante, F. S., & Mattioli, S. (2007). Grand rounds: Could

occupational exposure to n-hexane and other solvents precipitate visual failure in Leber hereditary optic neuropathy? *Environmental Health Perspectives*, *115*(1), 113–115. https://doi.org/10.1289/ehp.9245

Carelli, V., Ghelli, A., Ratta, M., Bacchilega, E., Sangiorgi, S., Mancini, R., Leuzzi, V., Cortelli, P., Montagna, P., Lugaresi, E., & Degli Esposti, M. (1997). Leber's hereditary optic neuropathy: Biochemical effect of 11778/ND4 and 3460/ND1 mutations and correlation with the mitochondrial genotype. *Neurology*, *48*(6), 1623–1632. https://doi.org/10.1212/WNL.48.6.1623

Carelli, V., La Morgia, C., Valentino, M. L., Barboni, P., Ross-Cisneros, F. N., & Sadun, A. A. (2009). Retinal ganglion cell neurodegeneration in mitochondrial inherited disorders. In *Biochimica et Biophysica Acta - Bioenergetics* (Vol. 1787, Issue 5, pp. 518–528). Biochim Biophys Acta. https://doi.org/10.1016/j.bbabio.2009.02.024

Carelli, V., Maresca, A., Caporali, L., Trifunov, S., Zanna, C., & Rugolo, M. (2015). Mitochondria: Biogenesis and mitophagy balance in segregation and clonal expansion of mitochondrial DNA mutations. In *International Journal of Biochemistry and Cell Biology* (Vol. 63, pp. 21–24). Int J Biochem Cell Biol. https://doi.org/10.1016/j.biocel.2015.01.023

Carelli, V., Morgia, C. La, Valentino, M. L., Rizzo, G., Carbonelli, M., De Negri, A. M., Sadun, F., Carta, A., Guerriero, S., Simonelli, F., Sadun, A. A., Aggarwal, D., Liguori, R., Avoni, P., Baruzzi, A., Zeviani, M., Montagna, P., & Barboni, P. (2011a). Idebenone treatment in Leber's hereditary optic neuropathy. In *Brain* (Vol. 134, Issue 9, pp. 1–5). Brain. https://doi.org/10.1093/brain/awr180

Carelli, V., Morgia, C. La, Valentino, M. L., Rizzo, G., Carbonelli, M., De Negri, A. M., Sadun, F., Carta, A., Guerriero, S., Simonelli, F., Sadun, A. A., Aggarwal, D., Liguori, R., Avoni, P., Baruzzi, A., Zeviani, M., Montagna, P., & Barboni, P. (2011b). Idebenone treatment in Leber's hereditary optic neuropathy. In *Brain* (Vol. 134, Issue 9, pp. 1–5). Brain. https://doi.org/10.1093/brain/awr180

Carelli, V., Musumeci, O., Caporali, L., Zanna, C., La Morgia, C., Del Dotto, V., Porcelli, A. M., Rugolo, M., Valentino, M. L., Iommarini, L., Maresca, A., Barboni, P., Carbonelli, M., Trombetta, C., Valente, E. M., Patergnani, S., Giorgi, C., Pinton, P., Rizzo, G., … Zeviani, M. (2015). Syndromic parkinsonism and dementia associated with OPA1 missense mutations. *Annals of Neurology*, *78*(1), 21–38. https://doi.org/10.1002/ana.24410

Carelli, V., Rugolo, M., Sgarbi, G., Ghelli, A., Zanna, C., Baracca, A., Lenaz, G., Napoli, E., Martinuzzi, A., & Solaini, G. (2004). Bioenergetics shapes cellular death pathways in Leber's hereditary optic neuropathy: A model of mitochondrial neurodegeneration. In *Biochimica et Biophysica Acta - Bioenergetics* (Vol. 1658, Issues 1–2, pp. 172–179). Biochim Biophys Acta. https://doi.org/10.1016/j.bbabio.2004.05.009

Catarino, C. B., von Livonius, B., Priglinger, C., Banik, R., Matloob, S., Tamhankar, M. A., Castillo, L., Friedburg, C., Halfpenny, C. A., Lincoln, J. A., Traber, G. L., Acaroglu, G., Black, G. C. M., Doncel, C., Fraser, C. L., Jakubaszko, J., Landau, K., Langenegger, S. J., Muñoz-Negrete, F. J., … Klopstock, T. (2020). Real-World Clinical Experience With Idebenone in the Treatment of Leber Hereditary Optic Neuropathy. *Journal of Neuro-Ophthalmology : The Official Journal of the North American Neuro-Ophthalmology Society*, *40*(4), 558–565. https://doi.org/10.1097/WNO.0000000000001023

Chang, J. K., Leso, A., Subaiea, G. M., Lahouel, A., Masoud, A., Mushtaq, F., Deeb, R., Eid, A., Dash, M., Bihaqi, S. W., & Zawia, N. H. (2018). Tolfenamic Acid: A Modifier of the Tau Protein and its Role in Cognition and Tauopathy. *Current Alzheimer Research*, *15*(7), 655–663. https://doi.org/10.2174/1567205015666180119104036

Chao De La Barca, J. M., Fogazza, M., Rugolo, M., Chupin, S., Del Dotto, V., Ghelli, A. M., Carelli, V., Simard, G., Procaccio, V., Bonneau, D., Lenaers, G., Reynier, P., & Zanna, C. (2020). Metabolomics hallmarks OPA1 variants correlating with their in vitro phenotype and predicting clinical severity. *Human Molecular Genetics*, *29*(8), 1319–1329.

https://doi.org/10.1093/hmg/ddaa047
Chen, H., Chomyn, A., & Chan, D. C. (2005). Disruption of fusion results in mitochondrial heterogeneity and dysfunction. *Journal of Biological Chemistry*, *280*(28), 26185–26192. https://doi.org/10.1074/jbc.M503062200
Chevrollier, A., Guillet, V., Loiseau, D., Gueguen, N., De Crescenzo, M. A. P., Verny, C., Ferre, M., Dollfus, H., Odent, S., Milea, D., Goizet, C., Amati-Bonneau, P., Procaccio, V., Bonneau, D., & Reynier, P. (2008). Hereditary optic neuropathies share a common mitochondrial coupling defect. *Annals of Neurology*, *63*(6), 794–798. https://doi.org/10.1002/ana.21385
Chicani, C., Chu, E., Ross-Cisneros, F., Rockwell, S., Murase, K., Thoolen, M., Miller, G., & Sadun, A. (2013). Treatment of Leber's hereditary optic neuropathy (LHON): Results using a novel quinone, EPI-743. *Investigative Ophthalmology & Visual Science*, *54*(15), 4574. https://iovs.arvojournals.org/article.aspx?articleid=2149447
Chinnery, P. F., & Hudson, G. (2013). Mitochondrial genetics. In *British Medical Bulletin* (Vol. 106, Issue 1, pp. 135–159). Br Med Bull. https://doi.org/10.1093/bmb/ldt017
Chitnis, T., & Weiner, H. L. (2017). CNS inflammation and neurodegeneration. *Journal of Clinical Investigation*, *127*(10), 3577–3587. https://doi.org/10.1172/JCI90609
Chun, B. Y., & Rizzo, J. F. (2017). Dominant Optic Atrophy and Leber's Hereditary Optic Neuropathy: Update on Clinical Features and Current Therapeutic Approaches. *Seminars in Pediatric Neurology*, *24*(2), 129–134. https://doi.org/10.1016/j.spen.2017.06.001
Cipolat, S., Rudka, T., Hartmann, D., Costa, V., Serneels, L., Craessaerts, K., Metzger, K., Frezza, C., Annaert, W., D'Adamio, L., Derks, C., Dejaegere, T., Pellegrini, L., D'Hooge, R., Scorrano, L., & De Strooper, B. (2006). Mitochondrial Rhomboid PARL Regulates Cytochrome c Release during Apoptosis via OPA1-Dependent Cristae Remodeling. *Cell*, *126*(1), 163–175. https://doi.org/10.1016/j.cell.2006.06.021
Civiletto, G., Varanita, T., Cerutti, R., Gorletta, T., Barbaro, S., Marchet, S., Lamperti, C., Viscomi, C., Scorrano, L., & Zeviani, M. (2015). Opa1 overexpression ameliorates the phenotype of two mitochondrial disease mouse models. *Cell Metabolism*, *21*(6), 845–854. https://doi.org/10.1016/j.cmet.2015.04.016
Cogliati, S., Frezza, C., Soriano, M. E., Varanita, T., Quintana-Cabrera, R., Corrado, M., Cipolat, S., Costa, V., Casarin, A., Gomes, L. C., Perales-Clemente, E., Salviati, L., Fernandez-Silva, P., Enriquez, J. A., & Scorrano, L. (2013). Mitochondrial cristae shape determines respiratory chain supercomplexes assembly and respiratory efficiency. *Cell*, *155*(1), 160–171. https://doi.org/10.1016/j.cell.2013.08.032
Costa, V., Giacomello, M., Hudec, R., Lopreiato, R., Ermak, G., Lim, D., Malorni, W., Davies, K. J. A., Carafoli, E., & Scorrano, L. (2010). Mitochondrial fission and cristae disruption increase the response of cell models of Huntington's disease to apoptotic stimuli. *EMBO Molecular Medicine*, *2*(12), 490–503. https://doi.org/10.1002/emmm.201000102
Crofts, A. R. (2004). The Q-cycle - A personal perspective. *Photosynthesis Research*, *80*(1–3), 223–243. https://doi.org/10.1023/B:PRES.0000030444.52579.10
Cuadrado, A., Rojo, A. I., Wells, G., Hayes, J. D., Cousin, S. P., Rumsey, W. L., Attucks, O. C., Franklin, S., Levonen, A. L., Kensler, T. W., & Dinkova-Kostova, A. T. (2019). Therapeutic targeting of the NRF2 and KEAP1 partnership in chronic diseases. In *Nature Reviews Drug Discovery* (Vol. 18, Issue 4, pp. 295–317). Nat Rev Drug Discov. https://doi.org/10.1038/s41573-018-0008-x
D'Angelo, L., Astro, E., De Luise, M., Kurelac, I., Umesh-Ganesh, N., Ding, S., Fearnley, I. M., Gasparre, G., Zeviani, M., Porcelli, A. M., Fernandez-Vizarra, E., & Iommarini, L. (2021). NDUFS3 depletion permits complex I maturation and reveals TMEM126A/OPA7 as an assembly factor binding the ND4-module intermediate. *Cell Reports*, *35*(3). https://doi.org/10.1016/j.celrep.2021.109002
Davies, V. J., Hollins, A. J., Piechota, M. J., Yip, W., Davies, J. R., White, K. E., Nicols, P. P., Boulton, M. E., & Votruba, M. (2007). Opa1 deficiency in a mouse model of autosomal

dominant optic atrophy impairs mitochondrial morphology, optic nerve structure and visual function. *Human Molecular Genetics*, *16*(11), 1307–1318. https://doi.org/10.1093/hmg/ddm079

Degli Esposti, M., Ngo, A., McMullen, G. L., Ghelli, A., Sparla, F., Benelli, B., Ratta, M., & Linnane, A. W. (1996). The specificity of mitochondrial complex I for ubiquinones. *Biochemical Journal*, *313*(1), 327–334. https://doi.org/10.1042/bj3130327

Del Dotto, V., Fogazza, M., Carelli, V., Rugolo, M., & Zanna, C. (2018). Eight human OPA1 isoforms, long and short: What are they for? In *Biochimica et Biophysica Acta - Bioenergetics* (Vol. 1859, Issue 4, pp. 263–269). Biochim Biophys Acta Bioenerg. https://doi.org/10.1016/j.bbabio.2018.01.005

Del Dotto, V., Fogazza, M., Lenaers, G., Rugolo, M., Carelli, V., & Zanna, C. (2018). OPA1: How much do we know to approach therapy? *Pharmacological Research*, *131*, 199–210. https://doi.org/10.1016/j.phrs.2018.02.018

Del Dotto, V., Fogazza, M., Musiani, F., Maresca, A., Aleo, S. J., Caporali, L., La Morgia, C., Nolli, C., Lodi, T., Goffrini, P., Chan, D., Carelli, V., Rugolo, M., Baruffini, E., & Zanna, C. (2018). Deciphering OPA1 mutations pathogenicity by combined analysis of human, mouse and yeast cell models. *Biochimica et Biophysica Acta - Molecular Basis of Disease*, *1864*(10), 3496–3514. https://doi.org/10.1016/j.bbadis.2018.08.004

Del Dotto, V., Mishra, P., Vidoni, S., Fogazza, M., Maresca, A., Caporali, L., McCaffery, J. M., Cappelletti, M., Baruffini, E., Lenaers, G., Chan, D., Rugolo, M., Carelli, V., & Zanna, C. (2017). OPA1 Isoforms in the Hierarchical Organization of Mitochondrial Functions. *Cell Reports*, *19*(12), 2557–2571. https://doi.org/10.1016/j.celrep.2017.05.073

Delettre, C., Griffoin, J. M., Kaplan, J., Dollfus, H., Lorenz, B., Faivre, L., Lenaers, G., Belenguer, P., & Hamel, C. P. (2001). Mutation spectrum and splicing variants in the OPA1 gene. *Human Genetics*, *109*(6), 584–591. https://doi.org/10.1007/s00439-001-0633-y

Ding, C., Wu, Z., Huang, L., Wang, Y., Xue, J., Chen, S., Deng, Z., Wang, L., Song, Z., & Chen, S. (2015). Mitofilin and CHCHD6 physically interact with Sam50 to sustain cristae structure. *Scientific Reports*, *5*. https://doi.org/10.1038/srep16064

Dinkova-Kostova, A. T., Fahey, J. W., & Talalay, P. (2004). Chemical Structures of Inducers of Nicotinamide Quinone Oxidoreductase 1 (NQO1). *Methods in Enzymology*, *382*, 423–448. https://doi.org/10.1016/S0076-6879(04)82023-8

Dinkova-Kostova, A. T., & Talalay, P. (2010). NAD(P)H:quinone acceptor oxidoreductase 1 (NQO1), a multifunctional antioxidant enzyme and exceptionally versatile cytoprotector. In *Archives of Biochemistry and Biophysics* (Vol. 501, Issue 1, pp. 116–123). Arch Biochem Biophys. https://doi.org/10.1016/j.abb.2010.03.019

DJ, K., K, A., A, A., MJ, A., H, A., A, A. A., H, A., CM, A., PD, A., K, A., PJ, A., SG, A., G, A., R, A., MK, A., M, A., P, A., PV, A., J, A.-G., … SM, Z. (2016). Guidelines for the use and interpretation of assays for monitoring autophagy (3rd edition). *Autophagy*, *12*(1), 1–222. https://doi.org/10.1080/15548627.2015.1100356

Elachouri, G., Vidoni, S., Zanna, C., Pattyn, A., Boukhaddaoui, H., Gaget, K., Yu-Wai-Man, P., Gasparre, G., Sarzi, E., Delettre, C., Olichon, A., Loiseau, D., Reynier, P., Chinnery, P. F., Rotig, A., Carelli, V., Hamel, C. P., Rugolo, M., & Lenaers, G. (2011). OPA1 links human mitochondrial genome maintenance to mtDNA replication and distribution. *Genome Research*, *21*(1), 12–20. https://doi.org/10.1101/gr.108696.110

Enríquez, J. A. (2016). Supramolecular Organization of Respiratory Complexes. In *Annual Review of Physiology* (Vol. 78, pp. 533–561). Annu Rev Physiol. https://doi.org/10.1146/annurev-physiol-021115-105031

Erb, M., Hoffmann-Enger, B., Deppe, H., Soeberdt, M., Haefeli, R. H., Rummey, C., Feurer, A., & Gueven, N. (2012). Features of idebenone and related short-chain quinones that rescue ATP levels under conditions of impaired mitochondrial complex I. *PLoS ONE*, *7*(4). https://doi.org/10.1371/journal.pone.0036153

Erickson, R. P. (1972). Leber's optic atrophy, a possible example of maternal inheritance. *American Journal of Human Genetics*, *24*(3), 348–349. https://pubmed.ncbi.nlm.nih.gov/5063796/

Fato, R., Bergamini, C., Leoni, S., & Lenaz, G. (2008). Mitochondrial production of reactive oxygen species: Role of Complex I and quinone analogues. *BioFactors*, *32*(1–4), 31–39. https://doi.org/10.1002/biof.5520320105

Fernandez-Vizarra, E., & Zeviani, M. (2021). Mitochondrial disorders of the OXPHOS system. In *FEBS Letters* (Vol. 595, Issue 8, pp. 1062–1106). FEBS Lett. https://doi.org/10.1002/1873-3468.13995

Fiedorczuk, K., & Sazanov, L. A. (2018). Mammalian Mitochondrial Complex I Structure and Disease-Causing Mutations. In *Trends in Cell Biology* (Vol. 28, Issue 10, pp. 835–867). Trends Cell Biol. https://doi.org/10.1016/j.tcb.2018.06.006

Fimognari, C., Lenzi, M., Cantelli-Forti, G., & Hrelia, P. (2008). Induction of differentiation in human promyelocytic cells by the isothiocyanate sulforaphane. *In Vivo*, *22*(3), 317–320. https://pubmed.ncbi.nlm.nih.gov/18610742/

Floreani, M., Napoli, E., Martinuzzi, A., Pantano, G., De Riva, V., Trevisan, R., Bisetto, E., Valente, L., Carelli, V., & Dabbeni-Sala, F. (2005). Antioxidant defences in cybrids harboring mtDNA mutations associated with Leber's hereditary optic neuropathy. *FEBS Journal*, *272*(5), 1124–1135. https://doi.org/10.1111/j.1742-4658.2004.04542.x

Formosa, L. E., Dibley, M. G., Stroud, D. A., & Ryan, M. T. (2018). Building a complex complex: Assembly of mitochondrial respiratory chain complex I. In *Seminars in Cell and Developmental Biology* (Vol. 76, pp. 154–162). Semin Cell Dev Biol. https://doi.org/10.1016/j.semcdb.2017.08.011

Freya, T. G., & Mannellab, C. A. (2000). The internal structure of mitochondria. In *Trends in Biochemical Sciences* (Vol. 25, Issue 7, pp. 319–324). Trends Biochem Sci. https://doi.org/10.1016/S0968-0004(00)01609-1

Frezza, C., Cipolat, S., Martins de Brito, O., Micaroni, M., Beznoussenko, G. V., Rudka, T., Bartoli, D., Polishuck, R. S., Danial, N. N., De Strooper, B., & Scorrano, L. (2006). OPA1 Controls Apoptotic Cristae Remodeling Independently from Mitochondrial Fusion. *Cell*, *126*(1), 177–189. https://doi.org/10.1016/j.cell.2006.06.025

Galemou Yoga, E., Schiller, J., & Zickermann, V. (2021). Ubiquinone Binding and Reduction by Complex I—Open Questions and Mechanistic Implications. In *Frontiers in Chemistry* (Vol. 9). Front Chem. https://doi.org/10.3389/fchem.2021.672851

Ge, Y., Shi, X., Boopathy, S., McDonald, J., Smith, A. W., & Chao, L. H. (2020). Two forms of opa1 cooperate to complete fusion of the mitochondrial inner-membrane. *ELife*, *9*. https://doi.org/10.7554/eLife.50973

Ghelli, A., Porcelli, A. M., Zanna, C., Martinuzzi, A., Carelli, V., & Rugolo, M. (2008). Protection against oxidant-induced apoptosis by exogenous glutathione in leber hereditary optic neuropathy cybrids. *Investigative Ophthalmology and Visual Science*, *49*(2), 671–676. https://doi.org/10.1167/iovs.07-0880

Ghochani, M., Nulton, J. D., Salamon, P., Frey, T. G., Rabinovitch, A., & Baljon, A. R. C. (2010). Tensile forces and shape entropy explain observed crista structure in mitochondria. *Biophysical Journal*, *99*(10), 3244–3254. https://doi.org/10.1016/j.bpj.2010.09.038

Gilkerson, R. W., Selker, J. M. L., & Capaldi, R. A. (2003). The cristal membrane of mitochondria is the principal site of oxidative phosphorylation. *FEBS Letters*, *546*(2–3), 355–358. https://doi.org/10.1016/S0014-5793(03)00633-1

Giordano, C., Iommarini, L., Giordano, L., Maresca, A., Pisano, A., Valentino, M. L., Caporali, L., Liguori, R., Deceglie, S., Roberti, M., Fanelli, F., Fracasso, F., Ross-Cisneros, F. N., D'adamo, P., Hudson, G., Pyle, A., Yu-Wai-Man, P., Chinnery, P. F., Zeviani, M., … Carelli, V. (2014). Efficient mitochondrial biogenesis drives incomplete penetrance in Leber's hereditary optic neuropathy. *Brain*, *137*(2), 335–353. https://doi.org/10.1093/brain/awt343

Giordano, L., Deceglie, S., D'Adamo, P., Valentino, M. L., La Morgia, C., Fracasso, F., Roberti,

M., Cappellari, M., Petrosillo, G., Ciaravolo, S., Parente, D., Giordano, C., Maresca, A., Iommarini, L., Del Dotto, V., Ghelli, A. M., Salomao, S. R., Berezovsky, A., Belfort, R., … Cantatore, P. (2015). Cigarette toxicity triggers Leber's hereditary optic neuropathy by affecting mtDNA copy number, oxidative phosphorylation and ROS detoxification pathways. *Cell Death and Disease*, *6*(12). https://doi.org/10.1038/cddis.2015.364

Giorgio, V., Petronilli, V., Ghelli, A., Carelli, V., Rugolo, M., Lenaz, G., & Bernardi, P. (2012). The effects of idebenone on mitochondrial bioenergetics. *Biochimica et Biophysica Acta - Bioenergetics*, *1817*(2), 363–369. https://doi.org/10.1016/j.bbabio.2011.10.012

Giorgio, V., Schiavone, M., Galber, C., Carini, M., Da Ros, T., Petronilli, V., Argenton, F., Carelli, V., Acosta Lopez, M. J., Salviati, L., Prato, M., & Bernardi, P. (2018). The idebenone metabolite QS10 restores electron transfer in complex I and coenzyme Q defects. In *Biochimica et Biophysica Acta - Bioenergetics* (Vol. 1859, Issue 9, pp. 901–908). Biochim Biophys Acta Bioenerg. https://doi.org/10.1016/j.bbabio.2018.04.006

Giudice, A., & Montella, M. (2006). Activation of the Nrf2-ARE signaling pathway: A promising strategy in cancer prevention. In *BioEssays* (Vol. 28, Issue 2, pp. 169–181). Bioessays. https://doi.org/10.1002/bies.20359

Grazioli, S., & Pugin, J. (2018). Mitochondrial damage-associated molecular patterns: From inflammatory signaling to human diseases. In *Frontiers in Immunology* (Vol. 9, Issue MAY). Front Immunol. https://doi.org/10.3389/fimmu.2018.00832

Grba, D. N., & Hirst, J. (2020). Mitochondrial complex I structure reveals ordered water molecules for catalysis and proton translocation. *Nature Structural and Molecular Biology*, *27*(10), 892–900. https://doi.org/10.1038/s41594-020-0473-x

Griparic, L., Van Der Wel, N. N., Orozco, I. J., Peters, P. J., & Van Der Bliek, A. M. (2004). Loss of the Intermembrane Space Protein Mgm1/OPA1 Induces Swelling and Localized Constrictions along the Lengths of Mitochondria. *Journal of Biological Chemistry*, *279*(18), 18792–18798. https://doi.org/10.1074/jbc.M400920200

Guan, P. P., & Wang, P. (2019). Integrated communications between cyclooxygenase-2 and Alzheimer's disease. In *FASEB Journal* (Vol. 33, Issue 1, pp. 13–33). FASEB J. https://doi.org/10.1096/fj.201800355RRRR

Guarani, V., McNeill, E. M., Paulo, J. A., Huttlin, E. L., Fröhlich, F., Gygi, S. P., Vactor, D. Van, & Wade Harper, J. (2015). QIL1 is a novel mitochondrial protein required for MICOS complex stability and cristae morphology. *ELife*, *4*(MAY), 1–23. https://doi.org/10.7554/eLife.06265

Guerrero-Castillo, S., Baertling, F., Kownatzki, D., Wessels, H. J., Arnold, S., Brandt, U., & Nijtmans, L. (2017). The Assembly Pathway of Mitochondrial Respiratory Chain Complex I. *Cell Metabolism*, *25*(1), 128–139. https://doi.org/10.1016/j.cmet.2016.09.002

Guo, M. Y., Shang, L., Hu, Y. Y., Jiang, L. P., Wan, Y. Y., Zhou, Q. Q., Zhang, K., Liao, H. F., Yi, J. L., & Han, X. J. (2018). The role of Cdk5-mediated Drp1 phosphorylation in Aβ 1-42 induced mitochondrial fission and neuronal apoptosis. *Journal of Cellular Biochemistry*, *119*(6), 4815–4825. https://doi.org/10.1002/jcb.26680

Gutiérrez-Fernández, J., Kaszuba, K., Minhas, G. S., Baradaran, R., Tambalo, M., Gallagher, D. T., & Sazanov, L. A. (2020). Key role of quinone in the mechanism of respiratory complex I. *Nature Communications*, *11*(1). https://doi.org/10.1038/s41467-020-17957-0

Haefeli, R. H., Erb, M., Gemperli, A. C., Robay, D., Fruh, I., Anklin, C., Dallmann, R., & Gueven, N. (2011). NQo1-dependent redox cycling of idebenone: Effects on cellular redox potential and energy levels. *PLoS ONE*, *6*(3). https://doi.org/10.1371/journal.pone.0017963

Hamed, A. R., Hegazy, M. E. F., Higgins, M., Mohamed, T. A., Abdel-Azim, N. S., Pare, P. W., & Dinkova-Kostova, A. T. (2016). Potency of extracts from selected Egyptian plants as inducers of the Nrf2-dependent chemopreventive enzyme NQO1. In *Journal of Natural Medicines* (Vol. 70, Issue 3, pp. 683–688). J Nat Med. https://doi.org/10.1007/s11418-016-0994-0

Heitz, F. D., Erb, M., Anklin, C., Robay, D., Pernet, V., & Gueven, N. (2012). Idebenone Protects

against Retinal Damage and Loss of Vision in a Mouse Model of Leber's Hereditary Optic Neuropathy. *PLoS ONE*, *7*(9). https://doi.org/10.1371/journal.pone.0045182

Herkenne, S., Ek, O., Zamberlan, M., Pellattiero, A., Chergova, M., Chivite, I., Novotná, E., Rigoni, G., Fonseca, T. B., Samardzic, D., Agnellini, A., Bean, C., Di Benedetto, G., Tiso, N., Argenton, F., Viola, A., Soriano, M. E., Giacomello, M., Ziviani, E., … Scorrano, L. (2020). Developmental and Tumor Angiogenesis Requires the Mitochondria-Shaping Protein Opa1. *Cell Metabolism*, *31*(5), 987-1003.e8. https://doi.org/10.1016/j.cmet.2020.04.007

Hirst, J. (2013). Mitochondrial complex i. In *Annual Review of Biochemistry* (Vol. 82, pp. 551–575). Annu Rev Biochem. https://doi.org/10.1146/annurev-biochem-070511-103700

Holmström, K. M., Kostov, R. V., & Dinkova-Kostova, A. T. (2016). The multifaceted role of Nrf2 in mitochondrial function. In *Current Opinion in Toxicology* (Vol. 2, pp. 80–91). Curr Opin Toxicol. https://doi.org/10.1016/j.cotox.2016.10.002

Hudson, G., Amati-Bonneau, P., Blakely, E. L., Stewart, J. D., He, L., Schaefer, A. M., Griffiths, P. G., Ahlqvist, K., Suomalainen, A., Reynier, P., McFarland, R., Turnbull, D. M., Chinnery, P. F., & Taylor, R. W. (2008). Mutation of OPA1 causes dominant optic atrophy with external ophthalmoplegia, ataxia, deafness and multiple mitochondrial DNA deletions: A novel disorder of mtDNA maintenance. *Brain*, *131*(2), 329–337. https://doi.org/10.1093/brain/awm272

Hudson, G., Carelli, V., Spruijt, L., Gerards, M., Mowbray, C., Achilli, A., Pyle, A., Elson, J., Howell, N., La Morgia, C., Valentino, M. L., Huoponen, K., Savontaus, M. L., Nikoskelainen, E., Sadun, A. A., Salomao, S. R., Belfort, R., Griffiths, P., Man, P. Y. W., … Chinnery, P. F. (2007). Clinical expression of leber hereditary optic neuropathy is affected by the mitochondrial DNA-haplogroup background. *American Journal of Human Genetics*, *81*(2), 228–233. https://doi.org/10.1086/519394

Hung, S. S. C., McCaughey, T., Swann, O., Pébay, A., & Hewitt, A. W. (2016). Genome engineering in ophthalmology: Application of CRISPR/Cas to the treatment of eye disease. In *Progress in Retinal and Eye Research* (Vol. 53, pp. 1–20). Prog Retin Eye Res. https://doi.org/10.1016/j.preteyeres.2016.05.001

Iommarini, L., Ghelli, A., Gasparre, G., & Porcelli, A. M. (2017). Mitochondrial metabolism and energy sensing in tumor progression. In *Biochimica et Biophysica Acta - Bioenergetics* (Vol. 1858, Issue 8, pp. 582–590). Biochim Biophys Acta Bioenerg. https://doi.org/10.1016/j.bbabio.2017.02.006

Ishihara, T., Ban-Ishihara, R., Maeda, M., Matsunaga, Y., Ichimura, A., Kyogoku, S., Aoki, H., Katada, S., Nakada, K., Nomura, M., Mizushima, N., Mihara, K., & Ishihara, N. (2015). Dynamics of Mitochondrial DNA Nucleoids Regulated by Mitochondrial Fission Is Essential for Maintenance of Homogeneously Active Mitochondria during Neonatal Heart Development. *Molecular and Cellular Biology*, *35*(1), 211–223. https://doi.org/10.1128/mcb.01054-14

Jaber, S., & Polster, B. M. (2015). Idebenone and neuroprotection: antioxidant, pro-oxidant, or electron carrier? In *Journal of Bioenergetics and Biomembranes* (Vol. 47, Issues 1–2, pp. 111–118). J Bioenerg Biomembr. https://doi.org/10.1007/s10863-014-9571-y

Jahani-Asl, A., Huang, E., Irrcher, I., Rashidian, J., Ishihara, N., Lagace, D. C., Slack, R. S., & Park, D. S. (2015). CDK5 phosphorylates DRP1 and drives mitochondrial defects in NMDA-induced neuronal death. *Human Molecular Genetics*, *24*(16), 4573–4583. https://doi.org/10.1093/hmg/ddv188

Jones, B. A., & Fangman, W. L. (1992). Mitochondrial DNA maintenance in yeast requires a protein containing a region related to the GTP-binding domain of dynamin. *Genes and Development*, *6*(3), 380–389. https://doi.org/10.1101/gad.6.3.380

JR, F., A, M., J, Y., JM, M., & J, N. (2015). MICOS coordinates with respiratory complexes and lipids to establish mitochondrial inner membrane architecture. *ELife*, *4*(4), 1–61. https://doi.org/10.7554/ELIFE.07739

Kampjut, D., & Sazanov, L. A. (2020). The coupling mechanism of mammalian respiratory complex I. *Science*, *370*(6516). https://doi.org/10.1126/SCIENCE.ABC4209

Kane, M. S., Alban, J., Desquiret-Dumas, V., Gueguen, N., Ishak, L., Ferre, M., Amati-Bonneau, P., Procaccio, V., Bonneau, D., Lenaers, G., Reynier, P., & Chevrollier, A. (2017). Autophagy controls the pathogenicity of OPA1 mutations in dominant optic atrophy. *Journal of Cellular and Molecular Medicine*, *21*(10), 2284–2297. https://doi.org/10.1111/jcmm.13149

Kappos, L., Gold, R., Arnold, D. L., Bar-Or, A., Giovannoni, G., Selmaj, K., Sarda, S. P., Agarwal, S., Zhang, A., Sheikh, S. I., Seidman, E., & Dawson, K. T. (2014). Quality of life outcomes with BG-12 (dimethyl fumarate) in patients with relapsing-remitting multiple sclerosis: The DEFINE study. *Multiple Sclerosis*, *20*(2), 243–252. https://doi.org/10.1177/1352458513507817

Kaur, K., Gill, J. S., Bansal, P. K., & Deshmukh, R. (2017). Neuroinflammation - A major cause for striatal dopaminergic degeneration in Parkinson's disease. In *Journal of the Neurological Sciences* (Vol. 381, pp. 308–314). J Neurol Sci. https://doi.org/10.1016/j.jns.2017.08.3251

Kim, J. Y., Hwang, J. M., Ko, H. S., Seong, M. W., Park, B. J., & Park, S. S. (2005). Mitochondrial DNA content is decreased in autosomal dominant optic atrophy. *Neurology*, *64*(6), 966–972. https://doi.org/10.1212/01.WNL.0000157282.76715.B1

King, M. P., & Attardi, G. (1996). [27] Isolation of human cell lines lacking mitochondrial DNA. *Methods in Enzymology*, *264*, 304–312. https://doi.org/10.1016/s0076-6879(96)64029-4

King, M. S., Sharpley, M. S., & Hirst, J. (2009). Reduction of hydrophilic ubiquinones by the flavin in mitochondrial NADH:ubiquinone oxidoreductase (complex I) and production of reactive oxygen species. *Biochemistry*, *48*(9), 2053–2062. https://doi.org/10.1021/bi802282h

KJER, P. (1959). Infantile optic atrophy with dominant mode of inheritance: a clinical and genetic study of 19 Danish families. *Acta Ophthalmologica. Supplementum*, *164*(Supp 54), 1–147. https://pubmed.ncbi.nlm.nih.gov/13660776/

Klopstock, T., Metz, G., Yu-Wai-Man, P., Büchner, B., Gallenmüller, C., Bailie, M., Nwali, N., Griffiths, P. G., Von Livonius, B., Reznicek, L., Rouleau, J., Coppard, N., Meier, T., & Chinnery, P. F. (2013). Persistence of the treatment effect of idebenone in Leber's hereditary optic neuropathy. In *Brain* (Vol. 136, Issue 2). Brain. https://doi.org/10.1093/brain/aws279

Klopstock, Thomas, Yu-Wai-Man, P., Dimitriadis, K., Rouleau, J., Heck, S., Bailie, M., Atawan, A., Chattopadhyay, S., Schubert, M., Garip, A., Kernt, M., Petraki, D., Rummey, C., Leinonen, M., Metz, G., Griffiths, P. G., Meier, T., & Chinnery, P. F. (2011). A randomized placebo-controlled trial of idebenone in Leber's hereditary optic neuropathy. *Brain*, *134*(9), 2677–2686. https://doi.org/10.1093/brain/awr170

Laforge, M., Rodrigues, V., Silvestre, R., Gautier, C., Weil, R., Corti, O., & Estaquier, J. (2016). NF-κB pathway controls mitochondrial dynamics. *Cell Death and Differentiation*, *23*(1), 89–98. https://doi.org/10.1038/cdd.2015.42

Lamb, C. A., Yoshimori, T., & Tooze, S. A. (2013). The autophagosome: Origins unknown, biogenesis complex. In *Nature Reviews Molecular Cell Biology* (Vol. 14, Issue 12, pp. 759–774). Nat Rev Mol Cell Biol. https://doi.org/10.1038/nrm3696

Lenaers, G., Hamel, C., Delettre, C., Amati-Bonneau, P., Procaccio, V., Bonneau, D., Reynier, P., & Milea, D. (2012). Dominant optic atrophy. In *Orphanet Journal of Rare Diseases* (Vol. 7, Issue 1). Orphanet J Rare Dis. https://doi.org/10.1186/1750-1172-7-46

Lenaz, G., & Genova, M. L. (2010). Structure and organization of mitochondrial respiratory complexes: A new understanding of an old subject. In *Antioxidants and Redox Signaling* (Vol. 12, Issue 8, pp. 961–1008). Antioxid Redox Signal. https://doi.org/10.1089/ars.2009.2704

Letts, J. A., & Sazanov, L. A. (2017). Clarifying the supercomplex: The higher-order organization of the mitochondrial electron transport chain. In *Nature Structural and Molecular Biology* (Vol. 24, Issue 10, pp. 800–808). Nature Publishing Group. https://doi.org/10.1038/nsmb.3460

Liu, L., Feng, D., Chen, G., Chen, M., Zheng, Q., Song, P., Ma, Q., Zhu, C., Wang, R., Qi, W., Huang, L., Xue, P., Li, B., Wang, X., Jin, H., Wang, J., Yang, F., Liu, P., Zhu, Y., … Chen, Q.

(2012). Mitochondrial outer-membrane protein FUNDC1 mediates hypoxia-induced mitophagy in mammalian cells. *Nature Cell Biology*, *14*(2), 177–185. https://doi.org/10.1038/ncb2422

Liu, P., Li, Y., Yang, W., Liu, D., Ji, X., Chi, T., Guo, Z., Li, L., & Zou, L. (2019). Prevention of Huntington's disease-like behavioral deficits in R6/1 mouse by tolfenamic acid is associated with decreases in mutant huntingtin and oxidative stress. *Oxidative Medicine and Cellular Longevity*, *2019*. https://doi.org/10.1155/2019/4032428

Man, P. Y. W., Griffiths, P. G., Brown, D. T., Howell, N., Turnbull, D. M., & Chinnery, P. F. (2003). The epidemiology of leber hereditary optic neuropathy in the North East of England. *American Journal of Human Genetics*, *72*(2), 333–339. https://doi.org/10.1086/346066

Manickam, A., Michael, M., & Ramasamy, S. (2017). Mitochondrial genetics and therapeutic overview of Leber's hereditary optic neuropathy. In *Indian Journal of Ophthalmology* (Vol. 65, Issue 11, pp. 1087–1092). Indian J Ophthalmol. https://doi.org/10.4103/ijo.IJO_358_17

Mannella, C. A. (2006). Structure and dynamics of the mitochondrial inner membrane cristae. In *Biochimica et Biophysica Acta - Molecular Cell Research* (Vol. 1763, Issues 5–6, pp. 542–548). Biochim Biophys Acta. https://doi.org/10.1016/j.bbamcr.2006.04.006

Maresca, A., & Carelli, V. (2021). Molecular mechanisms behind inherited neurodegeneration of the optic nerve. In *Biomolecules* (Vol. 11, Issue 4). Biomolecules. https://doi.org/10.3390/biom11040496

Merkwirth, C., Dargazanli, S., Tatsuta, T., Geimer, S., Löwer, B., Wunderlich, F. T., Von Kleist-Retzow, J. C., Waisman, A., Westermann, B., & Langer, T. (2008). Prohibitins control cell proliferation and apoptosis by regulating OPA1-dependent cristae morphogenesis in mitochondria. *Genes and Development*, *22*(4), 476–488. https://doi.org/10.1101/gad.460708

Milenkovic, D., Blaza, J. N., Larsson, N. G., & Hirst, J. (2017). The Enigma of the Respiratory Chain Supercomplex. In *Cell Metabolism* (Vol. 25, Issue 4, pp. 765–776). Cell Metab. https://doi.org/10.1016/j.cmet.2017.03.009

Millet, A. M. C., Bertholet, A. M., Daloyau, M., Reynier, P., Galinier, A., Devin, A., Wissinguer, B., Belenguer, P., & Davezac, N. (2016). Loss of functional OPA1 unbalances redox state: Implications in dominant optic atrophy pathogenesis. *Annals of Clinical and Translational Neurology*, *3*(6), 408–421. https://doi.org/10.1002/acn3.305

Morán, M., Moreno-Lastres, D., Marín-Buera, L., Arenas, J., Martín, M. A., & Ugalde, C. (2012). Mitochondrial respiratory chain dysfunction: Implications in neurodegeneration. In *Free Radical Biology and Medicine* (Vol. 53, Issue 3, pp. 595–609). Free Radic Biol Med. https://doi.org/10.1016/j.freeradbiomed.2012.05.009

Nolli, C., Goffrini, P., Lazzaretti, M., Zanna, C., Vitale, R., Lodi, T., & Baruffini, E. (2015). Validation of a MGM1/OPA1 chimeric gene for functional analysis in yeast of mutations associated with dominant optic atrophy. *Mitochondrion*, *25*, 38–48. https://doi.org/10.1016/j.mito.2015.10.002

Nunnari, J., & Suomalainen, A. (2012). Mitochondria: In sickness and in health. In *Cell* (Vol. 148, Issue 6, pp. 1145–1159). Cell. https://doi.org/10.1016/j.cell.2012.02.035

Olichon, A., Baricault, L., Gas, N., Guillou, E., Valette, A., Belenguer, P., & Lenaers, G. (2003). Loss of OPA1 perturbates the mitochondrial inner membrane structure and integrity, leading to cytochrome c release and apoptosis. *Journal of Biological Chemistry*, *278*(10), 7743–7746. https://doi.org/10.1074/jbc.C200677200

Pajares, M., Jiménez-Moreno, N., García-Yagüe, Á. J., Escoll, M., de Ceballos, M. L., Van Leuven, F., Rábano, A., Yamamoto, M., Rojo, A. I., & Cuadrado, A. (2016). Transcription factor NFE2L2/NRF2 is a regulator of macroautophagy genes. *Autophagy*, *12*(10), 1902–1916. https://doi.org/10.1080/15548627.2016.1208889

Pathi, S., Li, X., & Safe, S. (2014). Tolfenamic acid inhibits colon cancer cell and tumor growth and induces degradation of specificity protein (Sp) transcription factors. *Molecular Carcinogenesis*, *53*(S1). https://doi.org/10.1002/mc.22010

Pesch, U. E. A., Leo-Kottler, B., Mayer, S., Jurklies, B., Kellner, U., Apfelstedt-Sylla, E., Zrenner, E., Alexander, C., & Wissinger, B. (2001). OPA1 mutations in patients with autosomal dominant optic atrophy and evidence for semi-dominant inheritance. *Human Molecular Genetics*, *10*(13), 1359–1368. https://doi.org/10.1093/hmg/10.13.1359

Petit, L., Khanna, H., & Punzo, C. (2016). Advances in gene therapy for diseases of the eye. In *Human Gene Therapy* (Vol. 27, Issue 8, pp. 563–579). Hum Gene Ther. https://doi.org/10.1089/hum.2016.040

Pfanner, N., van der Laan, M., Amati, P., Capaldi, R. A., Caudy, A. A., Chacinska, A., Darshi, M., Deckers, M., Hoppins, S., Icho, T., Jakobs, S., Ji, J., Kozjak-Pavlovic, V., Meisinger, C., Odgren, P. R., Park, S. K., Rehling, P., Reichert, A. S., Sheikh, M. S., … Nunnari, J. (2014). Uniform nomenclature for the mitochondrial contact site and cristae organizing system. In *Journal of Cell Biology* (Vol. 204, Issue 7, pp. 1083–1086). J Cell Biol. https://doi.org/10.1083/jcb.201401006

Pilz, Y. L., Bass, S. J., & Sherman, J. (2017). Revisión de las neuropatías ópticas mitocondriales: de las formas hereditarias a las adquiridas. In *Journal of Optometry* (Vol. 10, Issue 4, pp. 205–214). J Optom. https://doi.org/10.1016/j.optom.2016.09.003

Porcelli, A. M., Ghelli, A., Iommarini, L., Mariani, E., Hoque, M., Zanna, C., Gasparre, G., & Rugolo, M. (2008). The antioxidant function of Bcl-2 preserves cytoskeletal stability of cells with defective respiratory complex I. *Cellular and Molecular Life Sciences*, *65*(18), 2943–2951. https://doi.org/10.1007/s00018-008-8300-2

Protasoni, M., Pérez-Pérez, R., Lobo-Jarne, T., Harbour, M. E., Ding, S., Peñas, A., Diaz, F., Moraes, C. T., Fearnley, I. M., Zeviani, M., Ugalde, C., & Fernández-Vizarra, E. (2020). Respiratory supercomplexes act as a platform for complex III -mediated maturation of human mitochondrial complexes I and IV. *The EMBO Journal*, *39*(3). https://doi.org/10.15252/embj.2019102817

Pryde, K. R., & Hirst, J. (2011). Superoxide is produced by the reduced flavin in mitochondrial complex I: A single, unified mechanism that applies during both forward and reverse electron transfer. *Journal of Biological Chemistry*, *286*(20), 18056–18065. https://doi.org/10.1074/jbc.M110.186841

Rich, P. R. (2008). A perspective on Peter Mitchell and the chemiosmotic theory. In *Journal of Bioenergetics and Biomembranes* (Vol. 40, Issue 5, pp. 407–410). J Bioenerg Biomembr. https://doi.org/10.1007/s10863-008-9173-7

Robinson, B. H. (1996). [39] Use of fibroblast and lymphoblast cultures for detection of respiratory chain defects. *Methods in Enzymology*, *264*, 454–464. https://doi.org/10.1016/s0076-6879(96)64041-5

Rodríguez-Nuevo, A., Díaz-Ramos, A., Noguera, E., Díaz-Sáez, F., Duran, X., Muñoz, J. P., Romero, M., Plana, N., Sebastián, D., Tezze, C., Romanello, V., Ribas, F., Seco, J., Planet, E., Doctrow, S. R., González, J., Borràs, M., Liesa, M., Palacín, M., … Zorzano, A. (2018). Mitochondrial DNA and TLR9 drive muscle inflammation upon Opa1 deficiency. *The EMBO Journal*, *37*(10). https://doi.org/10.15252/embj.201796553

Romagnoli, M., La Morgia, C., Carbonelli, M., Di Vito, L., Amore, G., Zenesini, C., Cascavilla, M. L., Barboni, P., & Carelli, V. (2020). Idebenone increases chance of stabilization/recovery of visual acuity in OPA1-dominant optic atrophy. *Annals of Clinical and Translational Neurology*, *7*(4), 590–594. https://doi.org/10.1002/acn3.51026

Ropper, A. H. (2012). The "Poison Chair" Treatment for Multiple Sclerosis. *New England Journal of Medicine*, *367*(12), 1149–1150. https://doi.org/10.1056/nejme1209169

Ross, D., & Siegel, D. (2004). NAD(P)H:Quinone Oxidoreductase 1 (NQO1, DT-Diaphorase), Functions and Pharmacogenetics. *Methods in Enzymology*, *382*, 115–144. https://doi.org/10.1016/S0076-6879(04)82008-1

Ross, D., & Siegel, D. (2017). Functions of NQO1 in cellular protection and CoQ10 metabolism and its potential role as a redox sensitive molecular switch. In *Frontiers in Physiology* (Vol. 8,

Issue AUG, p. 595). Frontiers Media SA. https://doi.org/10.3389/fphys.2017.00595
Sagan, L. (1967). On the origin of mitosing cells. *Journal of Theoretical Biology*, *14*(3). https://doi.org/10.1016/0022-5193(67)90079-3
Sauvanet, C., Duvezin-Caubet, S., Salin, B., David, C., Massoni-Laporte, A., di Rago, J. P., & Rojo, M. (2012). Mitochondrial DNA Mutations Provoke Dominant Inhibition of Mitochondrial Inner Membrane Fusion. *PLoS ONE*, *7*(11). https://doi.org/10.1371/journal.pone.0049639
Shao, H. J., Lou, Z., Jeong, J. B., Kim, K. J., Lee, J., & Lee, S. H. (2015). Tolfenamic acid suppresses inflammatory stimuli-mediated activation of NF-κB signaling. *Biomolecules and Therapeutics*, *23*(1), 39–44. https://doi.org/10.4062/biomolther.2014.088
Siegel, D., McGuinness, S. M., Winski, S. L., & Ross, D. (1999). Genotype-phenotype relationships in studies of a polymorphism in NAD(P)H:quinone oxidoreductase 1. *Pharmacogenetics*, *9*(1), 113–121. https://doi.org/10.1097/00008571-199902000-00015
Song, Z., Chen, H., Fiket, M., Alexander, C., & Chan, D. C. (2007). OPA1 processing controls mitochondrial fusion and is regulated by mRNA splicing, membrane potential, and Yme1L. *Journal of Cell Biology*, *178*(5), 749–755. https://doi.org/10.1083/jcb.200704110
Stojanović, S., Sprinz, H., & Brede, O. (2001). Efficiency and mechanism of the antioxidant action of trans-resveratrol and its analogues in the radical liposome oxidation. *Archives of Biochemistry and Biophysics*, *391*(1), 79–89. https://doi.org/10.1006/abbi.2001.2388
Stroud, D. A., Surgenor, E. E., Formosa, L. E., Reljic, B., Frazier, A. E., Dibley, M. G., Osellame, L. D., Stait, T., Beilharz, T. H., Thorburn, D. R., Salim, A., & Ryan, M. T. (2016). Accessory subunits are integral for assembly and function of human mitochondrial complex i. *Nature*, *538*(7623), 123–126. https://doi.org/10.1038/nature19754
Subaiea, G. M., Adwan, L. I., Ahmed, A. H., Stevens, K. E., & Zawia, N. H. (2013). Short-term treatment with tolfenamic acid improves cognitive functions in alzheimer's disease mice. *Neurobiology of Aging*, *34*(10), 2421–2430. https://doi.org/10.1016/j.neurobiolaging.2013.04.002
Subaiea, G. M., Ahmed, A. H., Adwan, L. I., & Zawia, N. H. (2015). Reduction of amyloid-β deposition and attenuation of memory deficits by tolfenamic acid. *Journal of Alzheimer's Disease*, *43*(2), 425–433. https://doi.org/10.3233/JAD-132726
Sun, Q., Fan, J., Billiar, T. R., & Scott, M. J. (2017). Inflammasome and autophagy regulation: A two-way street. *Molecular Medicine*, *23*, 188–195. https://doi.org/10.2119/molmed.2017.00077
Taanman, J. W. (1999). The mitochondrial genome: Structure, transcription, translation and replication. In *Biochimica et Biophysica Acta - Bioenergetics* (Vol. 1410, Issue 2, pp. 103–123). Biochim Biophys Acta. https://doi.org/10.1016/S0005-2728(98)00161-3
Tadato, B., Heymann, J. A. W., Song, Z., Hinshaw, J. E., & Chan, D. C. (2010). OPA1 disease alleles causing dominant optic atrophy have defects in cardiolipin-stimulated GTP hydrolysis and membrane tubulation. *Human Molecular Genetics*, *19*(11), 2113–2122. https://doi.org/10.1093/hmg/ddq088
Tong, K. I., Kobayashi, A., Katsuoka, F., & Yamamoto, M. (2006). Two-site substrate recognition model for the Keap1-Nrf2 system: A hinge and latch mechanism. *Biological Chemistry*, *387*(10–11), 1311–1320. https://doi.org/10.1515/BC.2006.164
Traver, R. D., Siegel, D., Beall, H. D., Phillips, R. M., Gibson, N. W., Franklin, W. A., & Ross, D. (1997). Characterization of a polymorphism in NAD(P)H: Quinone oxidoreductase (DT-diaphorase). *British Journal of Cancer*, *75*(1), 69–75. https://doi.org/10.1038/bjc.1997.11
Trounce, I. A., Kim, Y. L., Jun, A. S., & Wallace, D. C. (1996). [42] Assessment of mitochondrial oxidative phosphorylation in patient muscle biopsies, lymphoblasts, and transmitochondrial cell lines. *Methods in Enzymology*, *264*, 484–509. https://doi.org/10.1016/s0076-6879(96)64044-0
van der Bliek, A. M., Shen, Q., & Kawajiri, S. (2013). Mechanisms of mitochondrial fission and

fusion. *Cold Spring Harbor Perspectives in Biology*, *5*(6). https://doi.org/10.1101/cshperspect.a011072

Vanduchova, A., Anzenbacher, P., & Anzenbacherova, E. (2019). Isothiocyanate from Broccoli, Sulforaphane, and Its Properties. In *Journal of Medicinal Food* (Vol. 22, Issue 2, pp. 121–126). J Med Food. https://doi.org/10.1089/jmf.2018.0024

Varanita, T., Soriano, M. E., Romanello, V., Zaglia, T., Quintana-Cabrera, R., Semenzato, M., Menabò, R., Costa, V., Civiletto, G., Pesce, P., Viscomi, C., Zeviani, M., Di Lisa, F., Mongillo, M., Sandri, M., & Scorrano, L. (2015). The Opa1-dependent mitochondrial cristae remodeling pathway controls atrophic, apoptotic, and ischemic tissue damage. *Cell Metabolism*, *21*(6), 834–844. https://doi.org/10.1016/j.cmet.2015.05.007

Varricchio, C., Beirne, K., Heard, C., Newland, B., Rozanowska, M., Brancale, A., & Votruba, M. (2020). The ying and yang of idebenone: Not too little, not too much – cell death in NQO1 deficient cells and the mouse retina. *Free Radical Biology and Medicine*, *152*, 551–560. https://doi.org/10.1016/j.freeradbiomed.2019.11.030

Vergani, L., Martinuzzi, A., Carelli, V., Cortelli, P., Montagna, P., Schievano, G., Carrozzo, R., Angelini, C., & Lugaresi, E. (1995). MtDNA mutations associated with leber's hereditary optic neuropathy: Studies on cytoplasmic hybrid (cybrid) cells. *Biochemical and Biophysical Research Communications*, *210*(3), 880–888. https://doi.org/10.1006/bbrc.1995.1740

Vinothkumar, K. R., Zhu, J., & Hirst, J. (2014). Architecture of mammalian respiratory complex I. *Nature*, *515*(7525), 80–84. https://doi.org/10.1038/nature13686

Viscomi, C., Bottani, E., & Zeviani, M. (2015). Emerging concepts in the therapy of mitochondrial disease. In *Biochimica et Biophysica Acta - Bioenergetics* (Vol. 1847, Issues 6–7, pp. 544–557). Biochim Biophys Acta. https://doi.org/10.1016/j.bbabio.2015.03.001

Votruba, M., Moore, A. T., & Bhattacharya, S. S. (1998). Clinical features, molecular genetics, and pathophysiology of dominant optic atrophy. In *Journal of Medical Genetics* (Vol. 35, Issue 10, pp. 793–800). J Med Genet. https://doi.org/10.1136/jmg.35.10.793

Wai, T., & Langer, T. (2016). Mitochondrial Dynamics and Metabolic Regulation. In *Trends in Endocrinology and Metabolism* (Vol. 27, Issue 2, pp. 105–117). Trends Endocrinol Metab. https://doi.org/10.1016/j.tem.2015.12.001

Walker, J. E. (1998). ATP synthesis by rotary catalysis (Nobel lecture). *Angewandte Chemie - International Edition*, *37*(17), 2308–2319. https://doi.org/10.1002/(SICI)1521-3773(19980918)37:17<2308::AID-ANIE2308>3.0.CO;2-W

Wallace, D. C., & Lott, M. T. (2017). Leber hereditary optic neuropathy: Exemplar of an mtDNA disease. In *Handbook of Experimental Pharmacology* (Vol. 240). Handb Exp Pharmacol. https://doi.org/10.1007/164_2017_2

Wesselborg, S., & Stork, B. (2015). Autophagy signal transduction by ATG proteins: From hierarchies to networks. In *Cellular and Molecular Life Sciences* (Vol. 72, Issue 24, pp. 4721–4757). Cell Mol Life Sci. https://doi.org/10.1007/s00018-015-2034-8

Willems, P. H. G. M., Rossignol, R., Dieteren, C. E. J., Murphy, M. P., & Koopman, W. J. H. (2015). Redox Homeostasis and Mitochondrial Dynamics. In *Cell Metabolism* (Vol. 22, Issue 2, pp. 207–218). Cell Metab. https://doi.org/10.1016/j.cmet.2015.06.006

Wilson, W. J., Afzali, M. F., Cummings, J. E., Legare, M. E., Tjalkens, R. B., Allen, C. P., Slayden, R. A., & Hanneman, W. H. (2016). Immune Modulation as an Effective Adjunct Post-exposure Therapeutic for B. pseudomallei. *PLoS Neglected Tropical Diseases*, *10*(10). https://doi.org/10.1371/journal.pntd.0005065

Wu, W., Zhao, D., Shah, S. Z. A., Zhang, X., Lai, M., Yang, D., Wu, X., Guan, Z., Li, J., Zhao, H., Li, W., Gao, H., Zhou, X., Qiao, J., & Yang, L. (2019). OPA1 overexpression ameliorates mitochondrial cristae remodeling, mitochondrial dysfunction, and neuronal apoptosis in prion diseases. *Cell Death and Disease*, *10*(10). https://doi.org/10.1038/s41419-019-1953-y

Yang, J., Zhou, R., & Ma, Z. (2019). Autophagy and Energy Metabolism. In *Advances in Experimental Medicine and Biology* (Vol. 1206, pp. 329–357). Adv Exp Med Biol.

https://doi.org/10.1007/978-981-15-0602-4_16
Yang, L., Long, Q., Liu, J., Tang, H., Li, Y., Bao, F., Qin, D., Pei, D., & Liu, X. (2015). Mitochondrial fusion provides an “initial metabolic complementation” controlled by mtDNA. *Cellular and Molecular Life Sciences*, *72*(13), 2585–2598. https://doi.org/10.1007/s00018-015-1863-9
Yoo, S. M., & Jung, Y. K. (2018). A molecular approach to mitophagy and mitochondrial dynamics. In *Molecules and Cells* (Vol. 41, Issue 1, pp. 18–26). Mol Cells. https://doi.org/10.14348/molcells.2018.2277
Yu-Wai-Man, P., Votruba, M., Moore, A. T., & Chinnery, P. F. (2014). Treatment strategies for inherited optic neuropathies: Past, present and future. *Eye (Basingstoke)*, *28*(5), 521–537. https://doi.org/10.1038/eye.2014.37
Yu-Wai-Man, Patrick. (2015). Therapeutic Approaches to Inherited Optic Neuropathies. *Seminars in Neurology*, *35*(5), 578–586. https://doi.org/10.1055/s-0035-1563574
Yu-Wai-Man, Patrick, & Chinnery, P. F. (2013). Dominant optic atrophy: Novel OPA1 mutations and revised prevalence estimates. In *Ophthalmology* (Vol. 120, Issue 8). Ophthalmology. https://doi.org/10.1016/j.ophtha.2013.04.022
Yu-Wai-Man, Patrick, & Newman, N. J. (2017). Inherited eye-related disorders due to mitochondrial dysfunction. In *Human Molecular Genetics* (Vol. 26, Issue R1, pp. R12–R20). Hum Mol Genet. https://doi.org/10.1093/hmg/ddx182
Yu, L., Chen, Y., & Tooze, S. A. (2018). Autophagy pathway: Cellular and molecular mechanisms. In *Autophagy* (Vol. 14, Issue 2, pp. 207–215). Autophagy. https://doi.org/10.1080/15548627.2017.1378838
Zanna, C., Ghelli, A., Porcelli, A. M., Karbowski, M., Youle, R. J., Schimpf, S., Wissinger, B., Pinti, M., Cossarizza, A., Vidoni, S., Valentino, M. L., Rugolo, M., & Carelli, V. (2008). OPA1 mutations associated with dominant optic atrophy impair oxidative phosphorylation and mitochondrial fusion. *Brain*, *131*(2), 352–367. https://doi.org/10.1093/brain/awm335
Zeviani, M., & Carelli, V. (2007). Mitochondrial disorders. In *Current Opinion in Neurology* (Vol. 20, Issue 5, pp. 564–571). Curr Opin Neurol. https://doi.org/10.1097/WCO.0b013e3282ef58cd
Zhang, D. D. (2006). Mechanistic studies of the Nrf2-Keap1 signaling pathway. *Drug Metabolism Reviews*, *38*(4), 769–789. https://doi.org/10.1080/03602530600971974
Zhu, J., Vinothkumar, K. R., & Hirst, J. (2016). Structure of mammalian respiratory complex i. *Nature*, *536*(7616), 354–358. https://doi.org/10.1038/nature19095
Zorova, L. D., Popkov, V. A., Plotnikov, E. Y., Silachev, D. N., Pevzner, I. B., Jankauskas, S. S., Babenko, V. A., Zorov, S. D., Balakireva, A. V., Juhaszova, M., Sollott, S. J., & Zorov, D. B. (2018). Mitochondrial membrane potential. *Analytical Biochemistry*, *552*, 50–59. https://doi.org/10.1016/j.ab.2017.07.009